M.Sc. in Chemical Engineering Thesis

Optimal design and control of a catalytic distillation column. Case study: Ethyl *tert*-butyl ether (ETBE) synthesis column.

Eng. David Esteban Bernal Neira

Advisor: Jorge Mario Gómez Ramírez, Ph.D.

Universidad de los Andes

Engineering Faculty, Department of Chemical Engineering

Bogotá, May 9th 2016

Content table

Abstract

Process intensification has as objective to achieve higher yields in chemical processes. One example of this is the catalytic distillation, where chemical reaction and vapor-liquid separation are integrated into one single process equipment. This system is characterized for high nonlinearities in the mathematical model that describes it and as a critical unit for the whole process. The integration of the design and control of this system has been addressed in this work. Steady-state and dynamic models based on fundamental principles for this equipment have been proposed and solved into optimal design and control problems. A methodology for determining the weighting parameters in a tracking and economic objective function for optimal control has been proposed. The Ethyl tert-butyl ether production catalytic distillation column was chosen as case study. The optimal design problem proposed in this work had several considerations that other authors who covered the same topic neglected, and its results showed the necessity of implementing a detailed model. The optimal design and control problems have been solved sequentially and simultaneously when facing the system to a disturbance in the feed stream composition, and the simultaneous approach proved to obtain a solution that satisfied operational constraints of the system contrary to the sequential approach. Several dynamic models based on the index of the differential algebraic equations system are proposed and tested, showing their validity in the operation range. Finally, an advanced economic oriented nonlinear model predictive control is implemented and compared to the optimal control solution and a PI controller strategy, showing savings in the economic performance of the process while facing a disturbance in the molar composition in the butenes feed stream.

Resumen

La intensificación de procesos tiene como objetivo incrementar el rendimiento en los procesos químicos. Un ejemplo de esto es la destilación catalítica, donde la reacción química y la separación líquido vapor son integradas en un único equipo de proceso. Este sistema se caracteriza por la alta no-linealidad de los modelos matemáticos que lo describen y por ser una unidad crítica de todo el proceso. La integración de diseño y control de este sistema se ha llevado a cabo en este trabajo. Modelos de estado estable y dinámicos basados en principios fundamentales para este equipo han sido propuestos y resueltos en el marco de problemas de diseño y control óptimo. Se ha propuesto una metodología para determinar los parámetros de peso de funciones de seguimiento y económica incluidas en la función objetivo del problema de control óptimo. Una columna de destilación catalítica diseñada para la producción de Etíl tert-butíl éter fue seleccionada como caso de estudio. El problema de diseño óptimo propuesto en este trabajo tuvo varias consideraciones que otros autores que cubrieron el mismo tema despreciaron, y cuya respuesta demostró la necesidad de implementar el modelo detallado. El problema de diseño y control óptimo se ha solucionado de manera secuencial y simultánea al enfrentar al sistema a una perturbación en la composición de la corriente de alimentación, y la manera simultánea ha probado obtener la solución que satisface las restricciones operacionales del sistema al contrario de la aproximación secuencial. Varios modelos dinámicos basados en el índice del sistema de ecuaciones algebro-diferencial fueron propuestos y probados, demostrando su validez en el rango de operación del sistema. Finalmente, se ha implementado un control avanzado predictivo no lineal orientado económicamente, el cual ha sido comparado con la solución de control óptimo y con un sistema de controladores PI, mostrando ahorros en el rendimiento económico mientras enfrentaba una perturbación en la composición molar de alimentación de butenos.

1. Introduction

Most of the chemical processes include two of the most important operations, chemical reaction and thermodynamic separation. These two operations are used to be carried out in different equipment. The reactions take place in different equipment, called reactors (continuously stirred tank reactors -CSTR-, tubular reactors or batch reactors, among others), and are operated under different conditions. On the other hand, the separation is usually made by different unitary operations (distillation, extractions, crystallization, absorption, among others) being the distillation by far the most common one [1]. Distillation is the most popular liquid mixture separation technique in the chemical and in the oil industry. The energy requirement of this operation can represent up to 40% of the whole plant's energy requirement [2], [3].

Recycle streams are used between the reaction and separation sections to increase the yield and conversion, minimize the undesired products synthesis, improve the energetic efficiency and guarantee the controllability of these processes. Instead of carrying the reaction and separation in independent units, these operations can be carried out in a single equipment [1]. The implementation of these combined processes represents one of the most promising methodologies of process intensification. Economic and environmental considerations have led the industry to develop this kind of processes [4], which offer considerable benefits compared to the traditional multi-unit scheme.

Integrating reaction and product purification in a single multifunctional unit leads to considerable improvements compared to the traditional sequential approach such as: overcoming of the chemical equilibrium limitations, increment in product selectivity and the use of the reaction heat for the separation [5]. A limitation of this integration is that the "operational window" is reduced considerably as the conditions of the reaction and the separation must be satisfied simultaneously [1]. The general concept this process intensification is referred as Reactive Distillation (RD) and when a heterogeneous catalyst is involved it is referred as Catalytic Distillation (CD).

The operation of the distillation with a chemical reaction is important in the process, becoming into a critical unit and in certain cases a limiting unit, therefore its stable behavior must be guaranteed. This unit is very sensitive to perturbations, which means that a change in the operational conditions may affect the process dynamics compromising significantly the steady state operation, affecting the product purity, the energy consumption or the produced quantity [6].

Traditionally, the design of a process has been made in a sequential manner. First, a stationary analysis determines the process design and then a dynamic analysis determines its control law. Ziegler and Nichols [7] identified a direct relationship between the design of a process and its dynamic response under uncertainty, which compels to consider the process controllability in the first stages of the design [8], [9]. From this fact, the optimal control arises as a field where mathematical optimization tools are used to find the optimal profiles of operational variables for a certain process guaranteeing the product quality and the process profitability and security facing a periodic change or a perturbation to the system. Coupling the optimal design and optimal control results in a process that maximizes its profitability, assuring the specifications of its product even when the system is subjected to dynamic disturbances.

Taking into account these facts, the optimal design and control of a CD column becomes important. This kind of problems have a considerable mathematical complexity because of the interactions that exist between the coupled processes of separation and reaction. The modeling of these phenomena is highly nonlinear, which generates complications while solving it and the possibility of multiple solutions [10]. The stationary model for this system is presented in the section 4.1. The mathematical complexity of this type of problems is mainly that the set of equations that describe the dynamic behavior of the system is a differential algebraic system of equations (DAE), which requires certain mathematical reformulations for solving it. The DAE problems are reformulated into large-scale NonLinear Programming (NLP) problems using orthogonal collocation. The state of the art regarding the CD process and its dynamic optimization applications is presented in the section 3.

The optimal design and control of a CD column designed for the production of Ethyl *tert*-butyl ether (ETBE) has been proposed as the case study of this work. The ETBE is a chemical compound used as oxygenate for fuels and it is classified as semi-renewable, as it can be synthetized from the etherification of bioethanol and isobutene in the presence of an acid catalyst [11]. This case study is presented in depth in section 5. The optimal control problem had included tracking objectives and an economic objective, for instance a weighted sum of the objectives was used as objective function. A methodology for determining the weighting parameters of each objective was proposed, based on an offline multi-objective utopia tracking optimization [12].

A comparison is made between the sequential and the simultaneous approach in the optimal design and control for this equipment. The results show that both approaches result in different design parameters that affect the economic profit of the process, its controllability and the satisfaction of the operational constraints of the system. The different optimization problems solved in this work are presented in the section 6.

Several formulations of the dynamic model were proposed based on the description level and the assumptions that support them and resulted in different index DAE problems. This models were compared in terms of resulting NLP problem size (e.g. number of equations and variables) and results by solving an Optimal Control Problem (OCP). The different formulations of the dynamic problem represented with different DAE problems can be found in the section 4.2. Finally, a first approach to an advanced control strategy called Economic-Oriented Nonlinear Model Predictive Control (EO-NMPC) was implemented and compared to a PI (Proportional and Integral) controller, showing advantages of the EO-NMPC in terms of economic profit. The results from the optimization problems presented in this work are presented in the section 7, and the conclusions and future perspectives based on this work are shown in the section 8.

2. Objectives

2.1. General objectives

Implement an optimal design and control strategy for a catalytic distillation column for the ETBE production.

2.2. Specific Objectives

- Propose a rigorous stationary and dynamic model for a catalytic distillation column.
- Simulate the dynamic behavior of the catalytic distillation column.
- Obtain the solution of an optimal control problem for a catalytic distillation column.
- Propose an optimization strategy for the economic oriented optimal control of a catalytic distillation column.
- Include into the optimal control problem design parameters of the catalytic distillation column.

3. State of the art

Among the aspects that will be discussed in the state of the art of this project, it is worthy to make a classification of the different topics handled. In first place, a state of the art of catalytic distillation will be shown and the development of this topic through the years. Then the state of the art of dynamic optimization and optimal control of distillation systems will be explored.

3.1. Catalytic distillation

The combination of the reaction and thermodynamic separation phenomena in a single operation goes back to the decade of 1860 with the Solvay process for ammonia recovery [13]. In the decade of 1980 this kind of operations generated a great interest due to the massive demand of Methyl *tert*-butyl ether (MTBE) as fuel oxygenate. A significant achievement of reactive distillation was the innovation by Eastman Kodak where a whole production plant (reactions and purification) of Methyl acetate was condensed in a single unit of reactive distillation. This change reduced the total number of equipments from 11 to a single one capable of producing virtually pure products reducing considerably the investment and operational costs. A diagram of this process is presented in the Figure 1.

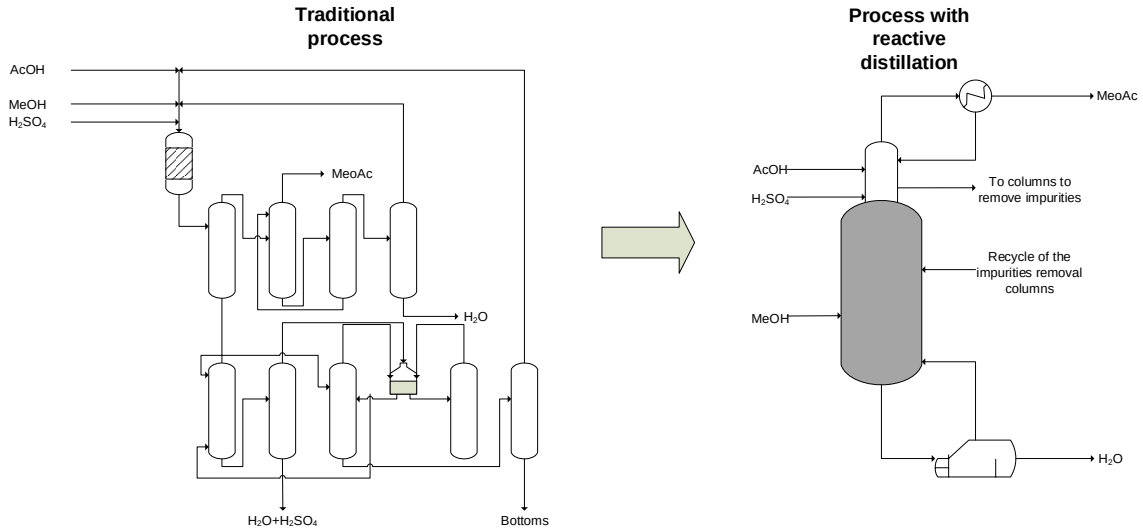

Figure 1. Traditional and reactive distillation processes for Methyl acetate production [5]

Since the implementation of this process, an explosion of scientific developments focused on RD and CD started. This fact can be observed in the increase of patents and articles number related with this topic, as seen in Figure 2.

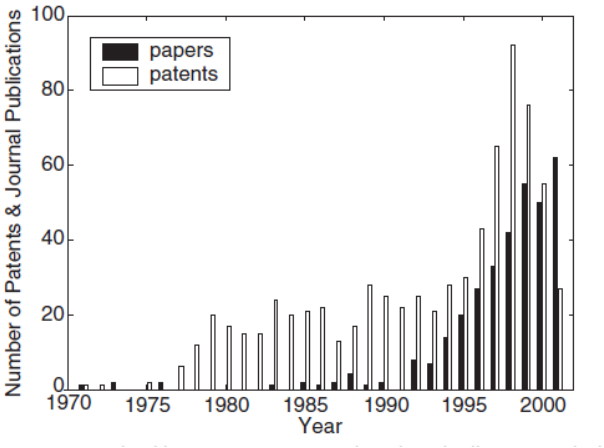

Figure 2. Patents and papers in indexed journals regarding reactive and catalytic distillation in the last decades [13]

Once explored the advantages of this operation, the applications in industry have diversified to esterifications, etherifications, hydrogenations, alkylation and hydrations, among others. All of these reactions are limited by chemical equilibrium, and due to the separation this limitation can be overcome, achieving high selectivities toward the desired product. Another advantage is that reactive separation can surpass the limitations given by the presence of azeotropes. Avoiding these limitations allows a reduction in operating costs and energetic integration. Table 1 presents a brief summary of the industrial applications for etherification reactions carried out by reactive and catalytic distillation. Table 1 only includes etherification since this is the reaction type of the case study. Other types of reactions examples carried out in the industry by reactive distillation like esterification, nitration, amination, amidation, hydrogenation, alkylation, hydration, among others can be found in the literature [5].

Table 1. Industrially important etherification reactions, either implemented on a commercial scale or investigated on laboratory scale, using reactive or catalytic distillation [13]

Reaction	Catalyst / column internals	Remarks on motives and achievements	References
methanol+isobutene ↔ methyl *tert*-butyl-ether (MTBE)	Amberlyst-15	to enhance the conversion of isobutene and achieve separation of isobutene from C_4 stream	[14], [15]
methanol+isoamylene ↔ *tert* amyl methyl ether (TAME)	ion-exchange resin	to enhance the conversion of isoamylene	[16], [17]
ethanol/bioethanol+isobutene ↔ ethyl *tert*-butyl-ether (ETBE)	Amberlyst-15 pellets, structured Amberlyst-15	to effectively utilize bioethanol and surpass equilibrium conversion	[18], [19]
isopropanol+propylene ↔ diisopropyl ether (DIPE)	ZSM 12, Amberlyst-36, Zeolite	a two stage process that uses water and propylene as feed	[20]
2-methyl-1-butane+ethanol ↔ *tert* amyl ethyl ether (TEEE)	Amberlist 16W, Amberlist 15W	to surpass the equilibrium limitations of the reaction	[21]

The *Clear Air Act* was a federal law in the United States of America which promoted the production of oxygenating ethers for fuels such as MTBE, ETBE and TAME [22] in the decade of 1970. The MTBE was the first kind of oxygenating ether produced in large scale for this purpose, thanks to its properties, which include an the increase in the gasoline octane number, an increase in the tolerance to water of the fuels and its high caloric value compared to other additives such as methanol and ethanol [13]. These facts made the MTBE the oxygenate with the fastest industrial development. The synthesis of this compound is performed by reactive distillation achieving conversions up to the 99% [1]. This operation replaced the traditional process of production which had equilibrium limited conversions between 90-95% and that produced a mixture difficult to separate due to the azeotropes generated between the MTBE and its reagents (isobutene and methanol).

In the first decade of the 2000's, several states of the USA (including California and New York) prohibited the MTBE as additive under environmental and health arguments [23]. Due to its high solubility in water, MTBE was detected in surface and ground water and land leading to losses of up to 30 billion dollars in remediation [24]. Because of the prohibition of MTBE and the increasing environmental concern, the ETBE emerges as an ideal substitute because of its physical and chemical properties and the fact that it can be synthetized from biological origin ethanol (organic material fermentation) making it semi-renewable [11].

3.2. Dynamic Optimization for distillation columns

A big leap was made in the field of dynamic chemical processes optimization because of the increasing development of dynamic simulation for large scale chemical processes[25]. The dynamic modeling of chemical processes results in a system of differential and algebraic equations (DAE). The optimal control is an example of dynamic optimization, which is one of the problems aimed to be solved in this work.

The control of a process varies its operational conditions, and not the variables involved in its design. The design variables are changed during a previous design phase of the process. The objective af the optimal control problem is to minimize or maximize certain performance indicator by satisfying the process dynamics and other operational constraints. The applications of the OCP include the startup, shut-down and set-point change in the operation of a process. Another application is to submit the process to a perturbation in the inlet conditions and find the profiles of the manipulated variables that are able to satisfy the imposed constraints. Simultaneously, this procedure can be performed while minimizing or maximizing an economic objective function, allowing the process to accomplish a dynamic behavior that results in the optimal economic profit.

Specifically, the optimal control problems (OCP) can be summarized in the following equations.

$$\min J = \mathcal{F}(t_f) + \int_{t_0}^{t_f} f(y(t), z(t), u(t), p(t))dt \tag{1.a}$$

$$\text{s.t.} \frac{dy}{dt} = f(y(t), z(t), u(t), p(t)), \tag{1.b}$$

$$y(t_0) = y_0 \tag{1.c}$$

$$h\big(y(t), z(t), u(t), p(t)\big) = 0 \tag{1.d}$$

$$g\big(y(t), z(t), u(t), p(t)\big) \leq 0 \tag{1.e}$$

Here y is the vector of differential variables, z the vector of algebraic variables and u the vector of the manipulated variables. In the case of a distillation column, the differential variables include the mass and energy holdups, the algebraic variables include the vapor and liquid flows and the control variables can be the reboiler duty and the reflux ratio. p represents the problem parameters, which for this problem can be the feed composition or the physical parameters of the components. The objective function J is the sum of two function, $\mathcal{F}$ and the time integral of $\oint$, which represent a terminal cost and the moving cost respectively. The terminal cost is only a function of the states at the final time t_f, while the moving cost considers the trajectory of the state and manipulated variables. Finally, y_0 represents the vector of initial conditions for the differential variables.

Because of the complexity of the problem states in Eq. 1, most cases do not count with an analytical solution, so there is a need of numerical methods as solving tool. In order to make clear the problem intended to be solved, the following section includes a brief introduction to the DAE problems and the Appendix B - OCP representation as NLP problem and solution algorithms illustrates some solving methods for dynamic optimization.

3.2.1. Differential Algebraic Equation (DAE) problems

The dynamic chemical process models based on fundamental principles are represented by sets of algebraic and differential equations (DAE). The algebraic equations represent the thermodynamic equilibrium or hydraulic constraints, and the differential constraints represent the mass, momentum and energy balances. The algebraic equations may also arise when model simplifications are made. For example, when the time-scale of the variables are different; some of them change rapidly and others very slowly in comparison.

The Hessenberg form of DAE systems is the one that will be used through this work. This is done since it is the most suitable representation for chemical processes, where the algebraic equations arise from the physical constraints of the problem. The semi-explicit DAE system is composed by a set of algebraic equations that represent the equality constraints. (2, 3) [26], [27].

$$\frac{dy}{dt} - f(y(t), z(t), u(t), p) = 0 \tag{2}$$

$$g(y(t), z(t), u(t), p) = 0 \tag{3}$$

There is no unified definition about the index of a DAE problem, but it is more difficult to solve when its index is higher. The different definitions of index include the differential index, the perturbation index and the traceability index. For large scale nonlinear problems the differential index of the DAE is the index definition that fits them the most, which is defined as

> "*The index is the integer s that represents the minimum number of differentiations of the DAE system required to represent an ODE or the variables $z(t)$ and $y(t)$*" [25].

The DAE problems that are index 0 are equivalent to ODE systems. The index one DAE-problems can be solved by discretization where, in each time step, an integration forward in time is made such that the algebraic equations of the model are solved. With the higher index models (≥2) this strategy cannot be used, since not all of the algebraic variables have a representation in the algebraic equations, which is the same as saying that the subsystem of algebraic equations is singular.

Among the several alternatives to solve a high index DAE problem, the order reductions technique is included. A disadvantage of this method is that, even though it allows solving the numeric integration problems, the size of the model is considerably increased due to the amount of new derivatives to be calculated. Because of the higher amount of new variables in this reformulated problem, it is expected to have higher computational times. On the other side, the direct solution is the equivalent to that of the reduced models if the consistent initial conditions are satisfied (e.g. solution of the stationary problem) for the high index DAE problems[25]. For distillation cases, the direct solution of the index 2 DAE is computationally more efficient that the solution of the equivalent index reduced DAE [28].

3.2.2. Optimal control cases for distillation columns

Although the optimal control theory started back in the 1960s decade [29], its first application into a distillation column was done by Pike et al. [30] in 1974. Due to the computational limitations of the time, this work simplified the mathematical model significantly. Nevertheless if was able to prove the reduction in operational costs.

From that moment on, with the development of increasingly powerful computers, the optimal control of distillation columns was made with more complex and rigorous models. A summary of the results in optimal control regarding distillation columns in the last years can be seen In the Table 2

Table 2. State of the art summary for optimal control in distillation columns

Author	Year	Problem	Mathematical programming field	Distillation type	Programming environment
Pike et al. [30]	1974	First study on the optimal control of distillation columns.	LP	Conventional	Does not report
Mohideen et al. [31]	1996	Comparison of the sequential and simultaneous design and control for distillation.	MIDO	Conventional	GAMS
Kim. [32]	1999	Optimal design and operation of a batch distillation column.	NLP	Batch	Does not report
Ross et al. [6]	1999	Sequential optimal control and design of a water, propanol and isopropanol distillation.	NLP	Conventional	gPROMS
Bansal et al. [33]	2000	Optimal control of a methanol-water distillation.	MIDO	Conventional	gPROMS/gOPT
Biegler et al. [34]	2002	Summary of the computational and mathematical methods for optimal control in distillation.	NLP	Conventional	AMPL
Bansal et al.	2002	Optimal control and design in a	MIDO	Conventional	GAMS/gPROMS

[35]		benzene-toluene distillation.			
Geogiadis et al. [36]	2002	Comparison of sequential and simultaneous optimal design and control (ODCP) in reactive distillation.	MIDO	Reactive	gPROMS
Low et al. [37]	2004	Application of genetic algorithms for a batch distillation optimal control.	MIDO	Batch	gPROMS
Raghunathan et al. [38]	2004	Dynamic optimization of a batch distillation column using rigorous models.	MPEC	Batch	AMPL
Panjwani et al. [39]	2005	Comparison in economic terms of the sequential and simultaneous design and control of a reactive distillation.	MIDO	Reactive	GAMS/gPROMS
Woinaroschy [40]	2008	*Strat-up* methodology proposal for distillation columns.	NLP	Conventional	Does not report
Miranda et al. [41]	2008	Optimal design and control (ODCP) of a CD column.	NLP	Catalytic	FORTRAN
López-Negrete et al. [9]	2009	Simultaneous optimal control and feed position for distillation.	MIDO	Conventional	GAMS
Damartziz et al. [42]	2009	Dynamic non equilibrium model (NEQ) for reactive distillation column.	NLP	Reactive	Does not report
Simon et al. [43]	2009	Choice of the physical equipment and optimal control of batch distillation column.	NLP	Batch	MATLAB
Moghadam et al. [44]	2012	Optimal control of a CD column through a linear quadratic (LQ) regulation.	LQ	Catalytic	Does not report
Ramos. et al [45]	2013	Optimal control of an extractive distillation column.	NLP	Extractive	GAMS

In order to make the novelty of this work clear the works of Miranda et al. [41] and Moghadam et al. [44] will be further explained. This is done because of the similarity with this work topic.

Miranda et al. [41] made an optimization (design and control) of a CD column for ETBE production. The Pontryagin's maximum principle was applied in this work to declare the optimality of the OCP solution. In this manner, they reduced the problem in order to be solved with integration techniques for ODEs. In this case they used a complete discretization and they proceeded with a NonLinear Programming (NLP) solution method. The problem was implemented in FORTRAN and solved using a Sequential Quadratic Programming (SQP) algorithm with the Newton-Raphson method. Control and economic objective functions were used.

Moghadam et al. [44] developed a linear quadratic (LQ) regulator for CD producing dimethyl ether (DME). A LQ regulator is a closed loop controller similar to a Model Predictive Control (MPC) with just one horizon of prediction. The linear model is obtained by linearization. The model used was a set of

differential hyperbolic and algebraic equations. Through an approximation of the equation of the Ricatti operator they can solve the OCP and implement a control system using a scheme of proportional integral (PI) controllers.

In first place, there are significant differences between the approximation to the problem made by Moghadam et al. [44] and the one proposed in this work. The set of differential hyperbolic equations used by these authors use all the terms as dimensionless quantities. This results in an advantage when trying to scale the process, but results unappropriated when trying to describe the state of the system as it intended in this project. In second place, the optimal control found by this work is based on linear and quadratic (LQ) approximations which are based in linearizations of the nonlinear variables close to the steady state of the process. This moves away from one of the objectives of this project, which seeks the resolution of the optimal control of the CD problem using equations based in fundamental principles.

The work by Miranda et al. [41] solves the OCP of the ETBE production CD process using a SQP algorithm implemented in FORTRAN. The algorithms discussed in the Appendix B - OCP representation as NLP problem and solution algorithms of this work are the ones that are going to be used to solve this problem, all implemented in GAMS: these algorithms have shown a better handling of large-scale NLP problems (as the dynamic analysis of a CD column is). The work of Miranda et al. [41] makes several simplifications of the fundamental equations model (e.g. no pressure drop across the column) in order to solve the design and optimal control problem. This sort of assumptions is going to be avoided in this work. The tray capacity constraints analyzed by this work were not taken into account by Miranda et al. Finally this work presents an advanced control strategy such as the Economic Oriented Nonlinear Model Predictive Control (EO.NMPC) apart of the solution of the sequential and the simultaneous ODCP problem solved by Miranda et al. [41].

3.2.3. Economic Oriented Non Linear Model Predictive Control

Since the first stages of development and implementation of the automatic control, the relationship between the operational considerations and the economic performance of the processes has been a topic of research [46]–[48]. Traditionally, both problems have been approached sequentially through a two-level structure, first the steady-state optimization and then the feedback control strategy [47].

The first level of this structure, also named Real-Time Optimization (RTO) and developed in the 1980's [46], seeks to establish business decisions and production schedules in real time based on a detailed steady-state model of the plant, intending to optimize the economic benefits in short time periods. The operational conditions (set-points) are implemented in the second level of the structure. The plant model parameters are constantly updated allowing it to withstand disturbances and reducing their long-term effects [48].

This two-level structure shows problems in its implementation, caused mainly by the difference of the time scales managed by both levels [48]. The RTO skips the dynamic behavior of the processes, generating inconsistent and hardly achievable *set-points* for the feedback control strategy.

The second level corresponds to the feedback control strategy, whose aim is to reach the production's goals estimated by the RTO and to ensure the stability of the process [46]. Traditionally for this level of

the structure the PID (Proportional, Integral and Derivative) controllers have been used, but these have been gradually replaced due to their tuning difficulties and poor capability of handling multivariate systems [48]. Since the 1970's, an interest in the implementation of advanced feedback control strategies such as Model Predictive Control (MPC)[49] has grown. This control strategy solves an OCP at certain periods of time, and uses a detailed model in order to predict the future behavior of the system as seen in the Figure 3. Among the several advantages of the MPC strategy, the most remarkable are: its capability to handle systems with multiple inputs and multiple outputs (MIMO) [50] and to handle constraints. Its implementation does not require wide knowledge of control theory and its tuning is relatively intuitive [49].

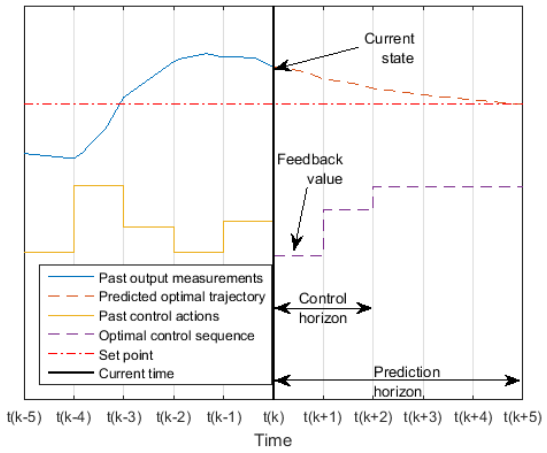

Figure 3. Illustration of the Model Predictive Control in the k^{th} time

The MPC strategy has been used in the process industry, but its implementations have normally used linear models that represent the non-linear systems with small disturbances from its operation point [28]. This implementations simplify the OCP, guaranteeing a global optimum and a faster convergence, but sacrificing the reliability of the model. In order to avoid such problems, nonlinear models can be implemented in MPC strategies (Non Linear Model Predictive Control NMPC) to make the prediction of the dynamic behavior closer to the real system's behavior, but increasing the complexity of the problem to solve. The tradeoff between the MPC and the NMPC is to have a very fast but inaccurate solution, or a solution that requires more solving time but is more precise.

The integration of the two levels of the implementation of process automatic control can be solved by proposing a simultaneous control structure that includes the dynamic behavior of the system and an economic objective. This is called the Economically-Oriented NMPC (EO-NMPC) [51]. This structure is based on the solution of a nonlinear OCP over the prediction time horizon that allows to establish the adequate behavior of the manipulated variables, maximizing the process profits and penalizing the deviations of the process' and product's specifications.

Several authors have defined these Nonlinear models as simplifications or empirical models in order to relieve the computational load of solving the OCP problems [52]–[54], since if the solution time of the OCP is greater than the sampling time, time delays and even instabilities can be introduced into the process. Due to these approximations, the predictions are limited to certain regions; therefore a model based on fundamental principles is proposed in this work. This sort of models can predict the behavior

of the system over all the operation conditions by implementing all the phenomenological equations that describe the system (e.g. material and energy balances, thermodynamic relations) in a large scale DAE system. The treatment to solve these kind of problems is described in the Appendix B - OCP representation as NLP problem and solution algorithms.

4. Catalytic distillation column model

This section presents the different models for the CD columns. The first part of this section presents the stationary model, while the second one presents the dynamic model. The dynamic models, based on the detail of the system description and the assumptions made to propose them result in different DAE index models; presented in this section.

The models used during this work rely on the fact that the catalytic distillation columns has separation and reactive stages in cross flow sieve trays. The separation and reactive stages will be considered as equilibrium stages, indexed by the letter n starting by the top of the column, being the condenser the equilibrium stage 1 and the reboiler the equilibrium stage NT. The components are indexed by the letter i up to the total amount of components by NC. Component molar balances (with or without the chemical reaction), phase equilibrium, summation equations, heat balances and hydraulic relationships for each stage are solved (MESH model) to determine composition, temperature, and flow profiles.

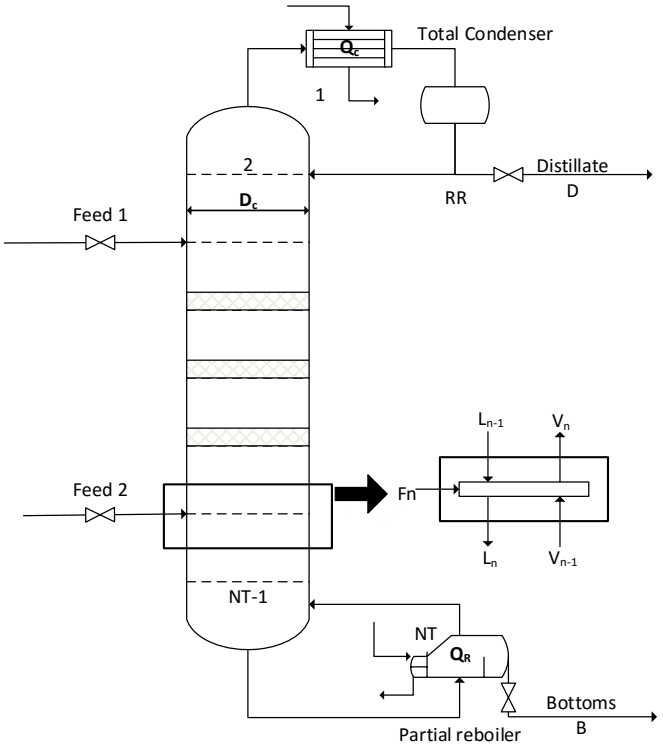

Figure 4. Sketch of a catalytic distillation column with 2 feeds

Some assumptions have been made in order to build the models described below.

- Thermodynamic equilibrium in each stage.
- Adiabatic operation.
- Total condenser and partial reboiler.
- No pressure drop at the reboiler.
- Constant mass accumulation in the condenser and the reboiler just in the liquid phase.

Some sets can be defined to make the formulation of the model more concrete.

Set definitions

$$C = \{1, \dots, NC\} \tag{4.a}$$

$$N = \{1, \dots, NT\} \tag{4.b}$$

$$Cond = 1 \subseteq N \tag{4.c}$$

$$Reb = NT \subseteq N \tag{4.d}$$

$$Cat \subseteq N \tag{4.e}$$

$$Sep = N \setminus Cond \setminus Reb \setminus Cat \tag{4.f}$$

where C is the Set of components, indexed in i; N is the Set of equilibrium stages, indexed in n; $Cond$ represents the condenser, Reb the reboiler, Cat the stages with catalyst and Sep the Separation cross flow tray stages.

Applying these assumptions and using the sets defined in Eq. 4, two different models arise, a steady-state model and a dynamic model.

4.1. Steady-state model

The following model is based on the stationary behavior of a CD column with a single reaction. This model will be used for the optimal design of the distillation column.

Total mole balance

$$V_{n+1} = L_n \left(1 + \frac{1}{RR}\right), \forall n \in Cond \tag{5.a}$$

$$F_n + L_{n-1} + V_{n+1} = L_n + V_n, \forall n \in Sep \tag{5.b}$$

$$F_n + L_{n-1} + V_{n+1} = L_n + V_n - m_{cat,n} \mathcal{R}_n \sum_{i \in C} \nu_i, \forall n \in Cat \tag{5.c}$$

$$L_{n-1} = L_n + V_n, \forall n \in Reb \tag{5.d}$$

where the vapor and liquid flows from the stage n are represented by V_n and L_n respectively, F_n is the feed flow to the stage n, RR is the molar reflux ratio, $m_{cat,n}$ is the catalyst mass in the stage n, $\mathcal{R}_n$ is the reaction rate and υ_i is the stoichiometric coefficient of component i in the reaction.

Partial mole balance

$$y_{n+1,i} = x_{n,i}, \forall i \in C, \forall n \in Cond \tag{6.a}$$

$$F_n z_{n,i} + L_{n-1} x_{n-1,i} + V_{n+1} y_{n+1,i} = L_n x_{n,i} + V_n y_{n,i}, \forall i \in C, \forall n \in Sep \quad (6.b)$$

$$F_n z_{n,i} + L_{n-1} x_{n-1,i} + V_{n+1} y_{n+1,i} = L_n x_{n,i} + V_n y_{n,i} - m_{cat,n} \mathcal{R}_n \nu_i, \forall i \in C, \forall n \in Cat \quad (6.c)$$

$$L_{n-1} x_{n-1,i} = L_n x_{n,i} + V_n y_{n,i}, \forall i \in C, \forall n \in Reb \quad (6.d)$$

where $x_{n,i}$ and $y_{n,i}$ represent the molar composition of component i in the equilibrium stage n in the liquid and vapor phases respectively, and $z_{n,i}$ is the molar composition of component i in the feed stream of stage n.

Energy balance

$$V_{n+1} H_{V,n+1} = L_n \left(1 + \frac{1}{RR}\right) H_{L,n} + Q_{Cond}, \forall n \in Cond \quad (7.a)$$

$$F_n H_{F,n} + L_{n-1} H_{L,n-1} + V_{n+1} H_{V,n+1} = L_n H_{L,n} + V_n H_{V,n}, \forall n \in Sep \cup Cat \quad (7.b)$$

$$Q_{Reb} + L_{n-1} H_{L,n-1} = L_n H_{L,n} + V_n H_{V,n}, \forall n \in Reb \quad (7.d)$$

where $H_{L,n}$ and $H_{V,n}$ represent the molar enthalpy in the equilibrium stage n of the liquid and vapor phases respectively, $H_{F,n}$ is the molar enthalpy of the feed stream of stage n, and Q_R and Q_C are the heat duties of reboiler and condenser respectively. It is worth to be noted that the reaction does not add any term to the energy balance since the reference status of the enthalpies is 298K, which makes the reaction heat equal to the difference of the formation enthalpy of the components [18].

Thermodynamic equilibrium

$$y_{n,i} = K_{n,i} x_{n,i}, i \in C, \forall n \in N \quad (8)$$

where $K_{n,i}$ is the equilibrium constant of component i in stage n. The equilibrium constant is given by the ratio of the vapor and liquid composition of a component in an equilibrium stage. According to the vapor and liquid equilibrium assumed, three different systems can arise: ideal system, ideal vapor system and real system. Because of its completeness, the definition of the equilibrium constant will be calculated using the real system which uses correction of non-ideality for the vapor and liquid phase as follows in the so called gamma-phi formulation.

$$K_{n,i} = \frac{P_i^{sat} \gamma_{n,i}}{P_n \varphi_{n,i}}, i \in C, \forall n \in N \quad (9)$$

where $\varphi_{n,i}$ is the fugacity coefficient of component i in stage n and describes the non-ideality in the vapor phase, $\gamma_{n,i}$ is the activity coefficient of component i in stage n and describes the non-ideality in the liquid phase, P_i^{sat} is the saturation pressure of component i in stage n, and P_n is the pressure at stage n.

Summation equations

$$\sum_{i \in C} \left(y_{n,i} - x_{n,i}\right) = 0, n \in N \quad (10)$$

These equations are included to satisfy that the sum of the compositions is equal to one in both vapor and liquid phase. Since the total mass balance is included in the equations, there is no need to include the two equations that force each phase's composition to sum to one.

Pressure behavior

$$P_n = P_{n-1} + \Delta P_n, \forall n \in N \tag{11.a}$$

$$\Delta P_n = f(D_C, L_n, V_n), \forall n \in N \tag{11.b}$$

The definition of the pressure drop of each stage ΔP_n is given by empiric relationships that depend on the design parameters of the distillation column (e.g. the column diameter), the physical properties of the mixture at the stage (e.g. the liquid and vapor densities) and the flows at that stage. The whole relationships can be found in the Section A.5. Hydraulic correlations.

All the physical properties were calculated using correlations found in the literature and are further explained in the Appendix A – Mathematical models.

4.2. Dynamic models

Based on the the MESH equations, a dynamic model for the CD column is proposed. Based on the detail of the equations describing the system, specifically regarding the vapor holdup, the Hessenberg index of the resulting model is 1 or 2. Index 2 models can be solved using the strategies described in the Section 3.2.1, but the mathematical properties of those problems, such as consistent initial conditions, can cause numerical instabilities. The DAE1 and DAE2 problems will be explained and also a reduced version of the DAE2 problem, called the DAE2r problem.

The last part of this section explains a hybrid model between the DAE2 and the DAE2r models called in this document DAE2h. This model uses the solution of the DAE2r model at the beginning of every finite element, while solving the DAE2 model for the collocation points inside of it.

4.2.1. Detailed differential algebraic model (DAE1)

This detailed model of the CD column is a DAE system of index 1. This model includes the vapor holdup for every stage, as defines in this section.

Total mole balance

$$\frac{dM_n}{dt} = V_{n+1} - L_n\left(1 + \frac{1}{RR}\right) = 0, \forall n \in Cond \tag{12.a}$$

$$\frac{dM_n}{dt} = F_n + L_{n-1} + V_{n+1} - L_n - V_n, \forall n \in Sep \tag{23.b}$$

$$\frac{dM_n}{dt} = F_n + L_{n-1} + V_{n+1} - L_n - V_n + m_{cat,n}\mathcal{R}_n \sum_{i \in C} \nu_i, \forall n \in Cat \tag{23.c}$$

$$\frac{dM_n}{dt} = L_{n-1} - L_n - V_n = 0, \forall n \in Reb \tag{23.d}$$

where M_n is the total mass holdup of the stage n and t is the time.

Partial mole balance

$$\frac{dM_{n,i}}{dt} = V_{n+1}y_{n+1,i} - L_n x_{n,i}\left(1 + \frac{1}{RR}\right), \forall i \in C, \forall n \in Cond \tag{13.a}$$

$$\frac{dM_{n,i}}{dt} = F_n z_{n,i} + L_{n-1}x_{n-1,i} + V_{n+1}y_{n+1,i} - L_n x_{n,i} - V_n y_{n,i}, \forall i \in C, \forall n \in Sep \quad (13.b)$$

$$\frac{dM_{n,i}}{dt} = F_n z_{n,i} + L_{n-1}x_{n-1,i} + V_{n+1}y_{n+1,i} - L_n x_{n,i} - V_n y_{n,i} + m_{cat,n}\mathcal{R}_n \nu_i, \forall i \in C, \forall n \in Cat \quad (13.c)$$

$$\frac{dM_{n,i}}{dt} = L_{n-1}x_{n-1,i} - L_n x_{n,i} - V_n y_{n,i}, \forall i \in C, \forall n \in Reb \quad (13.d)$$

where $M_{n,i}$ represents the molar partial holdup of component i in the equilibrium stage n.

Energy balance

$$\frac{dU_n}{dt} = V_{n+1}H_{V,n+1} - L_n\left(1 + \frac{1}{RR}\right)H_{L,n} - Q_{Cond}, \forall n \in Cond \quad (14.a)$$

$$\frac{dU_n}{dt} = F_n H_{F,n} + L_{n-1}H_{L,n-1} + V_{n+1}H_{V,n+1} - L_n H_{L,n} - V_n H_{V,n}, \forall n \in Sep + Cat \quad (14.b)$$

$$\frac{dU_n}{dt} = Q_{Reb} + L_{n-1}H_{L,n-1} - L_n H_{L,n} - V_n H_{V,n}, \forall n \in Reb \quad (14.c)$$

where U_n represents the internal energy holdup in the equilibrium stage n.

Total molar holdup

$$M_n = M_{L,n} + M_{V,n}, \forall n \in N \quad (15.a)$$

$$M_{V,n} = 0, \forall n \in Cond \cup Reb \quad (15.b)$$

where $M_{L,n}$ and $M_{V,n}$ represent the molar holdup in stage n of the liquid and vapor phase respectively. According to the assumptions stated afore, there is no vapor accumulation in condenser or reboiler.

Partial molar holdup

$$M_{n,i} = M_{L,n}x_{n,i} + M_{V,n}y_{n,i}, \forall n \in N \quad (16)$$

Thermodynamic equilibrium

$$y_{n,i} = K_{n,i}x_{n,i}, i \in C, \forall n \in N \quad (17)$$

Summation equations

$$\sum_{i \in C}\left(y_{n,i} - x_{n,i}\right) = 0, \forall n \in N \quad (18)$$

Internal energy

$$U_n \cong M_{V,n}\left(H_{V,n} - \frac{P_n}{\bar{\rho}_{V,n}}\right) + M_{L,n}H_{L,n}, \forall n \in N \quad (19)$$

where $\bar{\rho}_{V,n}$ is the molar density of the vapor phase in the stage n.

Stage capacity

$$\frac{M_{V,n}}{\bar{\rho}_{V,n}} + \frac{M_{L,n}}{\bar{\rho}_{L,n}} = \frac{\pi h_S {D_C}^2}{4}, \forall n \in N \quad (20)$$

where $\bar{\rho}_{L,n}$ is the molar density of the liquid phase in the stage n, h_s is the height of the stage and D_C is the column diameter.

Pressure behavior

$$P_n = P_{n-1} + \Delta P_n, \forall n \in N \tag{21.a}$$

$$\Delta P_n = f(D_C, L_n, V_n), \forall n \in N \tag{21.b}$$

As stated afore, the pressure drop is calculated through the hydraulic correlations in the A.5. Hydraulic correlations appendix. These correlations also influence the liquid and vapor flows across the column.

This model is an index 1 DAE, as stablished by Schulz [55]. This model has two degrees of freedom (e.g. the reboiler duty and the molar reflux ratio), which will be the control variables when solving the OCP.

4.2.2. Simplified differential algebraic model (DAE2)

In order to simplify the previous model, several assumptions can be made based on the physical behavior of the system. These assumptions have been used by several authors to reduce the complexity of dynamic distillation column models [27], [28].

- Vapor hold-up negligible with respect to the liquid hold-up ($M_{V,n} \approx 0;\ \forall n \in N$). The density of the liquid phase is much greater than the density of the vapor phase.
- The pressure does not vary with time. It helps the problem to be less rigid.

It is important to point out that, under these assumptions, this model has $NT(NC+3)$ less variables and equations than the previous one. The new model can be described by the following algebraic and differential equations.

Total mole balance

$$\frac{dM_{L,n}}{dt} = V_{n+1} - L_n\left(1 + \frac{1}{RR}\right) = 0, \forall n \in Cond \tag{22.a}$$

$$\frac{dM_{L,n}}{dt} = F_n + L_{n-1} + V_{n+1} - L_n - V_n, \forall n \in Sep \tag{22.b}$$

$$\frac{dM_{L,n}}{dt} = F_n + L_{n-1} + V_{n+1} - L_n - V_n + m_{cat,n}\mathcal{R}_n \sum_{i \in C} \nu_i\,, \forall n \in Cat \tag{22.c}$$

$$\frac{dM_{L,n}}{dt} = L_{n-1} - L_n - V_n = 0, \forall n \in Reb \tag{22.d}$$

Partial mole balance

$$M_{L,n}\frac{dx_{n,i}}{dt} = V_{n+1}y_{n+1,i} - L_n x_{n,i}\left(1 + \frac{1}{RR}\right), \forall i \in C, \forall n \in Cond \tag{23.a}$$

$$M_{L,n}\frac{dx_{n,i}}{dt} = F_n z_{n,i} + L_{n-1}x_{n-1,i} + V_{n+1}y_{n+1,i} - L_n x_{n,i} - V_n y_{n,i}, \forall i \in C, \forall n \in Sep \tag{23.b}$$

$$M_{L,n}\frac{dx_{n,i}}{dt} = F_n z_{n,i} + L_{n-1}x_{n-1,i} + V_{n+1}y_{n+1,i} - L_n x_{n,i} - V_n y_{n,i} + m_{cat,n}\mathcal{R}_n \nu_i, \forall i \in C, \forall n \in Cat \tag{23.c}$$

$$M_{L,n}\frac{dx_{n,i}}{dt} = L_{n-1}x_{n-1,i} - L_n x_{n,i} - V_n y_{n,i}, \forall i \in C, \forall n \in Reb \quad (23.d)$$

Internal energy hold-up

$$U_n = M_{L,n}H_{L,n}, \forall n \in N \quad (24)$$

The energy balance (Eq. 14), thermodynamic equilibrium (Eq. 17), and summation equation (Eq. 18) are not shown for this model since they are the same equations presented for the previous one. The main differences with respect to the previous model are:

- The mass hold-ups of each tray corresponds just to the liquid phase.
- The composition of the liquid in each tray is a differential variable instead of an algebraic variable.
- The algebraic equations of the vapor flow rate, the plate capacity, and the total and partial hold-ups are no longer needed.

In this case the model is an index two DAE because the vapor flow rate of each stage does not have an algebraic representation in the subset of algebraic equations. Thus the change of this variable with respect to time cannot be known directly when a method to solve index one problems is applied. Nevertheless, the number of equations and variables is reduced significantly; as a result, the simplified model can be easily solved in computational terms. The degrees of freedom are the same of the previous model.

As the index of this system of differential equations is 2, the main problem is to find a consistent initial conditions. High index (≥2) DAE systems have a singular subsystem of algebraic equations when an initial value is set for the differential variables. In case that a non-consistent initial point for the differential variables is set, the numerical solution of the system may present an impulse behavior before the integration of the differential equations, resulting in a displacement of the real solution [56].

4.2.3. Index reduction technique and simplified differential algebraic model (DAE2r)

In order to solve the index two model using solution strategies of index one problems, it is necessary to reduce the index of the system. In this case a technique of differentiation and substitution reported by [57] is used. This technique is described next.

The internal energy equation (Eq. 29) is differentiated and it is replaced in the energy balance equations (Eq. 14). The new equations for the algebraic energy and partial mole balance of each stage are:

$$M_{L,n}\frac{dH_{L,n}}{dt} + \frac{dM_{L,n}}{dt}H_{L,n} = V_{n+1}H_{V,n+1} - L_n\left(1+\frac{1}{RR}\right)H_{L,n} - Q_{Cond}, \forall n \in Cond \quad (25.a)$$

$$M_{L,n}\frac{dH_{L,n}}{dt} + \frac{dM_{L,n}}{dt}H_{L,n} = F_n H_{F,n} + L_{n-1}H_{L,n-1} + V_{n+1}H_{V,n+1} - L_n H_{L,n} - V_n H_{V,n}, \forall n \in Sep \cup Cat \quad (25.b)$$

$$M_{L,n}\frac{dH_{L,n}}{dt} + \frac{dM_{L,n}}{dt}H_{L,n} = Q_{Reb} + L_{n-1}H_{L,n-1} - L_n H_{L,n} - V_n H_{V,n}, \forall n \in Reb \quad (25.c)$$

$$M_{L,n}\frac{dx_{i,n}}{dt} = F_n\left(z_{n,i} - x_{n,i}\right) + L_{n-1}\left(x_{n-1,i} - x_{n,i}\right) + V_{n+1}\left(y_{n+1,i} - x_{n,i}\right) - V_n\left(y_{n,i} - x_{n,i}\right) + m_{cat,n}\mathcal{R}_n\left(\nu_i - x_{n,i}\sum_{i\in C}\nu_i\right), \forall i \in C, \forall n \in Reb \quad (25.d)$$

The term $\frac{dM_{L,n}}{dt}$ can be known from the total mass balance of each stage (Eq. 25) and the term $\frac{dH_{L,n}}{dt}$ can be calculated analytically using the chain rule to differentiate the expression of the liquid specific enthalpy. Also, the derivative of the temperature respect to time (Eq. 26) is needed and it can be calculated using the vapor liquid equilibrium expression.

$$\frac{dT_n}{dt} = \frac{-\frac{1}{P_n}\sum_{i\in C}\left[\frac{x_{i,n}P_{i,n}^{sat}}{\varphi_{n,i}}\sum_{j\in C}\frac{\partial\gamma_{i,n}\left(x_j,T\right)}{\partial x_{j,n}}\frac{dx_{j,n}}{dt}\right] - \sum_{i\in C}\left(K_{i,n}\frac{dx_{i,n}}{dt}\right)}{\frac{1}{P_n}\left(\sum_{i\in C}\frac{x_{i,n}P_{i,n}^{sat}}{\varphi_{n,i}}\frac{\partial\gamma_{i,n}\left(x_{j,n},T_n\right)}{\partial T_n} + \sum_{i\in C}\frac{x_{i,n}\gamma_{i,n}}{\varphi_{n,i}}\frac{dP_{i,n}^{sat}}{dT_n}\right)}, \forall n \in N \quad (26)$$

The equations used in this study to calculate thermodynamic properties (e.g. P_i^{sat}, γ_i) can be found in the appendix A.3. Condition dependent physical properties and their respective derivatives have been calculated in the appendix A.6. Index reduction model derivatives When the algebraic energy balance is used instead of the differential balances, the variation of the vapor flow rate of each stage can be known in each instant of time. This reduced the index of the problem by one.

The advantage of reducing the Hessenberg index of the DAE model to 1 is that the subsystem of algebraic equations is nonsingular, and therefore a set of consistent initial condition can be defined and an adequate solution of the DAE system is guaranteed.

4.2.4. Index Hybrid differential algebraic model (DAE2h)

The main inconvenience with the DAE2 model is that without a consistent set of initial conditions the hidden constraints of the algebraic variables not included in the algebraic subsystem are not satisfied and therefore the solution will be displaced from its true manifold [56]. A steady state solution of the system always guarantees a consistent initial point for these problems [58], but for process control under continuous disturbances this is not realistic, due to the time change of the system. As proposed by Lozano et al. [27], after applying the index reduction technique the DAE2 and the DAE2r models are equivalent, and the DAE2r model can be used to define consistent initial conditions for the DAE2 model.

This approach has been successfully used for the NMPC of separations processes [27], [28] and proved to have advantages compared to the other models presented before. It reduces the problem size after discretization since the derivatives from the order reduction are only calculated at the first point of integration and reduces the computational time. The fact of integrating an index 2 DAE requires a numerical method with considerable stability and low integral error properties to avoid propagation of error in the algebraic variables [27]. A collocation method with at least three internal points has proven to be acceptable in terms of accuracy for solving index 2 DAE systems [27], [28], [59].

5. Case study

The case study treated during this work is the synthesis of ethyl *tert*-butyl ether (ETBE). This chemical compound is an oxygenating ether for fuels used as an alternative to the methyl *tert*-butyl ether (MTBE). The synthesis process of this chemical compound is going to be modeled as a CD through the reaction between ethanol and isobutene over an acid catalyst.

The worldwide regulations about reduction of carbon monoxide emissions have encouraged the addition of oxygenates to the gasoline [22]. The high octane number of these oxygenates can also be used to eliminate the leaded octane enhancers, such as tetramethyllead (TML) and tetraethyllead (TEL), from the gasoline blends [60]. The MTBE and the ethanol have been the most widely used oxygenates. MTBE appears to be the best choice due to its physicochemical properties: high oxygen content, low Reid vapor pressure (RVP), high octane, high energy content, and low cost [60]. On the other side, ethanol has an advantage because it is an environmental friendly alternative to fossil fuels and it can be produced from biomass. Newer regulations have banned the MTBE as an oxygenate due to the potential contamination of water sources [23]. ETBE has emerged as a potential replacement of both these oxygenates. It is less hydrophilic than either MTBE or ethanol, therefore it is less likely to permeate and pollute groundwater supplies [60]. ETBE can be produced using bio-ethanol and in the past years new developments have been made to offer an economic viable fermentative production of isobutene [61], giving the ETBE an environmental friendly origin. ETBE has a lower volatility than MTBE, which means that volatile organic compounds (VOC) emissions are lessened [60]. ETBE has few disadvantages compared to MTBE, which include a lower oxygen content (and much lower than ethanol) requiring higher volumetric fractions for gasoline blends and its higher production cost, that is its principal disadvantage compared to the other oxygenates. This disadvantage could disappear if ETBE was produced via reactive or catalytic distillation technology making it a competitive alternative to MTBE [60].

Nowadays the ETBE is produced in the industrial level in catalytic cracking or dehydrogenation units [62]. In these cases, there are two constraints over the raw materials: in the first place the ethanol must be of high purity in order to avoid side reactions, and in the second place a mixture of butenes must be used, in which the isobutene is the reactive and the n-butene is inert in the reaction.

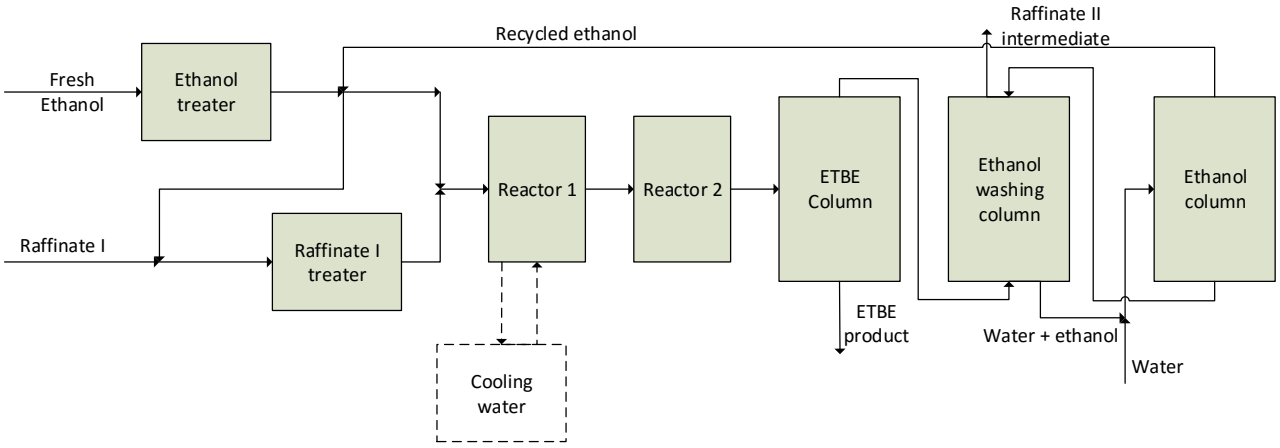

Figure 5. Block diagram of a conventional industrial ETBE production process [63]

The traditional production process of ETBE, shown in Figure 5, is composed of two reactors in series, and a separation section with two distillation columns and a liquid-liquid extraction column. The feed is initially purified in order to remove impurities capable of deactivating the catalyst in the reactors. This process is a potential candidate to apply CD. This process intensification may reduce considerably the amount of operations used and increase the conversion of the reactive, since the ETBE production reaction is limited by chemical equilibrium.

The synthesis of ETBE though CD has been studied and results of those studies [18], [62], [64], [65] have been promising. The case study was chosen then based of these studies' results.

The liquid phase reaction for the production of ETBE is carried out over an acid catalyst. It is a reversible and exothermic reaction (Eq. 27).

$$(CH_3)_2C = CH_2 + C_2H_5OH \rightleftharpoons (CH_3)_3COC_2H_5 \quad (27)$$

Additional side reactions may occur, like the dimerization of isobutene and the hydration of isobutene to isobutyric acid as seen in Eq. 28 and 29. It is possible to avoid these side reactions. The hydration of the isobutene is avoided by working in a anhydrous medium, and by using an excess in ethanol higher than 4%. This last condition avoids the dimerization by having the surface of the catalyst covered by ethanol [62].

$$(CH_3)_2C = CH_2 + (CH_3)_2C = CH_2 \rightleftharpoons [(CH_3)_2C = CH_2]_2 \quad (28)$$

$$(CH_3)_2C = CH_2 + H_2O \rightleftharpoons (CH_3)_3COH \quad (29)$$

The pseudo-homogeneous kinetics is based on the Langmiur, Hinshelwood, Hougen and Watson (LHHW) model. This model takes into account the kinetic factor, the driving force of the reaction and the adsorption over the catalyst. This mechanism assumes two active adsorption sites for the ethanol and one for the isobutene. Taking into account that the liquid is strongly non-ideal, the reaction rate is expressed in terms of the activity of the components γx instead of the molar composition [18]. The kinetic expression was obtained by Datta et al. [66] and described below.

$$\mathcal{R} = \frac{\kappa_{rate}(\gamma x)_{ETBE}^2 \left((\gamma x)_{IB} - \frac{(\gamma x)_{ETBE}}{\kappa_{Eq}(\gamma x)_{EtOH}}\right)}{(1 + \kappa_A(\gamma x)_{EtOH})^3} \tag{30}$$

where the reaction rate constants are given by the following expression.

$$\ln \kappa_{Eq} = 10.387 + \frac{4060.59}{T} - 2.89055 \ln T - 0.01915144(T) + 5.28586 * 10^{-5}(T)^2 - 5.32977 * 10^{-8}(T)^3 \tag{31}$$

$$\kappa_{rate} = 2.0606 * \exp\left(\frac{-60.4 * 10^3}{RT}\right) \tag{32}$$

$$\ln \kappa_A = -1.0707 + \frac{1323.1}{T} \tag{33}$$

where T is the temperature in Kelvins, and R is the ideal gas constant. The computation of this reaction rate has to be made in each reactive stage independently.

The reaction is carried on an Amberlyst 15 (A15) catalyst produced by Rohm and Haas®. This type of catalyst is a copolymer of styrene and divinylbenzene sulfone [67], with the physical characteristics listed in the Table 3.

Table 3. Physical properties of the A15 [67]

Property	Unit	Value
Surface area	[m^2/g]	53
Pore average size	[10^{-10} m]	300
Total pore volume	[ml/g]	0.40
Active sites concentration	[equivalents/kg]	4.8
Apparent density	[kg/m^3]	770

It should be noted that this catalyst is susceptible to be deactivated, in other words, the specific catalyst area and the number of active sites decrease with time due to the desulfonation [65].

The thermodynamic model used to describe the non-ideality of the liquid phase is the Non Random Two Liquid (NRTL) method. This model has been successfully used on other studies which covered strongly non-ideal liquid phase distillation systems for optimal control [28], and although the constants used for this model were not experimentally determined; they were adjusted from the vapor-liquid equilibrium data generated by the UNIFAC Dortmund, which is the model used by other authors to describe the non-ideality of the system described here [66].

The proposed CD column has 2 feed flows, one preferably of pure ethanol and the other a mixture of butenes normally of a molar composition of 30% of n-butene and 70% of isobutene.

6. Optimization problem

Based on the models presented in the Section 4, the optimization problems aimed to be solved can be formulated. These problems will be presented hereafter. These optimization problems are the optimal design, the optimal control and the simultaneous optimal design and control problem (ODCP) and the Economic Oriented NMPC (EO-NMPC) of a CD column designed for the production of ETBE.

6.1. Optimal Design formulation

The optimal design of a CD column is stated as a NLP problem, where the annualized cost of investment and operational cost are minimized subjected to nonlinear constraints. The design variables considered in this problem are continuous and include the column diameter, the stage height, the downcomer height and the tray areas. The design variables do not include the number of stages, or position of feeds and catalytic stages since those are integer variables and would require the formulation of a mixed integer nonlinear programming (MINLP) problem.

6.1.1. Optimization constraints

This problem is subjected to three sets of constraints: the model equations (as explained in Section 4.1), the product specification and the tray hydrodynamic constraints.

Product specification

The most straightforward way is to specify purity of one of the products in the bottom or in the top of the distillation column [18]. For this problem, the composition of ETBE has to be greater than a certain limit in the bottoms.

$$x_{NT,ETBE} \geq x_{NT,ETBE}^{min} \tag{34}$$

Tray hydrodynamic constraints

The tray hydrodynamic constraints are included in order to correlate geometrical parameters of the tray in order to:

- Ensure feasibility of the design from the geometrical point of view
- Allow the column to work within the tray capacity limits, avoiding effects such as: Entrainment flooding, downflow flooding and weeping-dumping.

Geometrical relations:

The geometrical relations used in this work are based on the sieve tray design stated in the Figure 6.

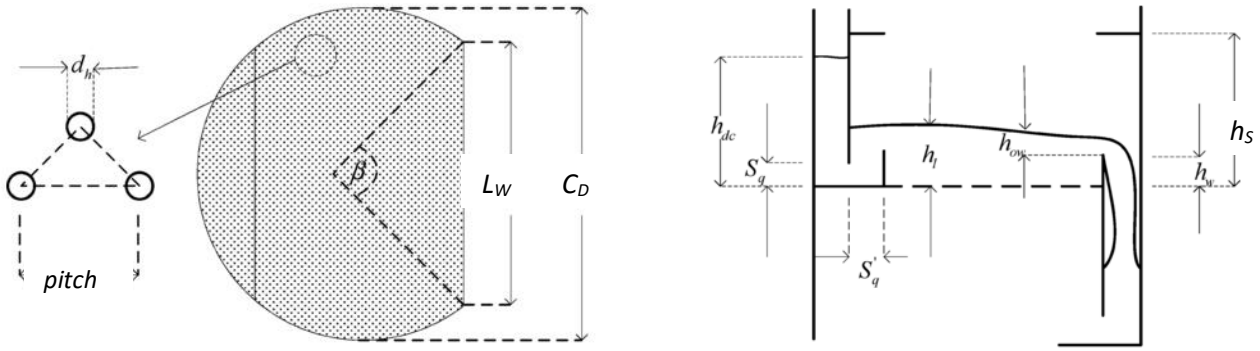

Figure 6. Diagram of plain and elevated view of the sieve-tray [18]

It can be noted that the holes are located in the corner of equilateral triangles, with a distance denoted as the $pitch$. For further considerations in this work, the hole diameter (d_h) and the $pitch$ are constant and satisfy the design ratio between 2.5 and 5.

Based on the Figure 6 arrangement, the following geometrical relationships can be obtained. Some building issues like the stage height or the downcomer height are determined from sizing correlation obtained by Kister [68] and Douglas [69].

Hole area

$$A_h = 0.907 A_a \left[\frac{d_h}{pitch}\right]^2 \tag{35}$$

Active area

$$A_a = A_T - 2A_{DC} \tag{36}$$

Downcomer area

$$A_{DC} = 0.5\left(\frac{C_D}{2}\right)^2 (\beta - \sin(\beta)) \tag{37}$$

$$\beta = 2\arcsin\left(\frac{L_W}{C_D}\right) \tag{38}$$

Weir Length

$$L_W = 0.7 D_C \tag{39}$$

Stage height

$$H_T \geq 1.15 \sum_{n \in N} h_S \tag{40}$$

Weir height

$$\frac{h_S}{20} \leq h_w \leq \frac{h_S}{3} \tag{41}$$

Tray Capacity Limits:

The tray capacity is limited by several hydraulic undesirable effects that affect the efficiency of the trays and the successful operation of the distillation column. Since one of the assumptions of the models described in this work is that there is thermodynamic equilibrium in the column, these undesirable effects must be avoided.

The undesirable effects analyzed here are the entrainment flooding, the downcomer flooding and the weeping. The vapor and liquid flowrates are related with the geometrical parameters of the column (e.g. the column diameter, the hole area) resulting in the phase velocities through several parts of the tray, which are the variables to be compared in order to prevent these undesirable effects.

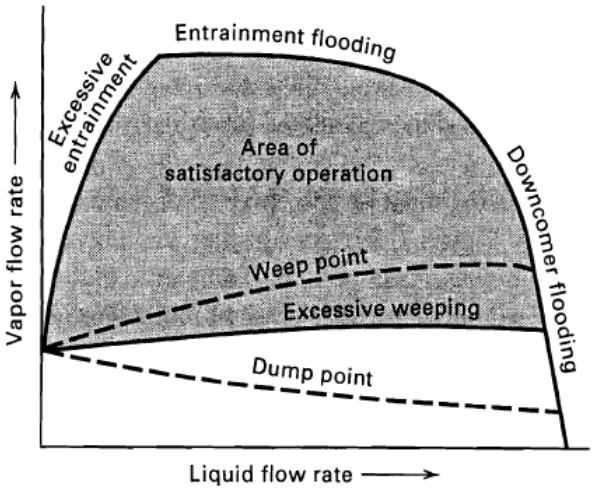

Figure 7. Sieve tray performance at various relative liquid and vapor flow rates [70]

Entrainment flooding

Flooding is the excessive accumulation of liquid in the column. The entrainment flooding occurs when the upward vapor velocity is high enough to suspend liquid droplets and carry them to the upper trays. The vapor velocity passing through the tray is defined as:

$$u_{V,n} = \frac{V_n}{A_T \bar{\rho}_{V,n}}, n \in Sep + Cat \tag{42}$$

The maximum allowed vapor velocity through the plate to avoid this behavior is given by:

$$u_{V,n}^{max} = C_{sbf} \sqrt{\frac{\rho_{L,n} - \rho_{V,n}}{\rho_{V,n}}}, n \in Sep + Cat \tag{43}$$

where the capacity parameter is given by the Kister and Hass correlation [68] as:

$$C_{sbf} = 0.37 \left(\frac{d_h^2 \sigma_n}{\rho_{L,n}}\right)^{0.125} \left(\frac{\rho_{V,n}}{\rho_{L,n}}\right)^{0.1} \left(\frac{h_S}{h_{cl}}\right)^{0.5} \tag{44}$$

where h_{cl} is the height of the clear liquid at the transition from froth to spray regimes and is given by:

$$h_{cl} = \frac{0.157 d_h^{0.833} p_h^{-0.79}}{1 + 1.04 * 10^{-4} \left(\frac{L_n}{\bar{\rho}_{L,n} L_W}\right)^{0.59} p_h^{-1.791}} \left(\frac{996}{\rho_{L,n}}\right)^{0.5\left(1 - \frac{0.91 d_h}{p_h}\right)} \quad (45)$$

The liquid velocity passing through the downcomer is defined as:

$$u_{L,n} = \frac{L_n}{A_{DC} \bar{\rho}_{L,n}}, n \in Sep + Cat \quad (46)$$

The maximum allowed liquid velocity in order to prevent entrainment flooding is given by:

$$u_{L,n}^{max} = \left(\sigma_n g \frac{\rho_{L,n} - \rho_{V,n}}{\rho_{L,n}^2}\right)^{1/4}, n \in Sep + Cat \quad (47)$$

Downflow flooding

The downflow flooding or downcomer flooding is when the column cannot handle the large amount of liquid available. To prevent this issue, excessive backup should be avoided.

The pressure balance equation, obtained by Cicile [71] is given by:

$$h_W + h_S \geq h_L + \frac{\Delta P + \Delta P_{DC}}{g\left(\rho_{L,n} - \rho_{V,n}\right)} \quad (48)$$

where h_l is the height of the liquid over the tray, determined as the sum of the stage weir height and the weir height crest.

$$h_L = h_W + h_{ow} \quad (49)$$

The pressure drop across the downcomer, called ΔP_{DC} is given by

$$\Delta P_{DC} = 1.62 \rho_{L,n} \left[\left(\frac{L_n}{\bar{\rho}_{L,n} S_q}\right)^2 + \left(\frac{V_n}{\bar{\rho}_{V,n} S_q'}\right)^2\right] \quad (50)$$

where S_q and S_q' are the downcomer cross areas as depicted in Figure 6.

Rearranging the terms in the pressure balance, the pressure drop of the liquid over the tray is constrained by the following term.

$$P_{ow} = h_{ow} g\left(\rho_{L,n} - \rho_{V,n}\right) \leq P_{ow}^{max} = h_S g\left(\rho_{L,n} - \rho_{V,n}\right) - (\Delta P + \Delta P_{DC}) \quad (51)$$

Weeping

When the vapor velocity through the tray holes is too low, the liquid starts draining through them. In order to avoid this phenomenon, the vapor velocity through the holes, defined as:

$$u_{h,n} = \frac{V_n}{A_h \bar{\rho}_{V,n}}, n \in Sep + Cat \quad (52)$$

must have a lower bound defined by Lockett equation [71] as:

$$u_{h,n}^{min} = \frac{0.68 \pm 0.12}{\sqrt{\frac{\rho_{V,n}}{\rho_{L,n} g h_{l,n} f a_n}}}, n \in Sep + Cat \tag{53}$$

6.1.2. Objective function

For the optimal design problem, the objective function is the minimization of the annualized cost of investment and operation of the CD column for the ETBE production. The investment term is given by the annualized capital cost (ACC) of 5 years operation. For this process, a cost of capital of 5% was assumed. The ACC includes the installed cost of the column shell, the trays, the reboiler, the condenser and the catalyst. The annual operation plan (AOP) included the consumption of raw materials, steam and cooling water and the sales of ETBE. This economic objective function was used based on the works of Gómez et al. [18] and Miranda et al. [41] for comparative means.

The objective function for the problem is then as follows:

$$\min Cost = \min\left(C_{inv} + C_{op}\right) \tag{54}$$

$$C_{inv} = AF\left(C_{CS} + C_t + C_{Reb,0} + C_{Ccond,0} + C_{cat}\right) \tag{55}$$

$$C_{op} = F_{EtOH} C_{EtOH} + F_{but} C_{but} - L_{NT} C_{ETBE} + C_H Q_{Reb} + C_W Q_{Cond} \tag{56}$$

where AF is the annualizing factor, F_{eth} and F_{but} are the ethanol and butanes feed flow rates respectively, and C_i is the cost corresponding to the i-th part of the objective function.

The installed costs of reboiler and condenser are linear functions of the heat duties of each equipment, as stated in several sources in the literature [18], [41], [72].

$$C_{Reb,0} = C_{Reb,1} + C_{Reb,2} Q_{Reb} \tag{57}$$

$$C_{Cond,0} = C_{Cond,1} + C_{Ccond,2} Q_{Cond} \tag{58}$$

Having this into account, the lump constants C_{Reb}, C_{Cond}, and C_0 can be defined as

$$C_{Reb} = C_H + AF C_{Reb,2} \tag{59}$$

$$C_{Cond} = C_W + AF C_{Cond,2} \tag{60}$$

$$C_0 = AF(C_{Reb,1} + C_{Cond,1}) \tag{61}$$

The value for C_0 has been assigned by Gomez et al. [18] and Ciric and Gu [73] as $10000/year.

The tray and column shell installation costs are determined by the correlations given by Douglas [69].

$$C_{CS} = \left(\frac{M\&S}{280}\right)(101.9 D_C^{1.066} H_T^{0.82} F_C) \tag{62}$$

$$C_t = \left(\frac{M\&S}{280}\right) 4.7 D_C^{1.55} \sum_{n \in Sep+Cat} (h_S) F_C' \tag{63}$$

where $M\&S$ is the Marshall and Swift index used for determining the prices of construction and installation and equipment. The value used for such index is the corresponding for 1994, 1050, as used

by Miranda et al. [41]. F_C and F_C' are cost factors determined by the operating pressure, the material of construction and the tray type. For the operating pressures, building material and tray types of the different studies about the case study [18], [41] result in $F_C = 1.15$ and $F_C' = 1.15$. These correlation are adjusted for plugging the diameter and the height in feet.

Using all these equations, the objective operating and investment costs become:

$$C_{inv} = C_0 + AF\left(\left(\frac{M\&S}{280}\right)\left(117.85D_C^{1.066}H_T^{0.82} + 4.7D_C^{1.55}\sum_{n\in Sep+Cat}(h_S)\right) + C_{cat}\right) \quad (64)$$

$$C_{op} = F_{EtOH}C_{EtOH} + F_{but}C_{but} - L_{NT}C_{ETBE} + C_{Reb}Q_{Reb} + C_{Cond}Q_{Cond} \quad (65)$$

The values used for the corresponding operation and the catalyst costs are given in the Table 4. It should be noted that the estimated production hours per year are 8000.

Table 4. Operating costs of the catalytic distillation column [18], [41], [72]

Cost	Value
Ethanol feed cost $\boldsymbol{C_{EtOH}}$	\$15/kmol
Butenes feed cost $\boldsymbol{C_{but}}$	\$8.25/kmol
ETBE product cost $\boldsymbol{C_{ETBE}}$	\$25.3/kmol
Reboiler overall duty cost $\boldsymbol{C_{Reb}}$	\$146.8/(kW.year)
Condenser overall duty cost $\boldsymbol{C_{Cond}}$	\$24.5/(kW.year)
Catalyst cost $\boldsymbol{C_{cat}}$	\$7.7/kg

6.2. Optimal Control formulation

The optimal control of a CD column is stated as an NLP problem. The quadratic error of the steady state's responses of the manipulated variables and the ETBE composition, added to the cost of operation is minimized, subject to nonlinear constraints. Therefore, it is tracking and economic minimization stated as a multi-objective optimization built as a linear combination of the different objectives.

6.2.1. Optimization constraints

This problem is subject to the dynamic model equations (as explained in Section 4.2) fully discretized using the orthogonal collocation method with Radau Roots explained in the Appendix B - OCP representation as NLP problem and solution algorithms, the steady state model explained in Section 4.1 for the initial point, and the product specification constraint stated in the last section. It should be noted that the tray capacity constraints are not included in the model, since the geometrical parameters of the column will not be modified during the optimization process.

Product specification

The product specification constraint is stated equally as in the optimal design optimization problem, but now it is imposed to all the time instants analyzed. This means:

$$x_{NT,ETBE,j,k} \geq x_{NT,ETBE}^{min}, \forall j = \{0, \dots, J\}, \forall k = \{0, \dots, K\} \tag{66}$$

where j is a finite element, and k a collocation point.

6.2.2. Objective function

The objective of an OCP is the minimization of the quadratic error of the controlled variables with respect to a set-point and the quadratic deviation of the manipulated variables with respect to a reference. Considering the discrete time representation of the problem and the fact that this information will be used during the whole prediction horizon (N_p) the objective function becomes:

$$\min J_{Track} = \min \sum_{i=0}^{N_p} \left(\alpha'_{ETBE} \left(x_{NT,ETBE}^{min} - x_{NT,ETBE,i} \right)^2 + \alpha'_{RR} (RR^{Ref} - RR_i)^2 + \alpha'_{Q_R} \left(Q_{Reb}^{Ref} - Q_{Reb,i} \right)^2 \right) \tag{67}$$

This formulation is asymptotically stable if the control law satisfies certain conditions that make the Eq. 67 a Lyapunov function [74], [75].

An OCP objective function with economic criteria can also be proposed. Here the objective will be an economic function of the system variables instead of a tracking function. For this particular case, the economic function is the operational cost determined in the section 6.1.2.

$$\min J_{Econ} = \min \sum_{i=0}^{N_p} \left(C_{op,i} \right) = \min \sum_{i=0}^{N_p} \left(F_{EtOH,i} C_{EtOH} + F_{but,i} C_{but} - L_{NT,i} C_{ETBE} + C_{Reb} Q_{Reb,i} + C_{Cond} Q_{Cond,i} \right) \tag{68}$$

The main disadvantage is that formulating an economic objective function does not guarantee that the function will be bounded on the infinite horizon or be a monotonic function, which affects the stability and robustness of the controller [74]. The nominal stability and robustness of the controller are guaranteed in case that the objective function is a Lyapunov function for a Economic Oriented nonlinear model predictive control (EO-NMPC) as shown by Huang et al. [76]. This result is valid also for any EO-NMPC considering only one prediction period, which is an OCP problem. The objective function has to satisfy Lipschitz continuity, the problem has to have an isolated local optimum and be greater than a monotonic unbounded function of the state variables and the problem [45], [76], [77]. In order to satisfy these conditions, a weighted sum of the objectives is proposed as follows.

$$\begin{aligned} \min J &= \min(\alpha_{Track} J_{Track} + \alpha_{Econ} J_{Econ}) \\ &= \min \Bigg(\alpha_{Track} \Bigg(\sum_{i=0}^{N_p} \Big(\alpha'_{ETBE} \left(x_{NT,ETBE}^{min} - x_{NT,ETBE,i} \right)^2 + \alpha'_{RR} (RR^{Ref} - RR_i)^2 \\ &\quad + \alpha'_{Q_R} \left(Q_{Reb}^{Ref} - Q_{Reb,i} \right)^2 \Big) \Bigg) + \alpha_{Econ} \left(\sum_{i=0}^{N_p} \left(C_{op,i} \right) \right) \Bigg) \end{aligned} \tag{69.a}$$

$$\alpha_{Track} + \alpha_{Econ} = 1 \tag{69.b}$$

$$\alpha_{Track}, \alpha_{Econ} \in [0,1) \tag{69.b}$$

The new objective function is strongly convex, due to the quadratic differences, guaranteeing the nominal stability of the system. The terms $\alpha_{Track}, \alpha_{Econ}$ represent the tradeoff between the tracking objective function and the economic objective function respectively [76], [78].

The weighting parameters can be expressed relative to the economic objective, such that:

$$\alpha_p = \frac{\alpha_p' \alpha_{Track}}{\alpha_{Econ}};\ \forall p \in \{ETBE, RR, Q_{Reb}\} \tag{70}$$

The resulting objective function is then the weighted sum of the tracking optimal control objective function and the operational costs. The tracking optimal control objective function is the squared error of the reboiler duty, the reflux ratio (the manipulated variables), and the ETBE composition at the bottoms compared to the reference of each variable. The reference values for the manipulated variables are the solution of the steady-state optimization, while the reference for the ETBE bottoms molar composition is the minimum composition, used as a set-point. The operational costs are the same as the operational costs mentioned in the optimal design optimization problem formulation.

$$\min J = \min \sum_{i=0}^{N_p} \left(\alpha_{ETBE} \left(x_{NT,ETBE}^{min} - x_{NT,ETBE,i} \right)^2 + \alpha_{RR} (RR^{Ref} - RR_i)^2 + \alpha_{Q_R} \left(Q_{Reb}^{Ref} - Q_{Reb,i} \right)^2 + C_{Op} \right) \tag{71}$$

where the α coefficients are the weighting parameters in the objective function. This objective function is similar to the one presented by Miranda et al. [41].

Weights determination

In order to define completely the objective function, the weighting parameter for each objective has to be determined. Representing all the weights relative to the economic part of the objective function, as in the Eq. 70, reduces the number of parameters in one.

The procedure to determine these weighting parameters is based on the work of Zavala et al. [12] where an online utopia tracking NMPC is proposed. Here, an offline approach of the utopia tracking of a multi-objective optimization strategy is proposed. The utopia point is a point that minimizes all the objectives simultaneously but cannot be achieved [79]. It is obtained by minimizing every objective independently and setting it as a lower bound for that objective. An upper bound for each objective is obtained also by taking the largest value of each objective among the other objectives minimization. The multi-objective optimization aims to find the closest possible solution to the utopia point. This work uses a $\mathcal{L}_1$ norm to determine the distance to the utopia point and that objective is represented by the following objective function.

$$\min |\boldsymbol{\phi} - \boldsymbol{\phi}^{Lo}| \tag{72}$$

where $\boldsymbol{\phi}$ is the vector of objectives and $\boldsymbol{\phi}^{Lo}$ is the utopia point. In order to scale all of the objectives, their range is used, which is defined as the $\mathcal{L}_1$ difference between their upper and lower bound [12]. With this modification the objective function becomes:

$$\min \left| \frac{\boldsymbol{\phi} - \boldsymbol{\phi}^{Lo}}{\boldsymbol{\phi}^{Up} - \boldsymbol{\phi}^{Lo}} \right| = \min \sum_{p \in \Phi} \frac{\phi_p - \phi_p^{Lo}}{\phi_p^{Up} - \phi_p^{Lo}} \tag{73}$$

where Φ is the set of objectives. It can be noticed that the absolute value from the $\mathcal{L}_1$ norm can be neglected because it is not possible for any objective to have a value lower that it's utopic point[80]. The objective function can be further modified in order to determine the weights as follows.

$$\min \sum_{p \in \Phi} \frac{\phi_p - \phi_p^{Lo}}{\phi_p^{Up} - \phi_p^{Lo}} = \min \left(\sum_{p \in \Phi} \frac{\phi_p}{\phi_p^{Up} - \phi_p^{Lo}} - \sum_{p \in \Phi} \frac{\phi_p^{Lo}}{\phi_p^{Up} - \phi_p^{Lo}} \right) \tag{74}$$

Since the second term in the last equation is a constant, solving the optimization problem of the Eq. 73 will result in the same variables values from Eq. 74 as stated in the following equation.

$$\operatorname{argmin} \left(\sum_{p \in \Phi} \frac{\phi_p}{\phi_p^{Up} - \phi_p^{Lo}} - \sum_{p \in \Phi} \frac{\phi_p^{Lo}}{\phi_p^{Up} - \phi_p^{Lo}} \right) = \operatorname{argmin} \left(\sum_{p \in \Phi} \frac{\phi_p}{\phi_p^{Up} - \phi_p^{Lo}} \right) \tag{75}$$

This means that the weighting parameters for each objective are determined as the difference between the upper and lower bound of each objective. This approach considers all the objectives equally important. In order to increase the convexity of the objective function, the tracking function can be preferred over the economic function as the quadratic terms included in it have a higher relative importance in the objective. For this case study, and taking into account that the weighting parameters are defined relative to the economic objective, the weighting parameters become:

$$\alpha_p = \frac{\alpha_{Track}}{\alpha_{Econ}} \frac{\phi_{Econ}^{Up} - \phi_{Econ}^{Lo}}{\phi_p^{Up} - \phi_p^{Lo}};\ \forall p \in \{ETBE, RR, Q_{Reb}\} \tag{76}$$

6.3. Simultaneous Optimal Design and Control formulation

The simultaneous ODCP of a CD column is formulated as an NLP problem. The objective is to minimize the error function of the steady state responses of the control variables and the ETBE composition, the cost of operation, and the investment cost. The multi-objective optimization problem is the minimization of a tracking function, together with the operational and investment costs. Apart of the state variables of the OCP problem, the simultaneous ODCP problem also considers as variables the continuous design variables considered in the optimal design problem.

6.3.1. Optimization constraints

The constraints of this model include the steady-state for the initial point and the dynamic models explained in Section 4, the product specification constraints and the tray capacity constraints. This problem will modify the dynamic response of the control variables and the geometrical parameters of the distillation column.

6.3.2. Objective function

The objective function in this case is the same as in the OCP adding the investment cost. The total objective function is:

$$\min J = \min C_{inv} + \sum_{i=0}^{N_p} \left(\alpha_{ETBE} \left(x_{NT,ETBE}^{min} - x_{NT,ETBE,i} \right)^2 + \alpha_{RR} (RR^{Ref} - RR_i)^2 + \alpha_{Q_R} \left(Q_{Reb}^{Ref} - Q_{Reb,i} \right)^2 + C_{Op,i} \right) \quad (77)$$

6.4. Economic Oriented Non Linear Model Predictive Control formulation

This optimization problem, as described in the section 3.2.3, is based on the recurrent solution of the OCP. The control law is defined taking only the first element of the solution of the OCP at each sampling time and only this element is provided as feedback to the system. The sampling time of the controller has been set in order to be the same as a finite element of the solution of the OCP, set as 300 seconds.

6.4.1. Optimization constraints

In order to define the constraints of this optimization problem, two assumptions were made. The first one is that there is no plant-model mismatch and the second one is that all the states are measurable and provided as feedback to the controller. The first assumption implies that the states predicted by the model will be the same as the ones measured, thus it is not necessary to consider the robustness of the controller. The second assumption allows neglecting the use of an observer (e.g. extended Kalman Filter, Moving Horizon estimator, Luenberg observer or Smith estimator [34]) for determining the state of the system at each sampling time.

The optimization constraints of the EO-NMPC will be the same as the ones of the OCP problem explained in the section 6.2.1. In this case, the design constraints included in the optimal design problem are neglected since this problem only considers the operation of the process.

It should be noticed that for the EO-NMPC problems, the manipulated variables (reboiler duty and reflux ratio) do not change at all times, but only change every sampling time. This is set in order to allow the OCP problem to be solved, task that requires a considerable amount of time.

6.4.2. Objective function

The objective of a model predictive control problem is to minimize the quadratic error of the controlled variables with respect to a set-point in a prediction horizon and the quadratic instant change of the manipulated variables in a control horizon ($N_u \leq N_p$). The control law is then the application of the OCP first element of the solution over the prediction horizon. The objective function of such problems applied to this case study, similar to the tracking OCP objective function in Eq. 67, is the following:

$$\min J_{NMPC} = \sum_{i=0}^{N_p} \left(\alpha'_{ETBE} \left(x_{NT,ETBE}^{min} - x_{NT,ETBE,i} \right)^2 \right) + \sum_{i=1}^{N_u} \left(\alpha'_{RR} (RR_i - RR_{i-1})^2 + \alpha'_{Q_R} \left(Q_{Reb,i} - Q_{Reb,i-1} \right)^2 \right) \quad (78)$$

There is a slight difference between the OCP tracking objective function and the NMPC objective function. The quadratic deviation of the instant change in the manipulated variables is minimized, instead of the deviation from a reference point.

The proposed EO-NMPC formulation has a different objective function since the objective becomes a weighted sum of an economic function of the system variables and the tracking terms presented in the

Eq. 78. In the case study, this economic function is the operational cost described in the section 6.1.2. A similar procedure to the one described in the section 6.2.2 is made to determine the resulting objective function.

$$\min J_{EO-NMPC} = \sum_{i=0}^{N_p} \left(\alpha_{ETBE} \left(x_{NT,ETBE}^{min} - x_{NT,ETBE,i} \right)^2 \right) + \sum_{i=1}^{N_u} \left(\alpha_{RR} (RR_i - RR_{i-1})^2 + \alpha_{Q_R} \left(Q_{Reb,i} - Q_{Reb,i-1} \right)^2 \right) + \sum_{i=0}^{N_p} C_{op,i} \quad (79)$$

The references [76], [78], [81] provide a deeper explanation regarding the stability properties and implementation of the EO-NMPC scheme presented here.

7. Results and Discussion

This work deals with the optimal design and optimal control of an ETBE production CD column. The results presented here will be classified according to the optimization problem being solved, from the problems mentioned in Section 6. There is an in-between section showing the results for the dynamic simulation of the system without solving an OCP. After the results of the sequential and simultaneous design and control there is a section showing a comparison among different DAE models and the results of the EO-NMPC compared to a PI controller. All the results exposed in this work were obtained using the algorithm CONOPT 3 [82] and implemented in GAMS 24.5 [83] and the examples were run in an Intel Core i5 2.70 GHz, 8.0 GB memory computer.

7.1. Optimal Design

The optimal design problem stated in section 6.1 was solved for two different studies of catalytic distillation columns found in the literature. The first application was in the column proposed by Miranda et al. [41] and the second were the columns designed by Gomez et al. [18] with the equilibrium and non-equilibrium models.

The column characteristics were obtained from Miranda et al. [41], where a 10 stages CD column was used to prove their algorithm of sequential and simultaneous design and control methodology. The column characteristics are stated in the Table 5.

Table 5. Distillation column characteristics from [41]

Characteristic	Unit	Value
Number of stages $\boldsymbol{NT}$	[-]	10
Number of reactive stages	[-]	3
Position of the catalyst	Stage	4,5,6
Ethanol feed stage	Stage	3
Butenes feed stage	Stage	8

$x_{NT,ETBE}^{min}$	[mol/mol]	0.83
Ethanol feed flow F_{EtOH}	[kmol/min]	1.7118
Ethanol feed temperature	[K]	323
Butenes feed temperature	[K]	342.38
Condenser pressure	[bar]	9.5
Distillation column height H_T	[m]	0.4572

The butenes feed flow was determined as a variable in the work of Miranda, therefore it was also left as a variable in this formulation. Some geometric characteristics from the trays were not stated in the original paper, which meant that in order to obtain results these values were assumed, always following the design rules given by the literature [68]. The assumed values were the tray thickness ε, equal to 2*10-3m, the hole diameter d_h, equal to 2*10-3m, and the $pitch$, equal to 9*10-3m (respecting the ration $2.5 \leq \frac{d_h}{pitch} \leq 5$).

The work made by Miranda et al. [41] considered three different scenarios, each one depending of the molar composition of the butenes stream. The three cases were with 0.275, 0.3, and 0.325 molar fraction of n-butene in the feed; being the rest isobutene. The three cases were named best-case, nominal and worse-case respectively, since the higher amount of isobutene allowed a higher production of ETBE. A fourth case was proposed by this work, which is fixing a molar fraction of 0.25 of n-butene in the feed, which will be named as worst-case.

To illustrate the obtained solution for the optimal design of the distillation column, the resulting profiles of the molar flows, temperature, pressure, molar fractions in liquid and vapor, and compressibility factor are presented in the Figure 8.

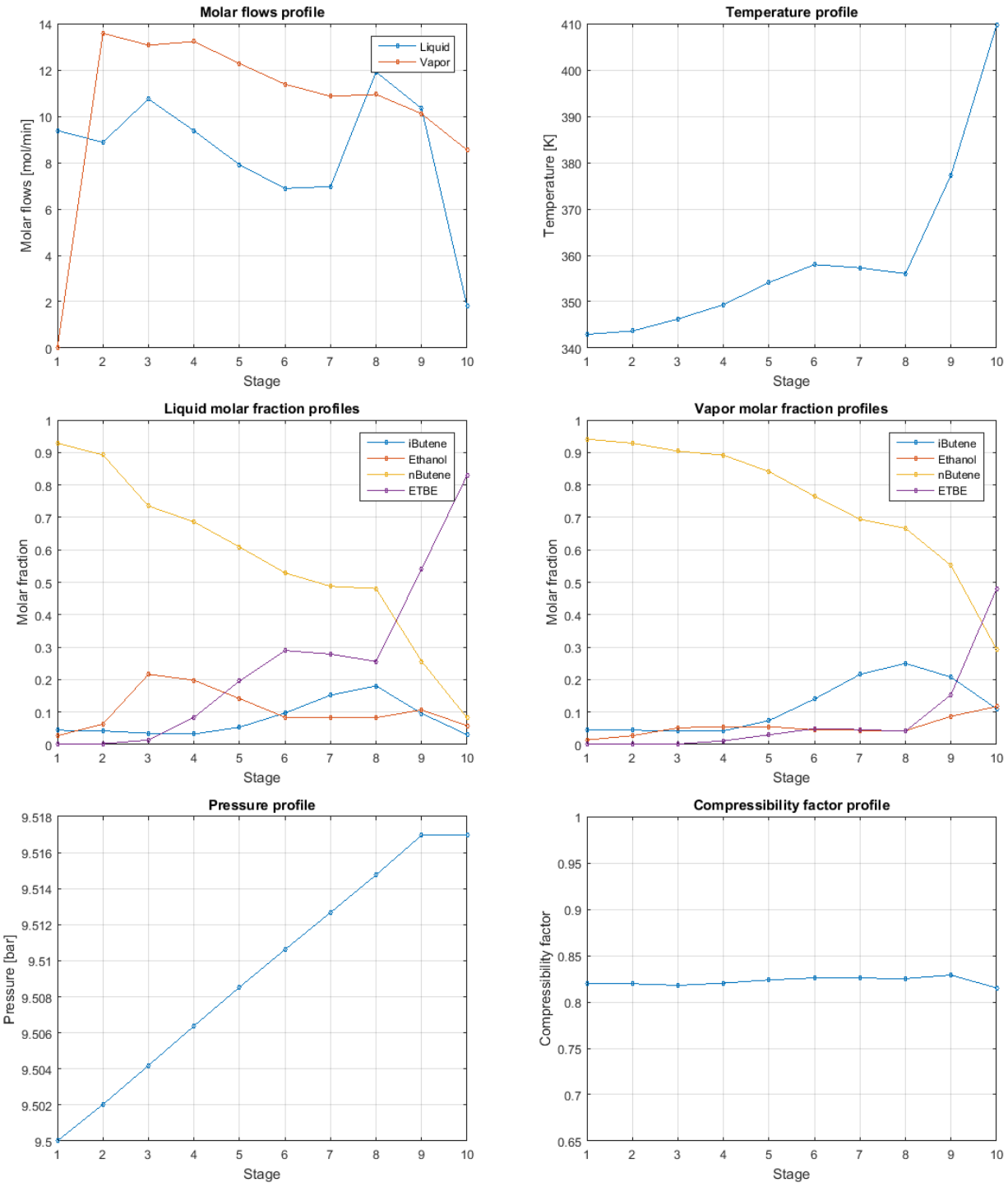

Figure 8. Profiles of the optimal design solution for the nominal case

The obtained profiles show an expected behavior. The ETBE is present in the lower trays as the reaction is the only source of this component. There is almost no pressure drop, which is of 0.018 bar for the whole column. The compressibility factor is around 0.82 for the whole column, which shows that the inclusion of an EOS was necessary to model this system. The operational parameters such as reflux ratio and reboiler duty is presented in the Table 6.

Once solved this problem, an interesting fact is that the optimal value obtained was different to the obtained solution by Miranda et al. For instance, the solution obtained using the parameters found by the authors with this work's model and the optimal design generated for this work were compared. This was done for the three cases, and the worst-case, and the main results are presented in the Table 6.

Table 6. Optimal design results

	Units	Worst-Case	Worse-case		Nominal		Best-case	
Isobutene feed composition	**[mol/mol]**	**0.25**	**0.275**		**0.3**		**0.325**	
Solution source		**This work**	**Miranda et al.**	**This work**	**Miranda et al.**	**This work**	**Miranda et al.**	**This work**
Column Diameter D_C	[m]	0.1214	0.0922	0.1155	0.09533	0.1110	0.09847	0.1066
Stage height h_S	[m]	0.0500	*0.0500*	0.0500	*0.0292*	0.0500	*0.0231*	0.0500
Downcomer height h_w	[m]	0.0166	*0.0166*	0.0166	*0.0082*	0.0166	*0.0033*	0.0166
Feed rate F_{but}	[mol/min]	7.515	4.533	6.491	4.907	5.774	5.359	5.207
Reboiler Duty Q_{Reb}	[kJ/min]	284.24	248.34	264.40	265.68	249.96	285.48	236.76
Molar reflux ratio RR	[-]	1.525	3.964	1.892	3.659	2.238	3.361	2.560
ETBE bottoms composition $x_{NT,ETBE}$	[mol/mol]	0.83000	**0.43688**	0.83000	**0.60215**	0.83000	**0.82015**	0.83000
Isobutene conversion	[mol/mol]	0.78038	0.84383	0.83143	0.87508	0.86027	0.88765	0.87889
Entrainment flooding?		No	No	No	No	No	No	No
Downcomer flooding?		No	**Yes**	No	**Yes**	No	**Yes**	No
Weeping?		No	No	No	No	No	No	No
Profit ETBE	[$/year]	21501	29260	21755	26003	21836	22917	21789
Annualized Investment cost	[$/year]	10156	10028	10148	10030	10142	10030	10033
Operating cost	[$/year]	42887	30982	38778	32514	35898	34358	33617
Total Cost	[$/year]	31543	11751	27171	16541	24205	21471	21890

* The results on italics do not correspond to data given by Miranda et al. [41], but obtained by the model used in this work. The values in bold are highlighted since reflect a violation of the design constraints.

It can be noticed that the differences in the models adopted in this work and by Miranda et al. [41] resulted in different solutions for the optimal design problem. The results obtained by the other authors were infeasible solutions for the models used in this work. For all three cases, the ETBE bottoms mole fraction is below the specified minimum of 0.83. All three cases presented at least one stage a height less than the minimum required to overcome the pressure difference across the downcomer, therefore resulting in downcomer flooding. The work by Miranda et al. [41] did not consider this undesired effect in their hydraulic constraints, but since the column is just 1.5 ft. tall and ten stages had to be placed in this height, that represented a design challenge. The optimal values obtained in this work resulted in logical values, increasing the column diameter allowed the tray capacity constraints to be satisfied, although it represented an increase in the overall cost. The obtained feed flow rates were higher than those obtained in the work by Miranda, but this fact was balanced with a lower molar reflux ratio.

The results also represent a logic behavior regarding the four different cases studied. The richer the feed was in isobutene, the lower feed flow was required (as the reaction generating ETBE is one to one with isobutene) and this decrease in feed flow rates resulted in a smaller column diameter and a lowerreboiler duty. With less flow rates of the butenes mixture, a higher conversion had to be achieved and that required a higher reflux ratio. The profit from the ETBE was proportional to the feed flow, the investment cost to the column diameter, and the operating cost depended strongly on the feed flows and the heat duties.

As the configuration of Miranda et al. [41] was used for the following sections, the results regarding the optimal design of the CD column proposed by Gómez et al. [18] are presented in the Appendix C – Second Case Study.

7.2. Dynamic Simulation

After obtaining the optimal design of the CD column from a steady state optimization, the next step was to make a dynamic simulation of the system. This was made by fixing the design parameters and the manipulated variables with the solutions from the steady state optimal design problem. A disturbance in the feed stream composition is applied to the system. This simulation was done in order to verify if the non-controlled dynamic case could produce a product within the desired specifications without changing its control variables values. In the case this does not hold, a control strategy would be required.

Two disturbances were applied to the system. The first one was a sinusoidal disturbance in the butenes feed composition. It was designed to oscillate with an amplitude of 5% and a period of two hours. Here the disturbance amplitude is the difference between the worst-case and the nominal-case scenarios. With the second disturbance was a step function decreasing the molar composition of the isobutene in the feed stream from 0.3 to 0.25 after 30 minutes of operation. The simulation time were 5 hours. The resulting disturbances in the n-butene feed molar composition were:

$$P_1: z_{nB} = 0.7 + 0.05 \sin\left(\pi * \frac{t[min]}{60}\right) \tag{80.a}$$

$$P_2: z_{nB} = \begin{cases} 0.7 \; if \; t[min] \leq 30 \\ 0.75 \; if \; t[min] > 30 \end{cases} \tag{80.b}$$

The rest of the butenes feed was completed with isobutene, and then the whole disturbances can be seen in the

Figure 9 below.

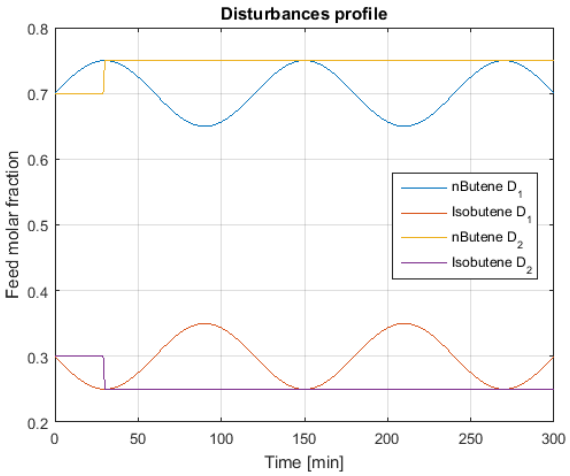

Figure 9. Disturbances profile

After using orthogonal collocation with the Radau roots, with 10 finite elements and 3 collocation points per element; the whole dynamic simulation was implemented. The results used for this simulation were the optimal design parameters for the nominal case obtained by this work, shown in the Table 6, as they satisfy the operational constraints for the initial time.

7.2.1. Sinusoidal disturbance

The main results of the dynamic simulation with a sinusoidal disturbance are shown in Figure 10.

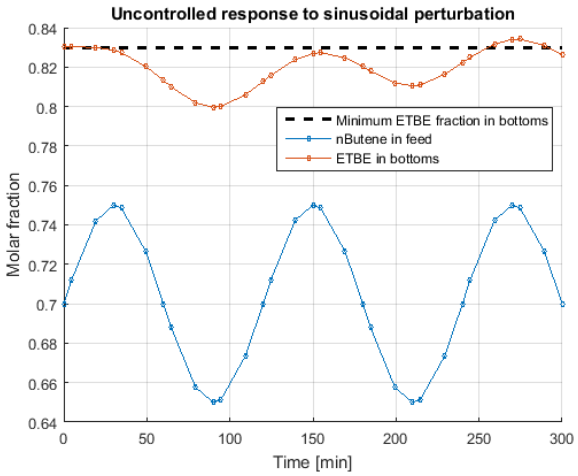

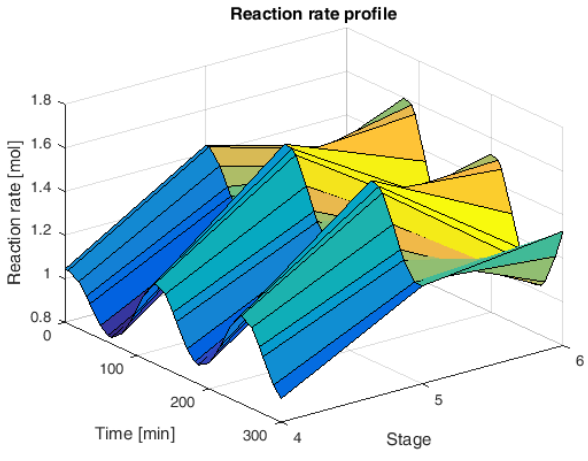

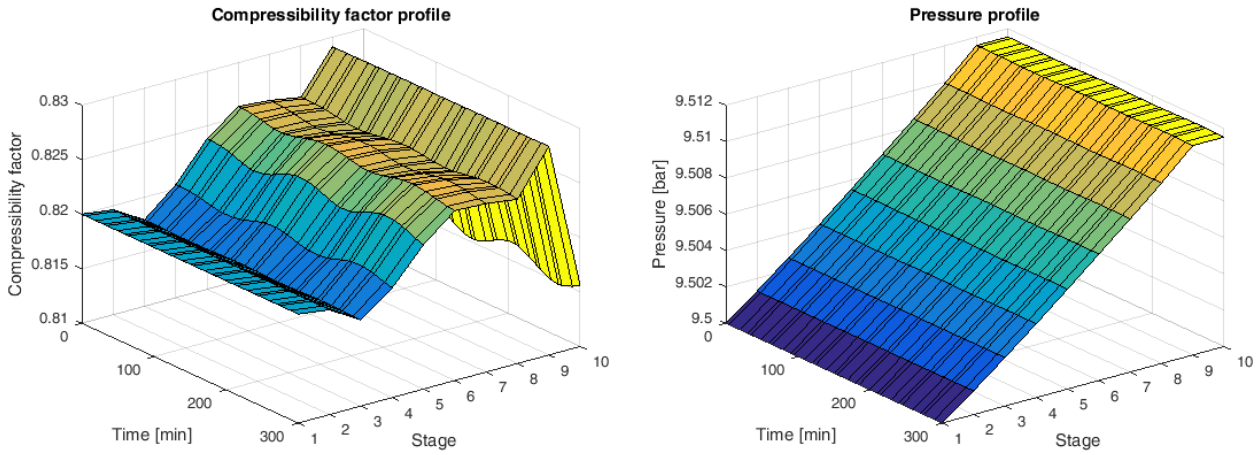

Figure 10. Main results for the dynamic simulation with a sinusoidal disturbance

The first result that can be seen from this simulation is that the uncontrolled response to the sinusoidal disturbance violates the minimum ETBE composition at the bottoms. This shows that in order to assure that the composition is above this minimum a control strategy is required. The three profiles shown here correspond to the dynamic response of the reaction rate, the compressibility factor, and the stage pressure. It can be noted that the response to the disturbance is considerable for the reaction rate, mild for the compressibility factor and negligible for the pressure. The standard deviation σ and relative deviation for all stages has been calculated and are shown in the Table 7 below.

Table 7. Standard and relative deviations for reaction rate, compressibility factor and stage pressure in dynamic simulation with a sinusoidal disturbance

Stage	Reaction rate		Compressibility factor		Stage pressure	
	$\sigma\left[\frac{mol}{kg_{cat}}\right]$	$\frac{\sigma}{\mathcal{R}}$ [%]	σ	$\frac{\sigma}{Z}$ [%]	$\sigma\,[bar]$	$\frac{\sigma}{P}$ [%]
1	-	-	9.38E-07	1.1E-04	0	0
2	-	-	4.88E-06	6.0E-04	1.51E-05	1.43E-06
3	-	-	4.06E-05	5.0E-03	3.87E-05	3.68E-06
4	0.1123	11.1169	3.21E-04	3.9E-02	8.19E-05	7.78E-06
5	0.1407	10.0764	4.51E-04	5.5E-02	1.26E-04	1.19E-05
6	0.1788	13.9901	2.58E-04	3.1E-02	1.44E-04	1.37E-05
7	-	-	2.15E-04	2.6E-02	1.56E-04	1.48E-05
8	-	-	1.83E-04	2.2E-02	1.81E-04	1.72E-05
9	-	-	1.36E-05	1.6E-03	1.84E-04	1.75E-05
10	-	-	7.77E-04	9.5E-02	1.84E-04	1.75E-05
Average	0.1439	11.7278	2.26E-04	0.0276	1.11E-04	1.06E-05

7.2.2. Step disturbance

The main results of the dynamic simulation with a step disturbance are shown below.

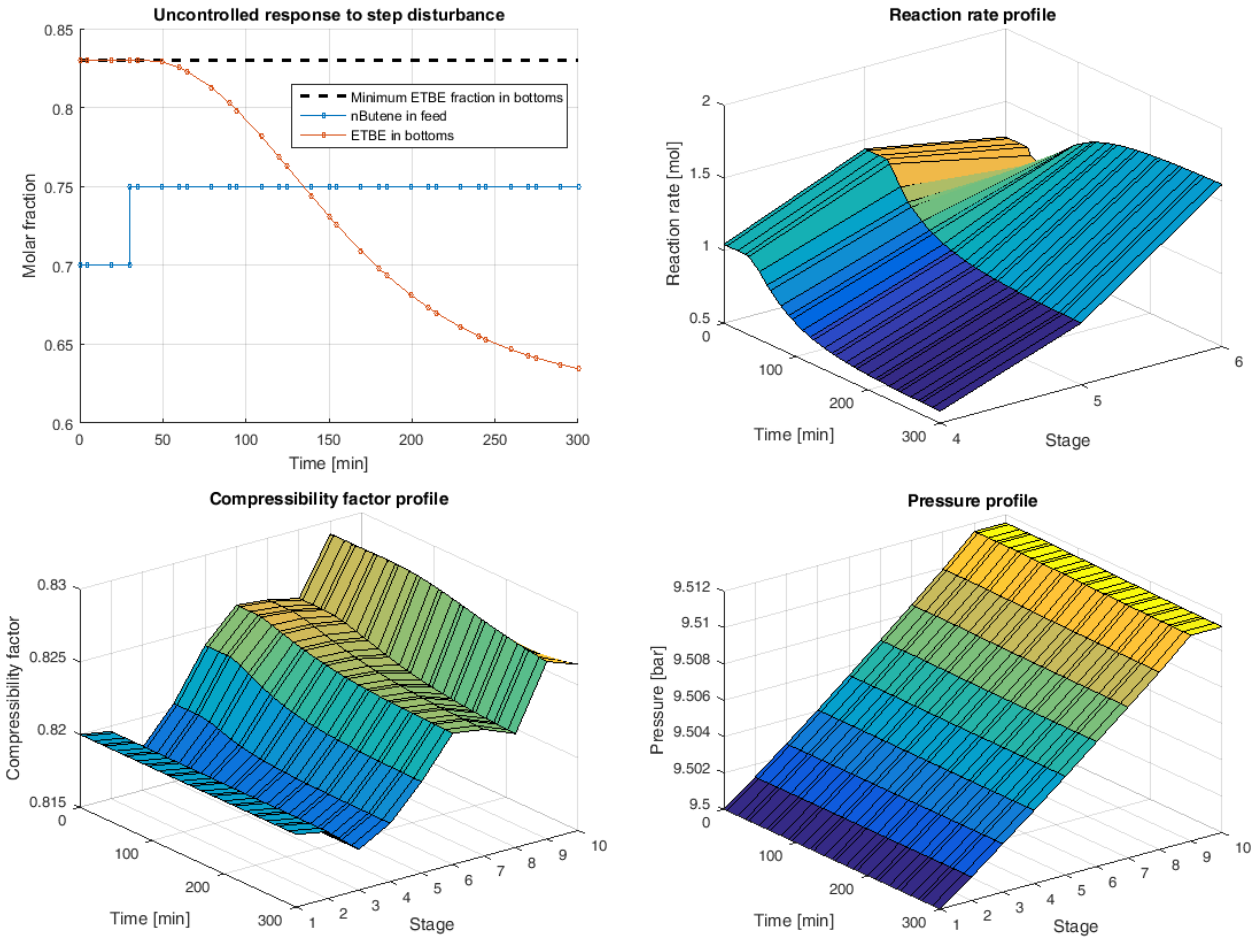

Figure 11. Main results for the dynamic simulation with a step disturbance

Similarly to the results from the sinusoidal disturbance, the uncontrolled response to the step perturbation results in violation of the minimum ETBE composition at the bottoms. Again this proves the need of a control strategy to satisfy this minimum composition constraint. The dynamic response of the reaction rate, the compressibility factor, and the stage pressure follow the same pattern for this disturbance as for the sinusoidal disturbance as it is considerable for the reaction rate, mild for the compressibility factor and negligible for the pressure.

Table 8. Standard and relative deviations for reaction rate, compressibility factor and stage pressure in dynamic simulation with a step disturbance

Stage	Reaction rate		Compressibility factor		Stage pressure	
	$\sigma\left[\frac{mol}{kg_{cat}}\right]$	$\frac{\sigma}{\mathcal{R}}$ [%]	σ	$\frac{\sigma}{Z}$ [%]	$\sigma\,[bar]$	$\frac{\sigma}{P}$ [%]
1	-	-	1.29E-06	1.6E-04	0	0
2	-	-	8.30E-06	1.0E-03	8.21E-06	7.80E-07
3	-	-	5.09E-05	6.2E-03	3.23E-05	3.07E-06
4	0.1676	23.1525	5.13E-04	6.2E-02	1.20E-04	1.14E-05
5	0.1795	16.8272	9.30E-04	1.1E-01	2.62E-04	2.49E-05
6	0.1529	10.4058	6.96E-04	8.4E-02	3.77E-04	3.59E-05
7	-	-	7.44E-04	9.0E-02	4.94E-04	4.70E-05
8	-	-	8.99E-04	1.1E-01	6.69E-04	6.36E-05
9	-	-	6.81E-04	8.2E-02	8.34E-04	7.93E-05
10	-	-	4.25E-03	5.2E-01	8.34E-04	7.93E-05
Average	0.1667	16.7952	8.77E-04	0.1067	3.63E-04	3.45E-05

The obtained results clearly show that the stage pressure is non-sensitive to a disturbance in the feed composition, either a step function or an oscillatory disturbance. The same can be remarked for the compressibility factor, but the reaction rate is strongly dependent on the feed composition. These results were shown because several studies in the literature have considered these variables as constants [84]. It has been shown that such an assumption may be valid for the stage pressure and the compressibility factor, but not for the reaction rate.

7.3. Optimal Control

Once stipulated the need of a control strategy for the system subject to a feed composition disturbance, an optimal control scheme has been used for defining it. The model used is the one presented in Section 6.2. The same simulation time, number of finite elements and number of collocation points as the dynamic simulation have been used for this OCP.

7.3.1. Weights determination

In order to determine completely the objective function of the OCP, the weighting parameters have to be defined. The procedure to determine such weighting parameters was described in Section 6.2.2 as an offline multi-objective utopia point tracking optimization. The procedure consisted in solving an OCP optimizing every objective independently. The optimal objective function value for each individual problem would define a lower bound for that objective and the largest value of the objective among all the other individual problem solutions defines its upper bound. Then the weighting parameters are

determined by Eq. 76. The coefficient $\frac{\alpha_{Track}}{\alpha_{Econ}}$ was determined to be equal to 5. This decision was made to avoid making the tracking and the economic objectives equally important for the objective function. The tracking objective was chosen arbitrarily 5 times more important, but since the quadratic terms in it were the responsible of the convexity of the objective function it allows the objective to approach a Lyapunov function as mentioned in the section 6.2.2. This last decision was taken after trial and error in the coefficient, aiming to obtain smooth responses profiles based on a methodology for determining the weighting parameters from Ramos et al. [45].

The results of the individual objectives optimization and the weighting parameters, for both disturbances described in Section 7.2 using the design parameters of the nominal-case optimization, are presented in the Table 9.

Table 9. Weighting parameters for the OCP objective function

Objective	Sinusoidal disturbance			Step disturbance		
	Lower bound ϕ^{Lo}	Upper bound ϕ^{Up}	Weighting parameter α	Lower bound ϕ^{Lo}	Upper bound ϕ^{Up}	Weighting parameter α
ETBE bottoms composition tracking [(mol/mol)^2] $\sum_{i=0}^{N_p}\left(x_{NT,ETBE}^{min} - x_{NT,ETBE,i}\right)^2$	1.08E-22	3.55E-1	1.85E+5	1.58E-22	7.51	1.03E+4
Reboiler duty quadratic deviation [(kJ/min)^2] $\sum_{i=0}^{N_p}\left(Q_{Reb}^{Ref} - Q_{Reb,i}\right)^2$	9.10E-15	9.40E+4	6.95E-1	6.48E-19	1.13E+5	6.85E-1
Reflux quadratic deviation [-] $\sum_{i=0}^{N_p}(RR^{Ref} - RR_i)^2$	7.80E-11	2.95E+2	2.22E+3	9.31E-13	2.18E+1	3.55E+2
Operation cost [$/year] $\sum_{i=0}^{N_p} C_{op,i}$	-117403.776	-104310.345	1.00	-99977.849	-84514.375	1.00

Having determined the weighting parameter for each part of the objective function, an OCP problem is solved. As the main aim of this problem is to make a sequential ODCP, two different cases from the optimal design solutions will be considered. The first one is the nominal case, which was the one designed to make the weighting parameters determination and that satisfies the operational constraint at the initial time. The second is the worst-case, which was the optimal design solution to the lowest composition in isobutene in the feed and which is also the most extreme condition for the disturbances.

7.3.2. Sinusoidal disturbance

The manipulated variables (molar reflux ratio and reboiler duty) profiles are shown in the Figure 12, together with the ETBE composition in the bottoms for the OCP solution to the sinusoidal disturbance. The obtained profiles were for the nominal-case and worst-case solutions of the optimal design problem. The manipulated variables profiles include the reference values of the variables, obtained also from the solution of the optimal design problem.

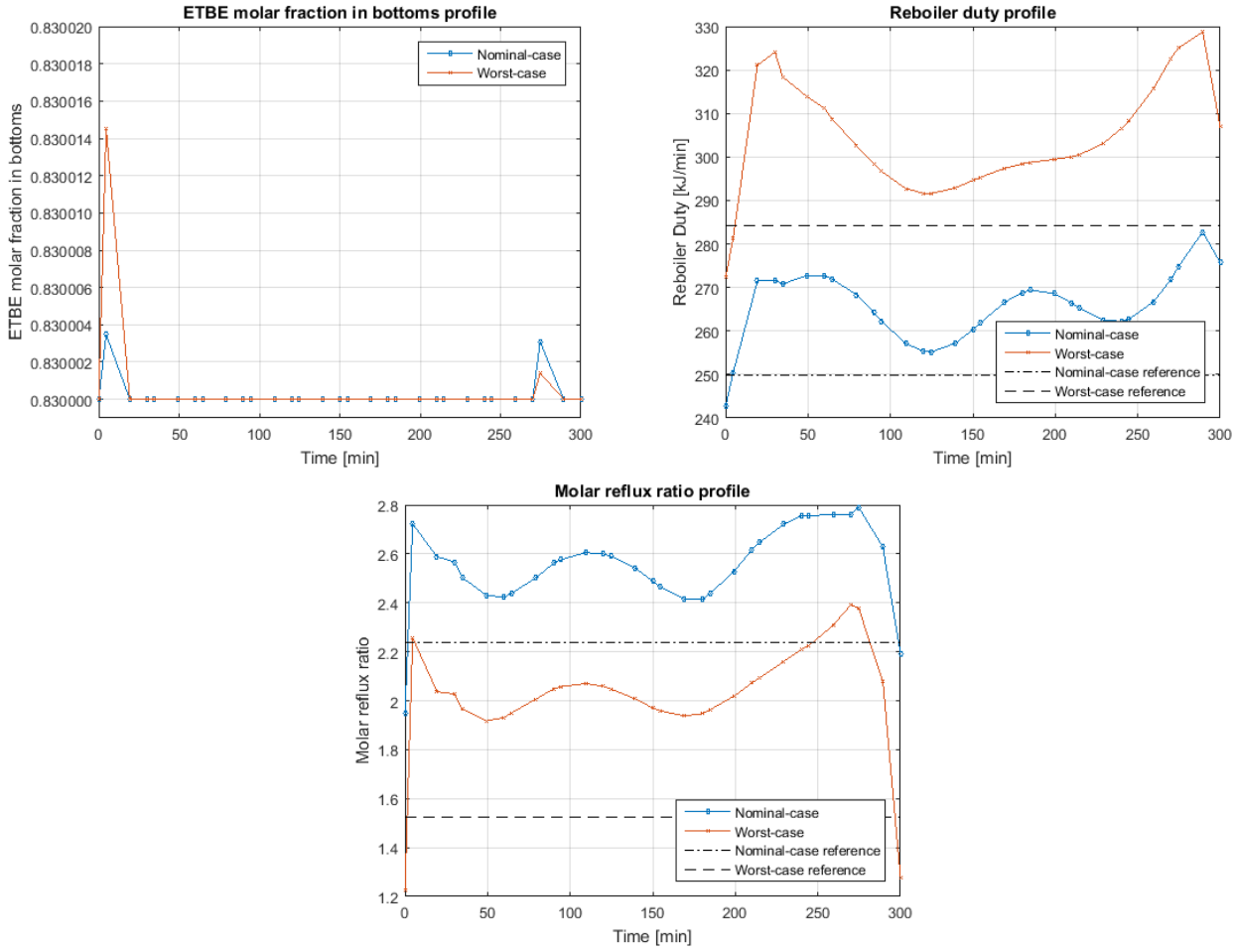

Figure 12. ETBE in bottoms and manipulated variables profiles for the OCP solution to the sinusoidal disturbance

It can be seen how both the molar reflux ratio and the reboiler duty change over time in order to always satisfy the purity constraint which is never violated. This constraint is active during most of the time horizon for two reasons. The first one, is that there is a penalty term for deviations from this minimal ETBE composition in the objective function, and secondly there are economic considerations in the objective function. Both of them are minimized and the effect is having the composition at its lower limit as long as possible. It can be noted that the manipulated variables responses are not synchronized with the disturbance. This can be explained for two reasons: the mass inertia of the system; which is the accumulation of mass in the column through time, and the nonlinearity of the reaction coupled with the separation.

The profiles of the nominal-case and the worst-case scenarios are similar among them, with certain displacement. The displacement has the same explanation as in the optimal design problem. The lower the molar fraction of isobutene in the feed stream, the more effort to achieve the purity of ETBE in bottoms and therefore the higher reboiler duty. The feed flow rate of butanes is also different between the two scenarios, being higher for the worst-case scenario, and therefore a lower conversion has to be achieved requiring a lower molar reflux ratio. As the initial conditions were the same as in the nominal-case, the reference values for the manipulated variables were closer to the profiles compared to the worst-case scenario.

Since this is an open loop control scheme, and there is an economic part in the objective function, in order to minimize the operational costs at the end of the time analyzed the control shuts down abruptly the reboiler duty and the molar reflux ratio as both of the manipulated variables are taken into account in the economic objective function. In the case of the reboiler duty it is directly included and in the case of the reflux ratio is indirectly included, when including the condenser cost. In the case of the worst-case scenario, this action is more noticeable. This is because the manipulated variables are farther from their reference values and this abrupt change is favored by both parts of the objective function: the tracking and the economic objectives.

7.3.3. Step disturbance

The OCP solution to the step disturbance introduced in the section 7.2.2 are presented in the Figure 13 below. The profiles shown here correspond to the same variables exposed in the previous section.

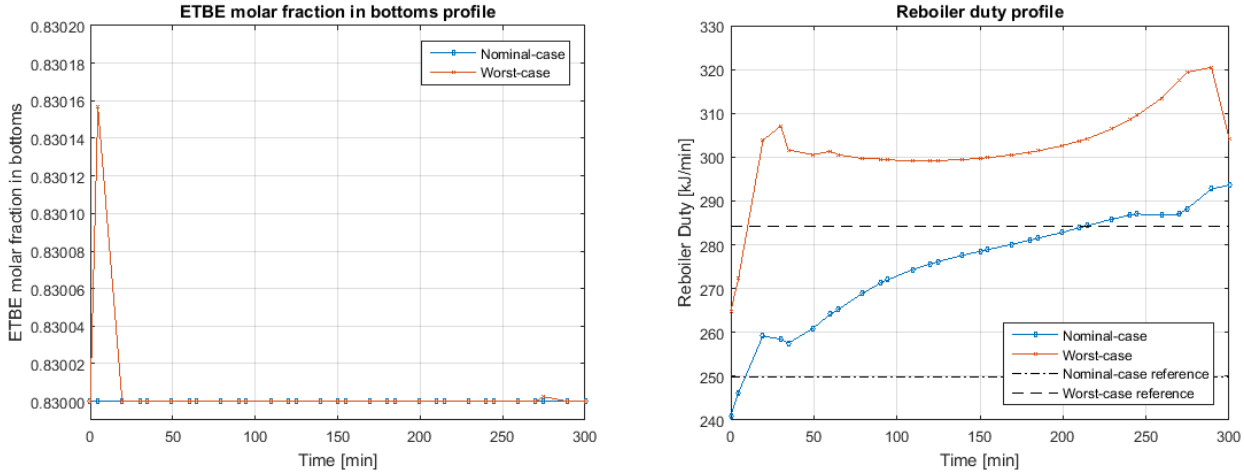

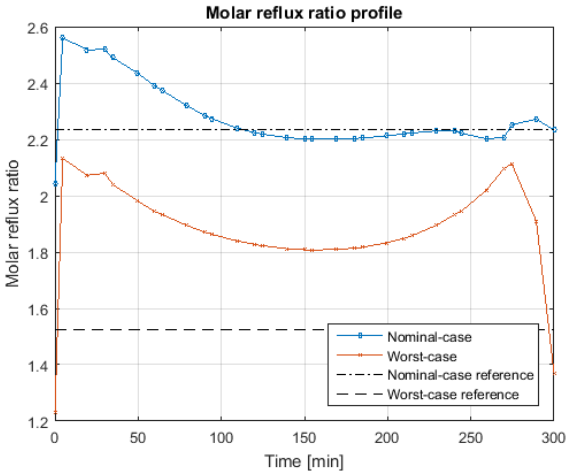

Figure 13. ETBE in bottoms and manipulated variables profiles for the OCP solution to the step disturbance

The results to the step disturbance also show that the manipulated variables have to be modified through time in order to satisfy the operational constraints of the system. The purity constraint is never violated and most of the time kept on its lower bound, because of the objective of the OCP. The step disturbance allows to notice the dynamic interaction of the manipulated variables and the feed composition, something that could be less clear with the response to the sinusoidal disturbance. As the amount of the inert n-butene in the feed increases, the reboiler duty has to increase to satisfy the purity constraint of the ETBE in the bottoms. At the same time, the reflux ratio increases to maintain the most amount of isobutene in the column to produce ETBE and it slowly decreases to get closer to its reference value.

The response to this disturbance again illustrates that the reference points obtained by the worst-case scenario in the optimal design problem are farther from the manipulated variables profiles than in the case of the nominal-case scenario. This fact increases the change in the last time steps of the solution, where both manipulated variables decrease abruptly towards the reference values.

7.4. Simultaneous Optimal Design and Control

For the simultaneous ODCP of the ETBE producing CD column, the objective function of the OCP problem also considers the installation cost of the equipment and the construction constraints. Apart of the state variables, continuous design variables are included in this optimization problem. As mentioned in Section 6.2.2, all the weighting parameters of the terms in the objective function are expressed relative to the economic objective. For instance for the investment cost C_{inv}, which is the extra part of the objective function compared to the OCP, there is no weighting parameter and the other terms have the same weighting parameters as in the OCP problem, reported in Table 9.

7.4.1. Sinusoidal disturbance

As in the section 7.3.2, the manipulated variables profiles and the ETBE molar composition in the bottoms are depicted in the Figure 14. The reference values shown here correspond to the solution of the initial condition of the problem, satisfying the purity constraint as an equality.

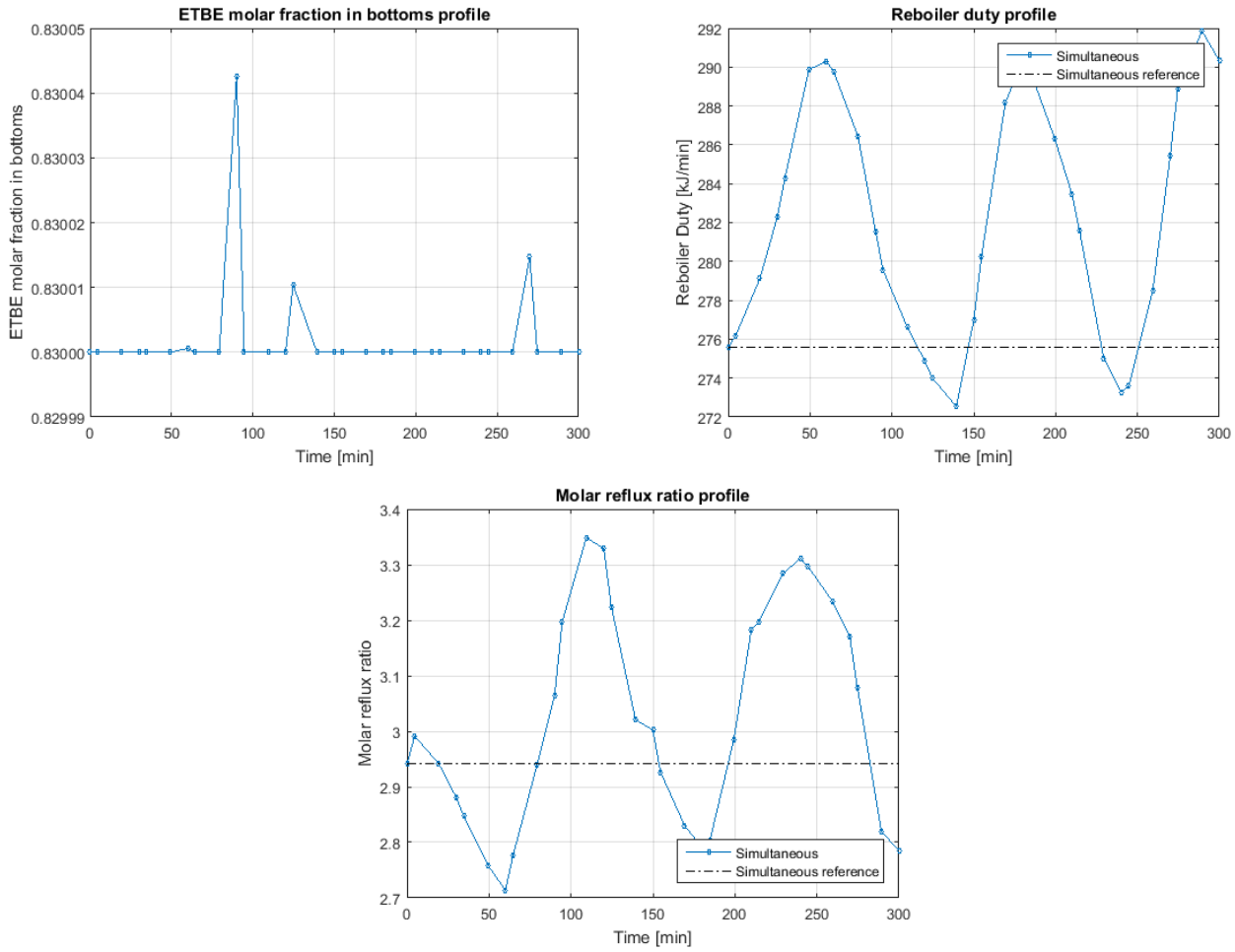

Figure 14. ETBE in bottoms and manipulated variables profiles for the simultaneous ODCP solution to the sinusoidal disturbance

The dynamic response of the ODCP solution is similar to the OCP solution. As in the Figure 12 and Figure 13, the purity constraint is never violated. The same final-time phenomena is observed, where the manipulated variables decrease abruptly to minimize the operational costs.

Besides obtaining the dynamic profiles of the manipulated variables, the simultaneous ODCP was interesting since the same design parameters are variables and the investment cost is also minimized. Comparing the sequential and the simultaneous ODCP solutions the following results are obtained.

Table 10.Comparison of the optimal solutions of the sequential and the simultaneous ODCP with a sinusoidal perturbation

	Unit	Sequential Worst-case	Sequential Nominal-case	Simultaneous
Column Diameter D_C	[m]	0.1214	0.1110	0.1106
Stage height h_S	[m]	0.0500	0.0500	0.0500
Downcomer height h_w	[m]	0.0166	0.0166	0.0166
Feed flow rate F_{but}	[mol/min]	7.514	5.772	5.266

Reference Reboiler Duty Q_{Reb}^{Ref}	[kJ/min]	284.22	249.85	275.56
Molar reflux ratio RR^{Ref}	[-]	1.525	2.237	2.941
Entrainment flooding?		No	No	No
Downcomer flooding?		**Yes**	No	No
Weeping?		**Yes**	**Yes**	No
Profit ETBE	[$/hr]	16.455	14.546	13.089
Annualized Investment cost	[$/year]	10156	10142	10141
Operating cost	[$/hr]	26.842	22.462	21.238
ETBE bottoms composition tracking $\sum_{i=0}^{N_p}\left(x_{NT,ETBE}^{min} - x_{NT,ETBE,i}\right)^2$	[(mol/mol)^2]	4.00E-7	4.06E-8	1.33E-6
Reboiler duty quadratic deviation $\sum_{i=0}^{N_p}\left(Q_{Reb}^{Ref} - Q_{Reb,i}\right)^2$	[(kJ/min)^2]	6070.62	3047.46	418.45
Reflux quadratic deviation $\sum_{i=0}^{N_p}(RR^{Ref} - RR_i)^2$	[-]	3.599	2.048	0.219

The geometrical parameters obtained for the simultaneous approach differ from the sequential solutions. The column designed has a smaller diameter compared to the sequential solutions and its feed flow rate is lower than the two sequential solutions. The reference reflux ratio is higher and the reboiler duty is lower than the sequential cases. It can be noticed that in terms of economic advantages, the investment cost for the simultaneous approach is lower than any of the sequential cases included in the Table 10. The profits from the ETBE sells are higher for both cases of sequential ODCPs. The worst-case scenario showed the best profits because of its large feed flow rate, but the operating costs of these approach are the highest too.

The tray capacity constraints are satisfied for the simultaneous approach, but for the sequential approach some of them are violated. This result is logic, since the geometrical parameters in the sequential approaches were obtained before knowing the disturbance of the system. On the other side, the simultaneous approach converged to a point which satisfies the tray capacity constraints and the dynamic equations, obtaining geometrical parameters suited to face the sinusoidal disturbance.

The two cases of sequential ODCP violate some of the tray capacity limits at some point of the simulated time. The Figure 15 shows the pressure over the weir on the second stage and the velocity through the holes in the tray for the last stage before the reboiler. As the stage next to the condenser

has the largest vapor flow rate in the column, it would be the stage where the downcomer flooding would happen. On the other side of the column, since the bottom stages have the largest liquid flows, the weeping is more likely to happen on those stages.

Finally regarding the controllability of the solutions obtained, the tracking objectives were evaluated at the solution for each approach. The nominal-case in the sequential approach was the one that had the best tracking objective from the controlled variable. The simultaneous approach had the lowest values for the tracking in the manipulated variables, which can be explained as the reference values were variables in this approach, while on the sequential approach those values were obtained in the steady-state optimization. The worst-case sequential approach had the largest tracking objectives since it was designed far from the initial condition of the system and the control had to force the system out of the reference values to satisfy the dynamic constraints.

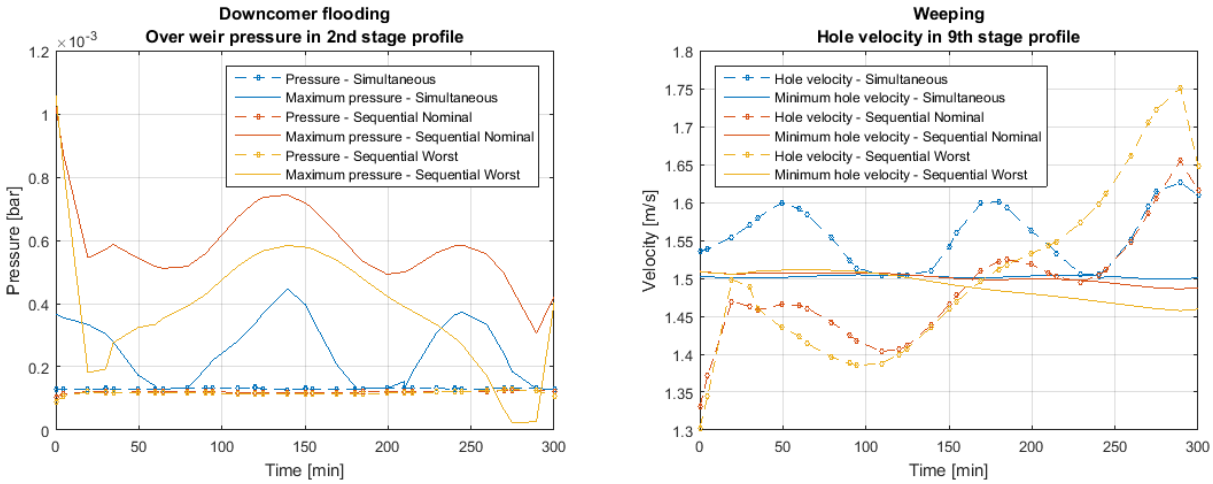

Figure 15. Over weir pressure and hole velocity profiles for the most likely stages to be affected by downcomer flooding and weeping for the sinusoidal disturbance

The worst-case sequential ODCP solution is beyond the tray capacity limits in terms of downcomer flooding and weeping. In the case of downcomer flooding, its second stage has an over weir pressure larger than the maximum allowed at the last time steps. Weeping occurs on the first time steps in the ninth stage for both the worst-case and the nominal case sequential ODCP.

Since the reflux ratio and the reboiler duty are manipulated over time, there are changes on the flows and not only on the compositions through the column. These changing flow rates have effect on the variables related to them, such as the stage pressure, the compressibility factor or the reaction rate. The given profiles are shown in the Figure 16.

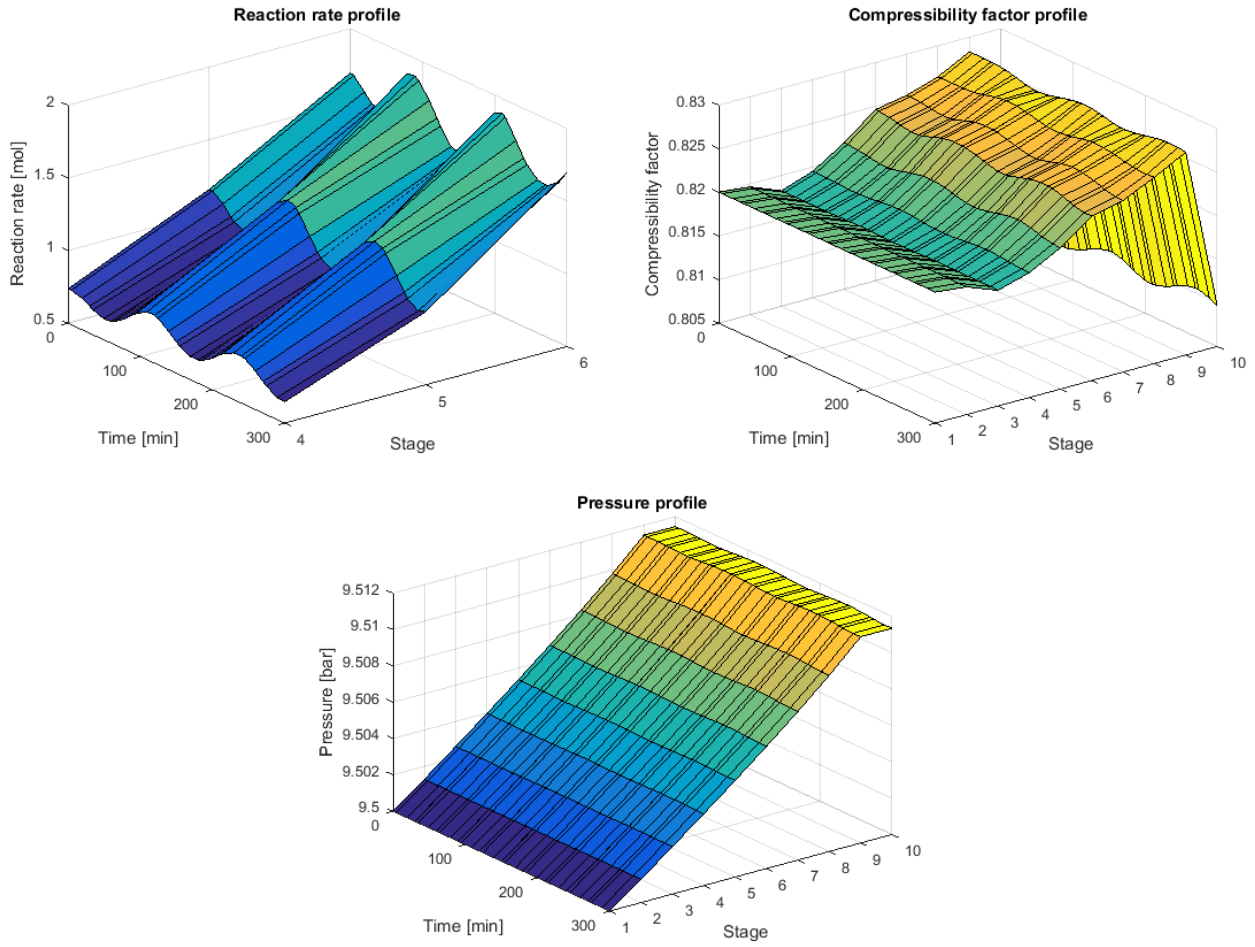

Figure 16. Dynamic behavior of reaction rate, compressibility factor and stage pressure in the ODCP solution with sinusoidal disturbance

As regarded in the dynamic simulation the reaction rate is more dependent than the compressibility factor and the stage pressure with time. The reaction rate appears to have been controlled indirectly by solving the OCDP and showing a higher rate in the lowest stage with catalyst.

The relative and standard deviations were calculated for this case and are presented in the Table 11.

Table 11. Standard and relative deviations for reaction rate, compressibility factor and stage pressure in the OCDP solution with sinusoidal disturbance

Stage	Reaction rate		Compressibility factor		Stage pressure	
	$\sigma\left[\frac{mol}{kg_{cat}}\right]$	$\frac{\sigma}{\mathcal{R}}$ [%]	σ	$\frac{\sigma}{Z}$ [%]	$\sigma\,[bar]$	$\frac{\sigma}{P}$ [%]
1	-	-	3.21E-06	3.91E-04	0	0
2	-	-	7.55E-06	9.21E-04	3.71E-06	3.71E-06
3	-	-	3.82E-05	4.67E-03	7.91E-06	7.91E-06

4	0.0623	8.5274	1.36E-04	1.66E-02	1.31E-05	1.35E-05
5	0.1201	10.5261	3.23E-04	3.93E-02	1.39E-05	2.09E-05
6	0.1271	7.5800	3.96E-04	4.80E-02	1.96E-05	2.89E-05
7	-	-	3.79E-04	4.59E-02	3.53E-05	3.75E-05
8	-	-	3.20E-04	3.87E-02	5.81E-05	4.50E-05
9	-	-	3.34E-04	4.04E-02	8.78E-05	4.87E-05
10	-	-	7.00E-04	8.64E-02	8.78E-05	4.87E-05
Average	0.1032	8.8812	2.64E-04	3.21E-02	3.24E-06	2.55E-05

It can be noticed again that the compressibility factor and the stages pressures dependence on the time is negligible. The optimal control solution has actually decreased the deviation of all three analyzed variables, making the assumption of no dynamic behavior for the pressure and the compressibility factor more valid. This will be useful when applying the different index DAE dynamic models to solve the OCP problem, which require an assumption of constant compressibility factor and pressure over time.

7.4.2. Step disturbance

The same methodology was adopted to compare the sequential and simultaneous approaches of the ODCP using the step disturbance introduced in the section 7.2.2. The profiles of the manipulated variables and the ETBE molar composition in the bottoms for the simultaneous approach are show in the Figure 17 below.

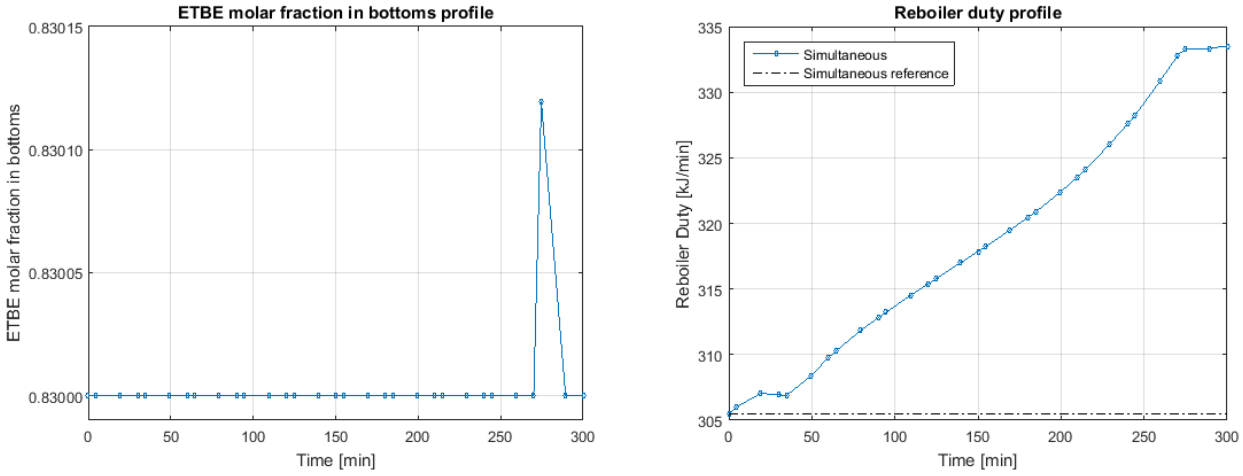

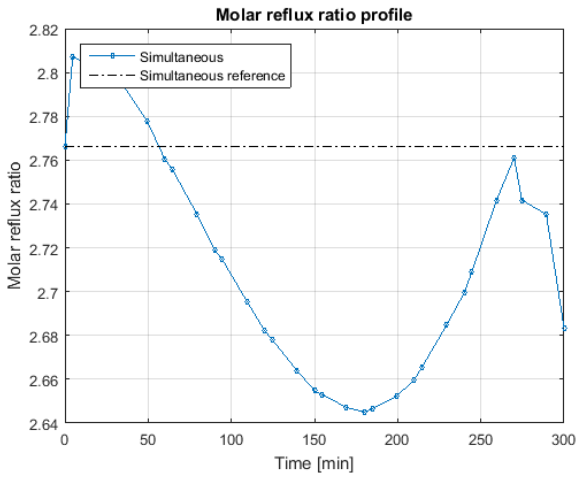

Figure 17. ETBE in bottoms and manipulated variables profiles for the simultaneous ODCP solution to the step disturbance

As all the cases of OCP exposed in this work, the ETBE purity constraint is never violated. The manipulated variables response to the step disturbance is again affected by an abrupt change in the last time steps to benefit the economic objective.

A similar table to the Table 11, reflecting the differences of the geometrical, economic and tray capacity phenomena between the sequential approached and the simultaneous for the step function is presented.

Table 12. Comparison of the optimal solutions of the sequential and the simultaneous ODCP with a step perturbation

	Unit	Sequential Worst-case	Sequential Nominal-case	Simultaneous
Column Diameter D_C	[m]	0.1214	0.1110	0.1284
Stage height h_S	[m]	0.0500	0.0500	0.0500
Downcomer height h_w	[m]	0.0166	0.0166	0.0166
Feed flow rate F_{but}	[mol/min]	7.514	5.772	6.219
Reference Reboiler Duty Q_{Reb}^{Ref}	[kJ/min]	284.22	249.85	305.49
Molar reflux ratio RR^{Ref}	[-]	1.525	2.237	2.766
Entrainment flooding?		No	No	No
Downcomer flooding?		**Yes**	No	No
Weeping?		**Yes**	**Yes**	No
Profit ETBE	[$/hr]	15.628	12.274	13.406
Investment cost	[$]	10156	10142	10039
Operating cost	[$/hr]	26.845	22.479	23.662

ETBE bottoms composition tracking $\sum_{i=0}^{N_p}\left(x_{NT,ETBE}^{min} - x_{NT,ETBE,i}\right)^2$	[(mol/mol)^2]	3.50E-7	1.08E-9	2.67E-5
Reboiler duty quadratic deviation $\sum_{i=0}^{N_p}\left(Q_{Reb}^{Ref} - Q_{Reb,i}\right)^2$	[(kJ/min)^2]	9042.07	6935.88	1242.219
Reflux quadratic deviation $\sum_{i=0}^{N_p}(RR^{Ref} - RR_i)^2$	[-]	2.954	0.477	0.027

The simultaneous ODCP solution resulted in a column with a larger diameter than any of the sequential approach solutions to the problem. This larger diameter was required to hold the tray capacity constraints with the large reference reboiler duty and reflux ratio obtained. Even when the flow rate is lower than the worst-case sequential solution, the amount of mass in the column due to the high reflux required a larger column in diameter. The profit for the ETBE obtained for the simultaneous ODCP solution lies in between the sequential solutions, same as the operating cost. As the investment cost is proportional to the column diameter, the simultaneous approach converged to a higher investment cost than the other two cases.

The same trend from the sinusoidal disturbance is obtained with the step disturbance in terms of the tracking objectives. The worst-case sequential approach had the largest of the manipulated variables tracking objectives, while the simultaneous had the lowest. The nominal case had the lowest ETBE bottoms set-point tracking objective.

In order to verify the tray capacity constraints, hole velocity and over weir pressure for the critical stages results for each approach are presented in the Figure 18.

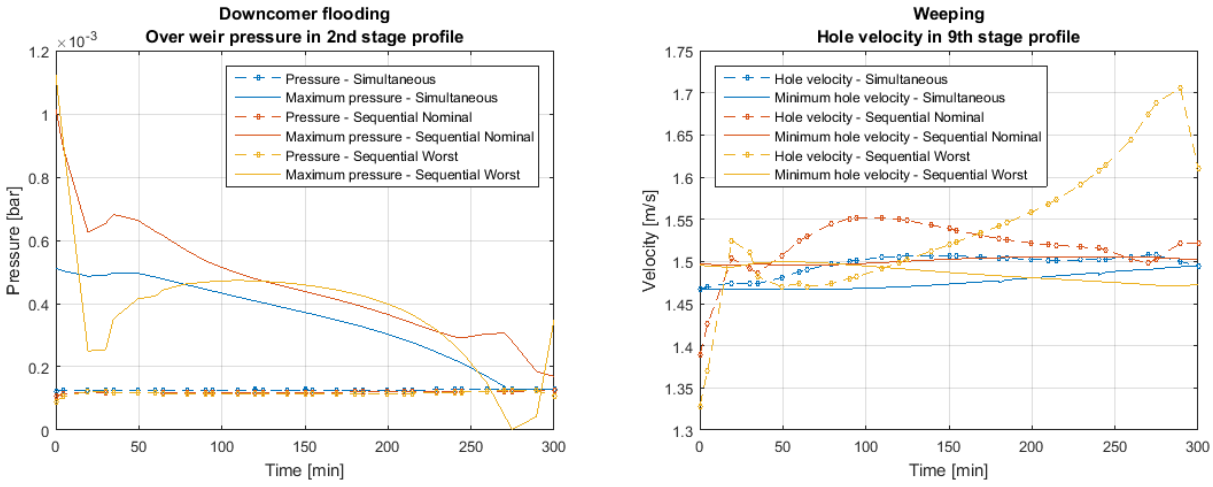

Figure 18. Over weir pressure and hole velocity profiles for the most likely stages to be affected by downcomer flooding and weeping for the step disturbance

For the step disturbance, the worst-case sequential approach resulted in a column which exceeds the tray capacity limits in terms of over weir pressure in the second stage and hole velocity of the 9th stage, resulting in downcomer flooding and weeping respectively. The nominal sequential approach also surpassed the limits of the hole velocity in the 9th stage. The simultaneous approach respected all the tray capacity limits.

For the completeness of this work a dynamic analysis of the reaction rate, the compressibility factor and the pressure is analyzed. The profiles are shown in the Figure 19.

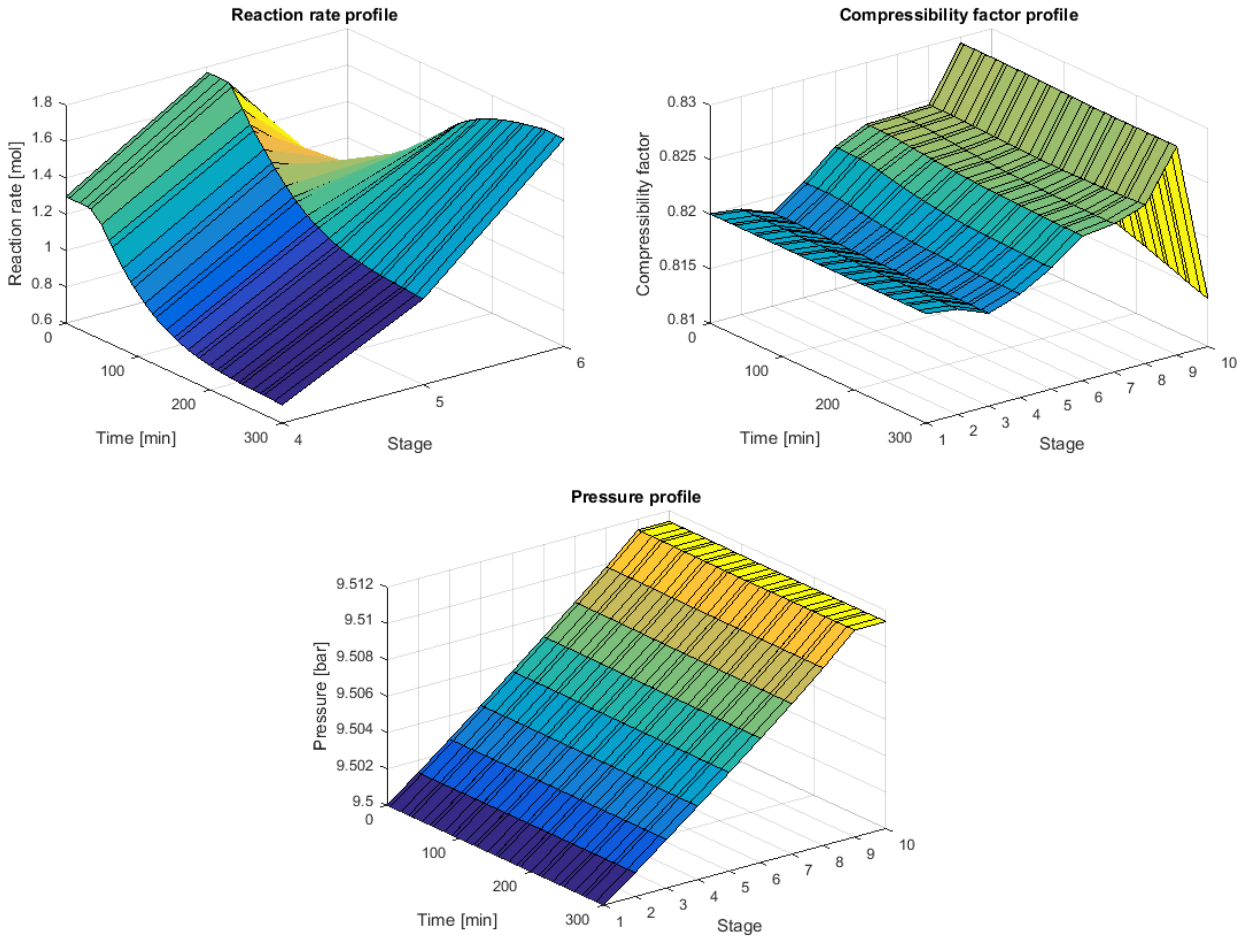

Figure 19. Dynamic behavior of reaction rate, compressibility factor and stage pressure in the ODCP solution with step disturbance

As in the dynamic simulations and the simultaneous ODCP with a sinusoidal disturbance, the standard deviation for the reaction rate, the compressibility factor and the stage pressure are determined in the Table 13.

Table 13. Standard and relative deviations for reaction rate, compressibility factor and stage pressure in the OCDP solution with step disturbance

Stage	Reaction rate		Compressibility factor		Stage pressure	
	$\sigma\left[\frac{mol}{kg_{cat}}\right]$	$\frac{\sigma}{\mathcal{R}}$ [%]	σ	$\frac{\sigma}{Z}$ [%]	$\sigma\,[bar]$	$\frac{\sigma}{P}$ [%]
1	-	-	3.07E-06	3.74E-04	0	0
2	-	-	8.65E-06	1.06E-03	4.74E-06	4.99E-05
3	-	-	5.21E-05	6.37E-03	8.19E-06	8.62E-05
4	0.2209	24.4073	4.26E-04	5.19E-02	1.55E-05	0.0001635
5	0.2515	19.0442	7.05E-04	8.57E-02	2.39E-05	0.0002516
6	0.3390	24.2345	3.79E-04	4.60E-02	2.88E-05	0.0003029
7	-	-	3.09E-04	3.75E-02	2.89E-05	0.0003041
8	-	-	1.25E-04	1.52E-02	2.38E-05	0.0002507
9	-	-	1.33E-04	1.60E-02	1.52E-05	0.0001596
10	-	-	1.42E-03	1.73E-01	1.52E-05	0.0001596
Average	0.2705	22.5620	3.56E-04	4.34E-02	1.64E-05	1.73E-04

It is remarkable that the solution of the simultaneous OCDP problem with a step disturbance resulted in the response with the largest standard deviation for the three variables analyzed. This result is due to the not very smooth responses of the manipulated variables, which had effect in the flow rates inside the column and in the variables listed in the Table 13.

7.5. Comparison of different DAE formulations

Based on the profiles of compressibility factor and pressure shown in the Figure 10, the Figure 11 and the Figure 16, the dynamic behavior of these variables can be neglected. All this models were an implementation of the DAE1 dynamic model, which included detailed hydraulic correlations, vapor hold-ups and dynamic response of all variables. This allows the implementation of the different DAE models presented in Section 4.2. The design parameters chosen for this comparison were the obtained by the nominal-case sequential optimization. This case was chosen over the simultaneous approach solution because it was the approach that had the smallest tracking objective respect to the set point in the ETBE bottoms molar composition. Four different formulations of the optimal control problem were proposed. These formulations varied in how detailed the model was and the Hessenberg index of the DAE systems. From this point the detailed model will be denoted as DAE1, the simplified model will be denoted as DAE2, the index reduced simplified model will be denoted as DAE2r, and the hybrid model of the DAE2 and the DAE2r will be denoted as DAE2h. These models are based on the work of Lozano et al. [27]

This comparison is made in order to verify the equivalence of the models and their validity for the OCP solution. The simultaneous ODCP problem was not considered to be tested with the different DAE models since all of them, except for the DAE1, assume constant pressure and the compressibility factor. Since the design of a process must be as detailed as possible; the detailed model was used in the optimal design parts of this work which include Sections 7.1 and 7.4.

The size of the different DAE models after the discretization using orthogonal collocation with 10 finite elements and 3 collocations points is shown in the Table 14. The discretization method of the DAE systems is explained in detail in the Appendix B - OCP representation as NLP problem and solution algorithms.

Table 14. Number of equations and variables for the different DAE optimal control formulations

	DAE1	DAE2	DAE2r	DAE2h
Number of equations	42099	28291	79110	41010
Number of variables	42272	28402	79211	41111

From the Table 14, note that the amount of equations and variables for the DAE1 formulation is considerably more than from the DAE2 model. This is because the DAE1 formulation includes the hydraulic correlations and the time evaluation for the compressibility factor and the stage pressure. The DAE2r is the formulation with the highest number of equations and variables, as the intermediate variables obtained by the derivatives expressions appear. The DAE2h formulation has less equations and variables than the DAE2r formulation as it only calculates the derivatives on the finite elements boundaries, and not in the collocation points.

Once the models were implemented, the OCP was solved with each formulation using the weighting parameters explained in Table 9. The manipulated variables, the ETBE molar bottoms composition, the reboiler temperature and the condenser duty profiles are presented in the Figure 20 and the Figure 21. The temperature in the reboiler and the condenser duty are used as indicators of the fidelity of the formulations to the DAE1. The reboiler temperature is the most likely to be measured in a real system to control the behavior of the process, as it is the stage with the largest change in temperature and the product is obtained from the bottoms.

7.5.1. Sinusoidal disturbance

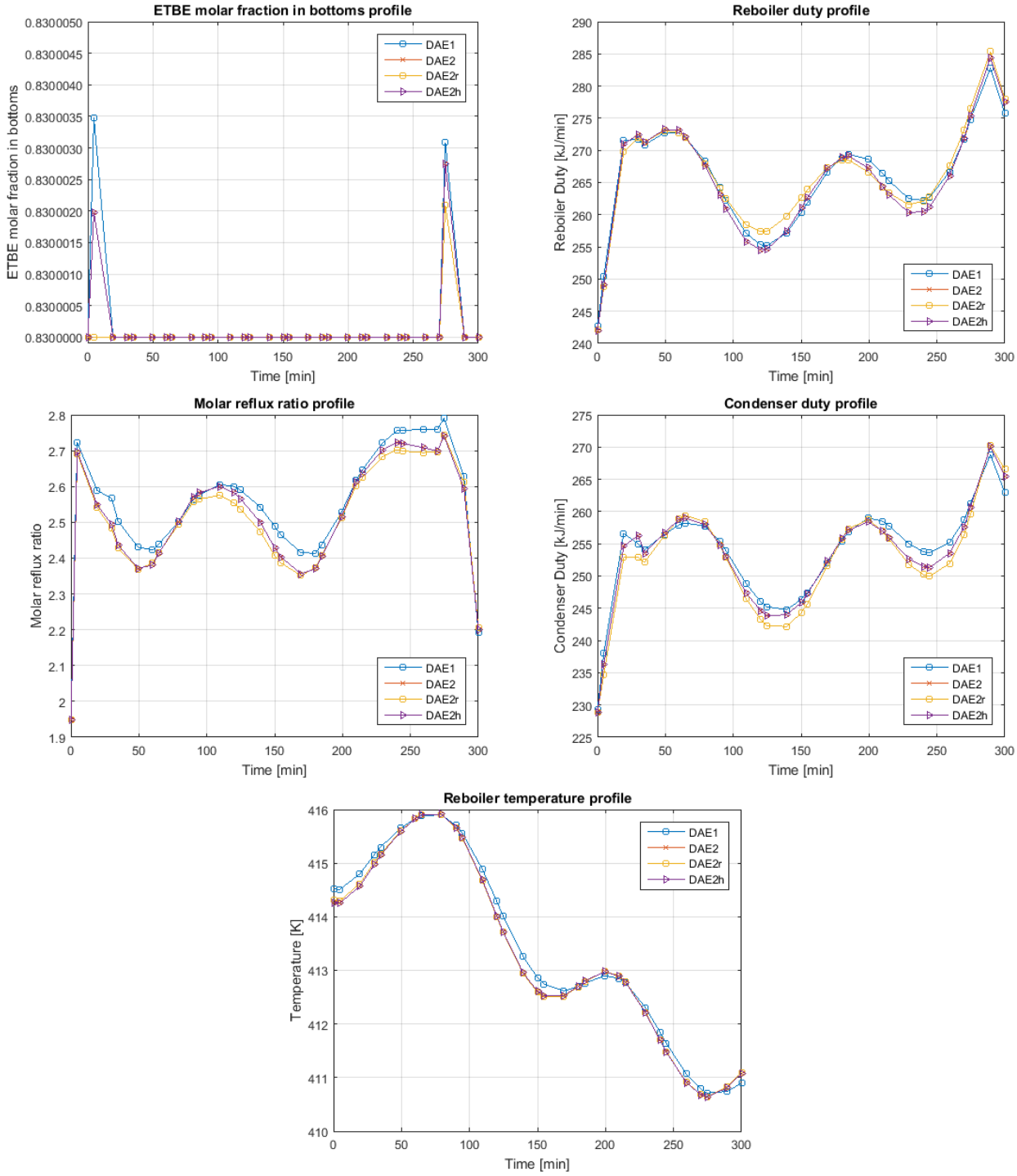

Figure 20. ETBE in bottoms, manipulated variables, reboiler temperature and condenser duty profiles for the OCP solution with the different DAE models subject to the sinusoidal disturbance

All of the models appear to have a very similar solution to the OCP problem. Even if the detailed DAE1 model considers the dynamics of the compressibility factor and the stage pressure, the profiles obtained are very similar. In order to compare the accuracy of the models relative to the DAE1 a mean

absolute error (MAE) in the manipulated variables and the ETBE bottoms molar composition is calculated and presented in the Table 15.

Table 15. Mean absolute error of the manipulated variables, the ETBE bottoms molar composition, the condenser duty and the reboiler temperature of the DAE models respect to the DAE1 solution for the sinusoidal disturbance

	Units	DAE2	DAE2r	DAE2h
Reboiler Duty Q_{Reb}	[kJ/min]	0.9047	1.1206	0.9047
Molar reflux ratio RR	[-]	0.0339	0.0427	0.0339
ETBE bottoms composition $x_{NT,ETBE}$	[mol/mol]	4.586E-6	1.117E-6	4.586E-6
Condenser Duty Q_{Cond}	[kJ/min]	0.9668	4.2837	3.5359
Reboiler temperature T_{Reb}	[K]	0.1292	0.1275	0.1292

7.5.2. Step disturbance

The same analysis was made using the step disturbance presented in Section 7.2.2. The profiles of the selected variables are shown in the Figure 21.

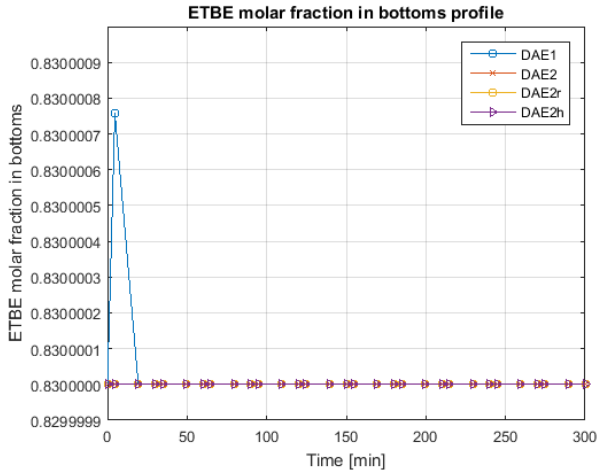

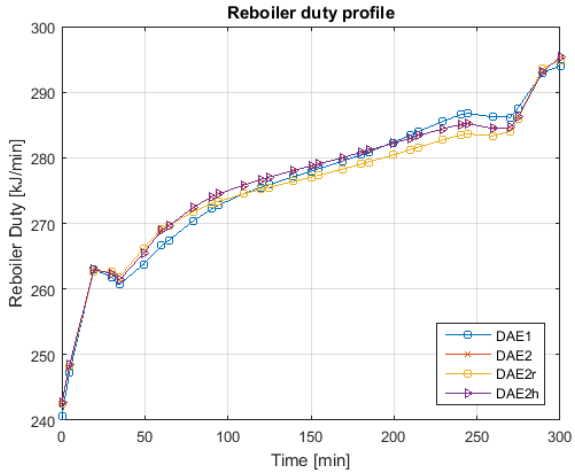

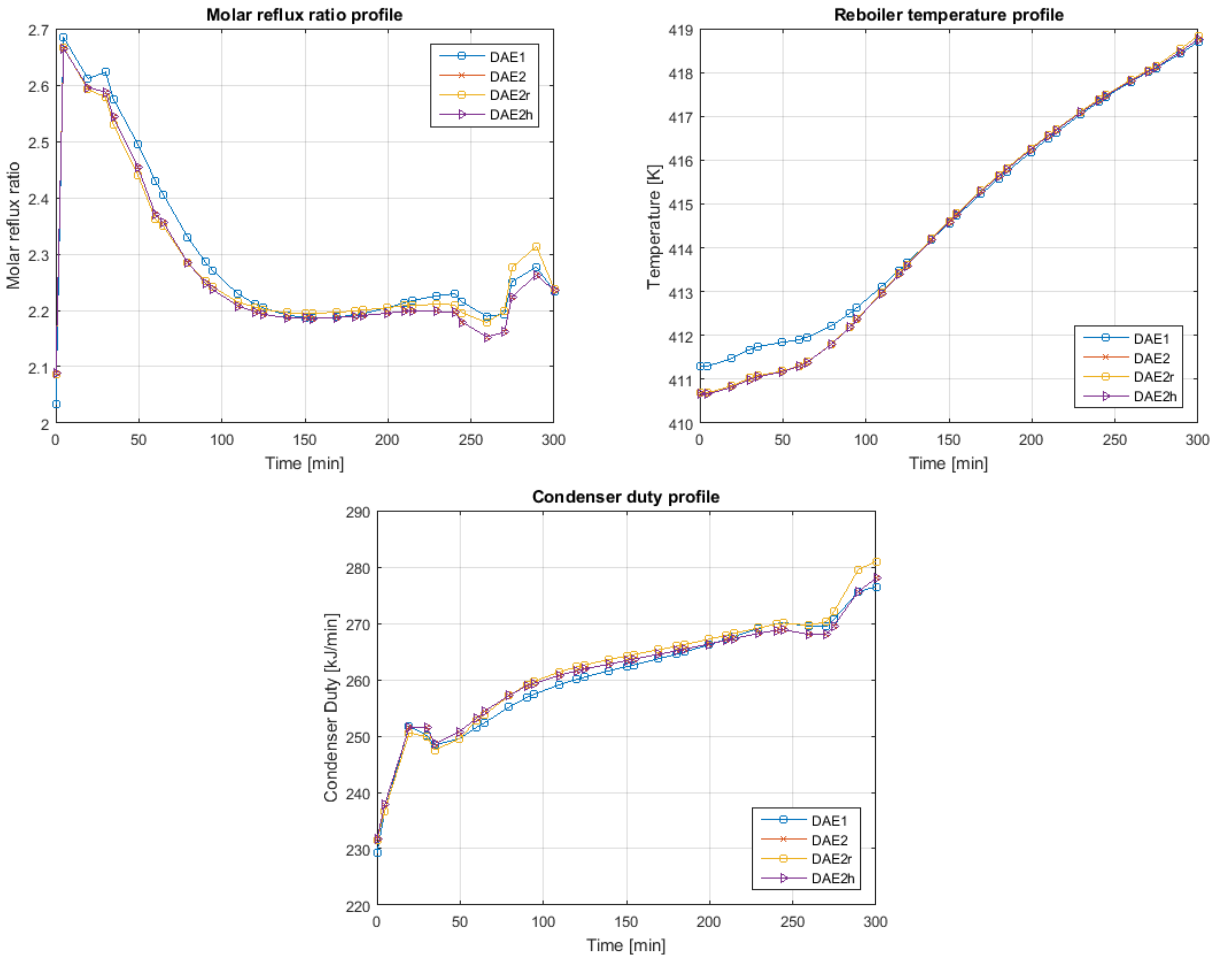

Figure 21. ETBE in bottoms, manipulated variables, reboiler temperature and condenser duty profiles for the OCP solution with the different DAE models subject to the step disturbance

Note that there is a great similarity among the profiles of the different DAE formulations. A MAE analysis is made in the same variables with the step disturbance obtaining the results present in the Table 17.

Table 16. Mean absolute error of the manipulated variables , the ETBE bottoms molar composition, the condenser duty and the reboiler temperature of the DAE models respect to the DAE1 solution for the step disturbance

	Units	DAE2	DAE2r	DAE2h
Reboiler Duty Q_{Reb}	[kJ/min]	1.1346	1.5180	1.1346
Molar reflux ratio RR	[-]	0.0241	0.0219	0.0241
ETBE bottoms composition $x_{NT,ETBE}$	[mol/mol]	1.892E-6	1.892E-6	1.892E-6
Condenser Duty Q_{Cond}	[kJ/min]	5.9317	6.1386	6.1127
Reboiler temperature T_{Reb}	[K]	0.2261	0.2336	0.2261

The difference between the DAE2 and the DAE2h models is negligible. On the other side the DAE2r presents slight differences when compared to the modified models and its solution is closer to the DAE1 model solution. Although the analytical solution of the DAE2r and the DAE2h models should be the same, there are differences in the solutions obtained for these two models. According to Lozano et al. [27], the factors that can originate these differences are the collocation method and the drift-off phenomena observed when an equation is replaced by its differential equivalent. As mentioned in Table B.1, the truncation error for the collocation methods varies among the differential and algebraic equations. As the accuracy is higher for the algebraic variables, the solutions may differ. This is because the DAE2r model includes the algebraic variables for all the collocation points, while the DAE2h just in the limits of the finite elements. On the other side, replacing the energy balance by its differential equivalent could originate a drift-off that moved the solution away from its true manifold[85].

This comparison was made in order to determine the validity of the DAE models for the case study. As mentioned by other authors [27], [28], [57], the application of simplified DAE models increases the computational efficiency of solving optimal control problems. As long as the assumptions that support the use of these models hold as shown in the OCP results, there is always a potential of using them. One application, where the efficient solution of optimal control problems is required is the NMPC, in which an OCP must be solved in a certain period of time less than the sampling time. This must be done to avoid time delays and instabilities and assure the controllability of the process. An example of that implementation is shown in the following section.

7.6. Economic Oriented Non Linear Model Predictive Control

The recursive solution of OCP problems and the application of the control policy dictated by the first element of the solution was implemented into an Economic-Oriented NMPC. The formulation of the optimization problem is described in the section 6.4. As mentioned in that section, the objective function differs from the objective functions used on the previous sections. The first modification is that the manipulated variables do not vary during the whole time, but are only modified every certain sampling time, determined to be 5 minutes. These manipulated variables were controlled not by considering the squared difference from a reference value, but by considering the squared instant difference. The control and prediction horizons may not be equal, which modified the sum of the manipulated variables deviation to reach until the control horizon lasted. The modification explained made the tuning of the weighting parameters defined before non-valid, so the methodology explained in the section 6.2.2 was applied for this objective function in order to determine these weighting parameters by solving it for the initial OCP to be solved.

The EO-NMPC is implemented to have a control and prediction horizon of 50 minutes, time where an OCP problem is solved, and the system will be disturbed with a step function in the butenes feed molar composition as presented in the section 7.2.2. The sampling time will be of 5 minutes and the system will be analyzed for 300 minutes. The dynamic model was chosen to be the DAE2h, due to the advantages in terms of computational time [27]. The obtained weighting parameters are presented in the Table 17.

Table 17. Weighting parameters for the EO-NMPC objective function

Objective	Lower bound ϕ^{Lo}	Upper bound ϕ^{Up}	Weighting parameter α
ETBE bottoms composition tracking $\sum_{i=0}^{N_p}\left(x_{NT,ETBE}^{min} - x_{NT,ETBE,i}\right)^2$	2.72	2.29E+3	2.05E-02
Reboiler duty instant quadratic deviation $\sum_{i=0}^{N_u}\left(Q_{Reb,i} - Q_{Reb,i-1}\right)^2$	1.48E-18	1.74E+5	1.56E+00
Reflux ratio instant quadratic deviation $\sum_{i=0}^{N_u}\left(RR_i - RR_{i-1}\right)^2$	1.04E-15	3.85E+1	3.46E-04
Operation cost $\sum_{i=0}^{N_p} C_{op,i}$	-906034.749	-794721.667	1.00

In order to compare the EO-NMPC control strategy, a Proportional and Integral (PI) controller was implemented. The PI control strategy uses two SISO PI, one manipulating the reboiler duty and the other the reflux ratio. The control strategy of both controllers was to control the ETBE molar composition in the bottoms. An optimization problem was proposed in order to minimize the quadratic difference of the ETBE molar bottoms composition with the set-point, leaving the gain and the time integral constant of both controllers as variables. The system is then disturbed by the same step disturbance as the EO-NMPC. The solution of this problem would result on a PI control strategy which has a simulation time of 300 minutes. The obtained tuning parameters for the PI control strategy are listed in the Table 18. Note that the purity constraint presented in the Section 6.2.2 was not included.

Table 18. Tuning parameters for optimal PI controllers

	Gain	Integral time constant [hr]
Reflux ratio control	$-37.382\ \frac{mol/min}{\%}$	1.457E-4
Reboiler duty control	$89946.656\ \frac{kJ/min}{\%}$	74.545

The effect of the reboiler duty on the ETBE bottoms composition is direct and the one of the reflux ratio is inverse. As the reboiler duty increases, the more volatile component on the CD boil benefiting the purity of the ETBE in the bottoms. As the reflux ratio increases, these more volatile components are

sent back into the column, decreasing the separation efficiency of the ETBE in it. Similar conclusions can be obtained from the signs of the gain in the optimal PI controllers tuning parameters.

After solving the EO-NMPC and implementing the PI control strategy, the system is disturbed with a decrease from 0.3 to 0.25 of isobutene molar feed fraction. The manipulated variables and the ETBE bottoms molar composition are shown in the Figure 22 below.

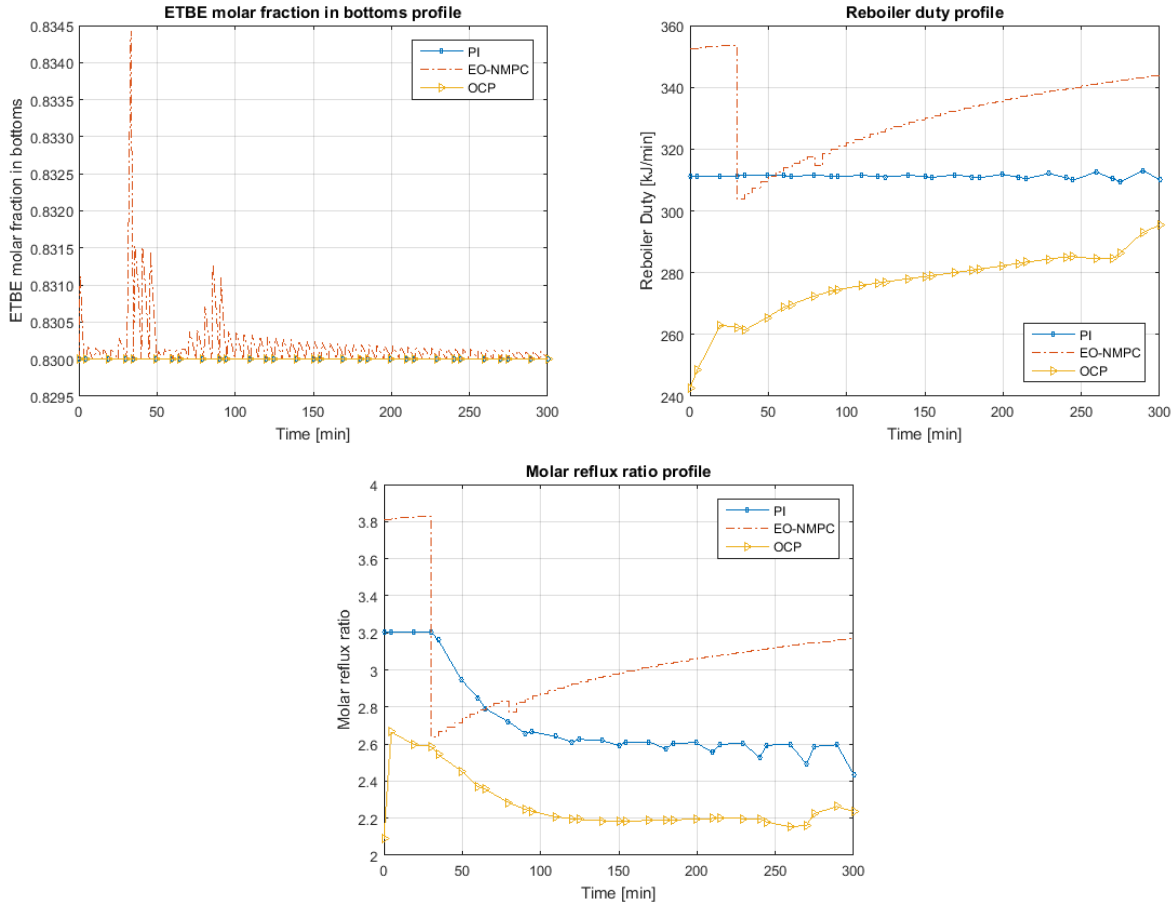

Figure 22. Control profiles for the step disturbance using PI, EO-NMPC and OCP control strategies

In the Figure 22, it can be seen that the two control strategies result in a different steady states after facing the disturbance. As the PI controller does not have economic considerations, the steady state achieved after 5 hour of operation is different from the one obtained by the NMPC and the OCP. The OCP solution shown in the Figure 22 corresponds to the DAE2h formulation.

The variation of the reboiler duty from the PI controller is almost none compared to the action of the EO-NMPC. The PI controller seems to have oscillation at the end of the simulation time. This fact is a problem from the control point of view, since the oscillation appears to grow with time. This could be originated by the action of the two controllers, which act upon each other incrementing the error over time. The response to the disturbance is based on a perfect forecast, for instance the EO-NMPC is able to respond almost immediately as the disturbance appears.

The EO-NMPC appears to stabilize the response of the system in the given time. On the other hand, the OCP problem varies the manipulated variables too rapidly. This fact affected the stability of the controller responses and are caused mainly because of the closed-loop and open-loop nature of the EO-NMPC and the OCP control strategy respectively.

A comparison in the economic performance of each control strategy is presented in the Table 19, where the economic profit at the end of the simulation time is stated.

Table 19. Economic performances of control strategies

	Economic Profit after 300 minutes [$]	EO-NMPC Economic advantage
PI	730306.7	5.76%
OCP	743466.2	4.06%
EO-NMPC	774919.8	-

Note that the EO-NMPC apart of stabilizing the system in the given time, has a 5.76% and 4.06% better economic performance in the solution of the control problem. This advantage in not negligible and can mean considerable savings by implementing it.

8. Conclusions and perspectives

In this work, a steady state and a dynamic model based on fundamental principles for a catalytic distillation column has been proposed. Using large scale NLP algorithms, the optimization of an ETBE production catalytic distillation column was performed. The proposed model included hydraulic constraints and product specification; and was solved for the steady-state and for the dynamic operation. The optimal design problem was solved in order to minimize the annualized cost of investment and operation, while satisfying operational constraints and the MESH model constraints. A comparison was made with the results of two other works regarding the same system, which considered certain simplifications over the model; showing that the completeness of the steady-state model is vital for a successful optimal design.

A dynamic simulation of the uncontrolled system was made in order to confirm the use of a control strategy to satisfy operational constraints. An optimal control problem was proposed by representing the DAE of the dynamic model as a large scale NLP problem using orthogonal collocation. The optimal control of the system subject to a sinusoidal and a step disturbance was implemented and successfully tested. It satisfies the operational constraints during the whole time horizon considered. The compressibility factor and the stage pressure did not vary with time given the disturbances analyzed in this work. This indicated that their dynamical behavior could be neglected. The reaction rate seems to be strongly affected by the disturbance in the feed composition, showing the considerable error that would mean to define its dynamics negligible.

Two different approaches have been considered to propose an optimal design and control of this unit, sequential and simultaneous. The sequential approach was based in the optimal design of the process

using the detailed steady state model subject to design constraints and later using the result of this optimization to propose an optimal control scheme. The simultaneous approach considered the design constraints and the investment cost together with the dynamic behavior of the system and solved an optimal design and control problem at once.

The dynamic optimization problems proposed took into account tracking and economic objective functions. In order to optimize both contradictory objectives, a weighted sum of them was taken as objective function. A methodology based on offline utopia tracking multiobjective optimization was proposed to determine the weighting parameters in the objective function.

The optimal design and control approaches were tested against different cases of composition in the butenes feed stream, ranging from 0.25 to 0.35 of isobutene molar fraction. In the dynamic case, a sinusoidal and a step disturbance were applied to the system. In both cases the simultaneous approach resulted in different design parameters compared to the sequential approaches. The sequential approaches could not satisfy the design specifications after the optimal control problem was solved, even if during the optimal design stage these constraints were satisfied and the design was made based on the worst-case scenario. On the other hand, the simultaneous approach solution satisfied the design specification for the whole analyzed time.

This work also compared the solutions to the OCP problem with the disturbances described before using different DAE models for the column. This comparison was made to show the validity of the simplified models in the range of the disturbances and its potential application on advanced control strategies. Finally, applying the DAE2h simplified model, an EO-NMPC problem was solved for the system and compared against the solution of a PI controller and the OCP solutions. As the NMPC control strategy requires a solution of an OCP for each sampling time, and the objective control also considered both tracking and economic objectives; the methodology proposed in this work was applied to determine the weighting parameters in the objective function. The implementation of the EO-NMPC control strategy meant saving of the order of 5% compared to the PI and the OCP control strategies with a step disturbance in the butenes feed stream composition.

Future work can head into two different directions. The first direction is regarding the ODCP problem, where improvements and refinements of the model can be made. In this work, only continuous design variables were considered. There are design variables of a catalytic distillation column which are discrete (e.g. stage number, feed position, catalytic stages number and position) which can be taken also into account in both the sequential and the simultaneous approaches. This would require to solve a Mixed Integer NonLinear Programming (MINLP) or a Mathematical Programming with Complementarity Constraints (MPCC) problem for the sequential case and a Mixed Integer Dynamic Optimization (MIDO) for the simultaneous approach. Future work can also be focused on the advanced control strategies, which were just introduced in this work. Model-Plant mismatch, different prediction and control horizons, measurement noise and many other refinements can be made in this direction. Other multiobjective optimization alternatives can be studied in order to improve the weighting parameter determination methodology proposed in this work.

Appendix A – Mathematical models

This work presents the optimization of a CD column for the production of ETBE. In order to construct this problem, mathematical models for the equation of state (EOS) (e.g. the non-ideality in the vapor phase), the activity equation (e.g. the non-ideality of the liquid phase), several physical properties, and the hydraulic correlations have to be implemented. This appendix describes these various models in detail.

A.1. Equation of state

There are many equations of state (EOS) models available in the literature. No single model is the best for all systems. In this work the Soave-Redlich-Kwong (SRK) EOS was used to estimate the needed properties such as enthalpy and density using the concept of departure function and compressibility factor.

The SRK EOS of state is

$$P = \frac{RT}{V-b} - \frac{a}{V(V+b)} \tag{A.1}$$

where

$$b_i = 0.08664\frac{RT_{C,i}}{P_{C,i}} \tag{A.2}$$

$$a_i = \alpha_i 0.42747\frac{R^2T_{C,i}^2}{P_{C,i}} \tag{A.3}$$

$$\alpha_i = \left[1 + m_i\left(1 - \left(\frac{T}{T_{C,m}}\right)^{1/2}\right)\right] \tag{A.4}$$

$$m_i = 0.48508 + 1.55171\omega_i - 0.15613\omega_i^2 \tag{A.5}$$

$$b = \sum_{i\in C} y_i b_i \tag{A.6}$$

$$a = \sum_{j\in C}\sum_{i\in C} y_j y_i \sqrt{a_j a_i} \tag{A.7}$$

$$A = \frac{aP}{(RT)^2} \tag{A.8}$$

$$B = \frac{bP}{RT} \tag{A.9}$$

Where $T_{C,i}$, $P_{C,i}$ and ω_i are the critical temperature, critical pressure and acentricity factor, respectively, of component i. y_i is the vapor mole fraction. In order to avoid the numerical error when evaluating a property when the temperature is higher than the critical temperature of a component, the mixture critical temperature $T_{C,m}$ is used. For the SRK model, the resulting expression for this property is [86]:

$$T_{C,m} = \frac{\left[\sum_{i \in C}\left(y_i \frac{T_{C,i}}{P_{C,i}^{0.5}}\right)\right]^2}{\sum_{i \in C}\left(y_i \frac{T_{C,i}}{P_{C,i}}\right)} \tag{A.10}$$

The compressibility factor Z con be calculated using the SRK EOS as:

$$Z^3 - Z^2 + (A - B - B^2)Z - AB = 0 \tag{A.11}$$

There are three roots for Eq. A.11. The smallest one corresponds to the liquid compressibility factor Z_L and the largest correspond to the vapor compressibility factor Z_V. The middle root has no meaning [87].

The fugacity coefficient can be then calculated using the compressibility factor as follows.

$$\varphi_i = \exp\left(\int_0^P \frac{Z-1}{P} dP\right) = \exp\left((Z-1)\frac{b_i}{b} - ln(Z-b) - \frac{a}{b}\left(2\sqrt{\frac{a_i}{a}} - \frac{b_i}{b}\right) ln\left(\frac{Z-b}{Z}\right)\right) \tag{A.12}$$

Departure functions are defined as the difference between the property in the real state and an ideal gas state at the same temperature. The enthalpy departure function using SRK EOS is:

$$H_V - H_V^{ig} = RT\left(Z - 1 - \int_V^\infty \left[T\left(\frac{\partial Z}{\partial T}\right)_V\right]\frac{dV}{V}\right) = RT(Z-1) + R(1+m_i)\left[\frac{A}{B}\frac{T}{a^{0.5}}\right] ln\left(\frac{Z-b}{Z}\right) \tag{A.13}$$

A.2. Constant physical properties

Several physical properties of the chemical compounds involved in the CD process are given. The following data is used for the determination of the remaining physical properties, the EOS, and the hydraulic correlations. The physical data was obtained in the Aspen Plus® [88] database and the Reis et al. [89] work.

Table A.1. Critical and constant physical properties of the compounds

	$P_C\ [bar]$	$T_C\ [K]$	ω	$MW\ \left[\frac{kg}{kmol}\right]$	$H^0\ \left[\frac{KJ}{mol}\right]$	$T_b@9.5bar\ [K]$
Isobutene	38.98675	417.9	0.19484	56.10752	-16.9147	341.7
Ethanol	60.35675	516.2	0.643558	46.06904	-234.963	421.9
n-Butene	39.18675	419.6	0.184495	56.10752	-0.125604	342.6
ETBE	28.32675	509.4	0.316231	102.17656	-313.9	438.8

A.3. Condition dependent physical properties

Ideal gas heat capacity of each component.

$$Cp_{V,i}^{ig} = C_{1c,i} + C_{2c,i}T + C_{3c,i}T^2 + C_{4c,i}T^3 + C_{5c,i}T^4 + C_{6c,i}T^5 \tag{A.14}$$

Table A.2. Ideal gas heat capacity coefficients, $\boldsymbol{T}$ in K, $\boldsymbol{Cp_{V,i}^{ig}}$ in kJ/(mol.K)

	C_{1c}	C_{2c}	C_{3c}	C_{4c}	C_{5c}	C_{6c}
Isobutene	0.016052191	0.000280432	-1.09E-07	9.10E-12	0	0
Ethanol	0.00901418	0.000214071	-8.39E-08	1.37E-12	0	0
n-Butene	-0.00299356	0.000353198	-1.99E-07	4.46E-11	0	0
ETBE	-0.014651654	0.000698631	-4.48E-07	1.16E-10	0	0

Specific vapor enthalpy of each component.

$$\begin{aligned} H_{V,i} &= H_{V,i}^{ig} + RT(Z-1) + R(1+m_i)\left[\frac{A}{B}\frac{T}{a^{0.5}}\right] ln\left(\frac{Z-b}{Z}\right) \\ &= H_i^0 + \int_{T_{ref}}^{T} Cp_{V,i}^{ig}\, dT + RT(Z-1) + R(1+m_i)\left[\frac{A}{B}\frac{T}{a^{0.5}}\right] ln\left(\frac{Z-b}{Z}\right) \\ &= H_i^0 + C_{1c,i}\left(T - T_{ref}\right) + \frac{C_{2c,i}}{2}\left(T^2 - T_{ref}^2\right) + \frac{C_{3c,i}}{3}\left(T^3 - T_{ref}^3\right) + \frac{C_{4c,i}}{4}\left(T^4 - T_{ref}^4\right) \\ &+ \frac{C_{5c,i}}{5}\left(T^5 - T_{ref}^5\right) + \frac{C_{6c,i}}{6}\left(T^6 - T_{ref}^6\right) + RT(Z-1) + R(1+m_i)\left[\frac{A}{B}\frac{T}{a^{0.5}}\right] ln\left(\frac{Z-b}{Z}\right) \end{aligned} \quad \text{(A.15)}$$

Specific mixture vapor enthalpy

$$H_V = \sum_{i \in C} y_i H_{V,i} \quad \text{(A.16)}$$

Specific vaporization enthalpy of each component.

$$\Delta H_{vap,i} = C_{1v,i}\left(1 - \frac{T}{T_{C,i}}\right)^{C_{2v,i} + C_{3v,i}\frac{T}{T_{C,i}} + C_{4v,i}\left(\frac{T}{T_{C,i}}\right)^2 + C_{5v,i}\left(\frac{T}{T_{C,i}}\right)^3} \quad \text{(A.17)}$$

Table A.3. Specific vaporization enthalpy coefficients, $\boldsymbol{T}$ in K, $\boldsymbol{\Delta H_{vap,i}}$ in kJ/mol

	C_{1v}	C_{2v}	C_{3v}	C_{4v}	C_{5v}
Isobutene	32.614	0.38073	0	0	0
Ethanol	55.789	0.31245	0	0	0
n-Butene	33.774	0.5107	-0.17304	0.05181	0
ETBE	45.29	0.27343	0.21645	-0.11756	0

Liquid heat capacity of each component.

$$Cp_{L,i} = C_{1l,i} + C_{2l,i}T + C_{3l,i}T^2 + C_{4l,i}T^3 + C_{5l,i}T^4 \quad \text{(A.18)}$$

Table A.4. Ideal gas heat capacity coefficients, $\boldsymbol{T}$ in K, $\boldsymbol{Cp_{L,i}}$ in kJ/(mol.K)

	C_{1l}	C_{2l}	C_{3l}	C_{4l}	C_{5l}
Isobutene	0.08768	0.0002171	-9.15E-07	2.27E-09	0
Ethanol	0.10264	-0.00013963	-3.03E-08	2.04E-09	0
n-Butene	0.18205	-0.001611	1.20E-05	-3.75E-08	4.50E-11
ETBE	0.11096	0.00031422	1.75E-07	0	0

Specific liquid enthalpy of each component.

$$H_{L,i}(T) = H_{L,i}(T_b) + \Delta H_{vap,i}(T_b) + \int_{T_b}^{T} Cp_{L,i}\, dT$$
$$= H_{L,i}(T_b) + \Delta H_{vap,i}(T_b) + C_{1l,i}(T - T_b) + \frac{C_{2l,i}}{2}(T^2 - T_b^2) + \frac{C_{3l,i}}{3}(T^3 - T_b^3) \quad \text{(A.19)}$$
$$+ \frac{C_{4l,i}}{4}(T^4 - T_b^4) + \frac{C_{5l,i}}{5}(T^5 - T_b^5)$$

It should be noted that this approximation to the liquid enthalpy was prosed due to the possibility of obtaining temperatures higher than some components critical temperature, leading to non-real answers for the vaporization enthalpy.

Specific mixture liquid enthalpy.

$$H_L = \sum_{i \in C} x_i H_{L,i} \quad \text{(A.20)}$$

Saturation pressure of each component.

$$\ln P_i^{sat} = C_{1sp,i} + \frac{C_{2sp,i}}{T + C_{3sp,i}} + C_{4sp,i}T + C_{5sp,i} \ln T + C_{6sp,i} T^{C_{7sp,i}} \quad \text{(A.21)}$$

Table A.5. Saturation pressure coefficients, $\boldsymbol{T}$ in K, $\boldsymbol{P_i^{sat}}$ in bar

	C_{1sp}	C_{2sp}	C_{3sp}	C_{4sp}	C_{5sp}	C_{6sp}	C_{7sp}
Isobutene	66.4970745	-4634.1	0	0	-8.9575	1.34E-05	2
Ethanol	61.7910745	-7122.3	0	0	-7.1424	2.89E-06	2
n-Butene	40.3230745	-4019.2	0	0	-4.5229	4.88E-17	6
ETBE	52.67507454	-5820.2	0	0	-6.1343	2.14E-17	6

Vapor mixture molar density

$$\bar{\rho}_V = \frac{P}{RTZ} \quad \text{(A.22)}$$

Vapor mixture mass density

$$\rho_V = \bar{\rho}_V \sum_{i \in C} MW_i y_i \tag{A.23}$$

Liquid molar density of each component.

$$\bar{\rho}_{L,i} = \frac{C_{1r,i}}{C_{2r,i}^{1+\left(1-\frac{T}{T_{C,m}}\right)^{C_{3r,i}}}} \tag{A.24}$$

Table A.6. Liquid density coefficients, $\boldsymbol{T}$ in K, $\boldsymbol{\bar{\rho}_{L,i}}$ in kmol/m^3

	C_{1r}	C_{2r}	C_{3r}
Isobutene	1.1446	0.2724	0.28172
Ethanol	1.6288	0.27469	0.23178
n-Butene	1.0877	0.26454	0.2843
ETBE	0.66333	0.26135	0.28571

Liquid mixture molar density

$$\bar{\rho}_L = \sum_{i \in C} x_i \bar{\rho}_{L,i} \tag{A.25}$$

Liquid mixture mass density

$$\rho_L = \bar{\rho}_L \sum_{i \in C} MW_i x_i \tag{A.26}$$

Interfacial surface tension of each component

$$\sigma_i = C_{1sig,i}\left(1 - \frac{T}{T_{C,m}}\right)^{\left(C_{2sig,i} + C_{3sig,i}\frac{T}{T_{C,m}} + C_{4sig,i}\left(\frac{T}{T_{C,m}}\right)^2\right)} \tag{A.27}$$

Table A.7. Interfacial surface tension coefficients, $\boldsymbol{T}$ in K, $\boldsymbol{\sigma_i}$ in N/m

	C_{1sig}	C_{2sig}	C_{3sig}	C_{4sig}
Isobutene	0.05544	1.2453	0	0
Ethanol	0.03764	-2.157E-5	1.025E-7	0
n-Butene	0.055945	1.2402	0	0
ETBE	0.071885	2.1204	-1.5583	0.76657

Interfacial mixture surface tension

$$\sigma = \sum_{i \in C} x_i \sigma_i \tag{A.28}$$

A.4. Thermodynamic model

The chosen thermodynamic model for predicting non-ideality in the liquid phase is the Non Random Two Liquid model (NRTL). That model is described by the following equations.

$$\ln \gamma_i = \frac{C_i}{S_i} + \sum_{k \in C} x_k \varepsilon_{ik} \quad \text{(A.29.a)}$$

$$\varepsilon_{ik} = \frac{G_{ik}}{S_k}\left(\tau_{ik} - \frac{C_k}{S_k}\right) \quad \text{(A.29.b)}$$

$$C_i = \sum_{j \in C} x_j G_{ji} \tau_{ji} \quad \text{(A.29.c)}$$

$$S_i = \sum_{j \in C} x_j G_{ji} \quad \text{(A.29.d)}$$

$$G_{ij} = \exp\left(-\alpha_{ij}\tau_{ij}\right) \quad \text{(A.29.e)}$$

$$\tau_{ij} = a_{ij} + \frac{b_{ij}}{T} \quad \text{(A.29.f)}$$

where the parameters a_{ij}, b_{ij} and α_{ij} are the interaction parameters used by the model. These parameters have been computed by the AspenPlus® [88] software from the vapor liquid equilibrium data generated by the UNIFAC model. The parameter a_{ij} of the system here analyzes is zero for all the combinations of chemical compounds. The other two parameters are shown in the tables below.

Table A.8. $\boldsymbol{b_{ij}}$ parameter of interaction for the NRTL model.

	Isobutene	Ethanol	n-Butene	ETBE
Isobutene	0	623.581001	107.526499	219.73407
Ethanol	141.963213	0	164.57256	187.104064
n-Butene	-93.2454642	595.529982	0	226.373398
ETBE	-172.59152	344.481315	-177.88565	0

Table A.9. $\boldsymbol{\alpha_{ij}}$ parameter of interaction for the NRTL model.

	Isobutene	Ethanol	n-Butene	ETBE
Isobutene	0	0.3	0.3	0.3
Ethanol	0.3	0	0.3	0.3
n-Butene	0.3	0.3	0	0.3
ETBE	0.3	0.3	0.3	0

A.5. Hydraulic correlations

The hydraulic correlations here presented are used to calculate the liquid and vapor flows in the distillation column. These correlations are also used for calculating the pressure drop across the column. The equations shown here have been successfully used in other studies of the same system [18] and were obtained from the works of Cicile [71], Zuiderweg [90] and Kister [68].

Flow factor

$$Fp_n = \frac{L_n/\rho_L}{V_n/\rho_V}\left(\frac{\rho_L[kg/m^3]}{\rho_V[kg/m^3]}\right)^{1/2}, n \in Sep + Cat \tag{A.30}$$

Liquid accumulation

$$M_{L,n} = 0.6\rho_L(A_T)(h_W^{0.5})\left(\frac{Fp_n A_T pitch}{L_W}\right)^{0.25}, n \in Sep + Cat \tag{A.31}$$

Aeration factor

$$fa_n = 0.981\exp\left(-0.411\left(\frac{V_n}{\rho_V}[m^3/s]\right)(\rho_V[kg/m^3])^{0.5}\left(\frac{1}{A_T}\right)\right), n \in Sep + Cat \tag{A.32}$$

Liquid height over the weir

$$h_{ow,n} = 0.6\left(\left(\frac{L_n}{\rho_L}[m^3/s]\right)\left(\frac{1}{L_W}\right)\right)^{2/3}, n \in Sep + Cat \tag{A.33}$$

Pressure drop due to the liquid

$$\Delta P_{L,n}[bar] = \frac{gfa_n(\rho_L[kg/m^3])\left(h_{ow,n} + h_W\right)}{1\text{x}10^5}, n \in Sep + Cat \tag{A.34}$$

Hole coefficient

$$K_h = (1\text{x}10^{-3})\left(880.6 - 67.7\frac{d_h}{\varepsilon} + 7.32\left(\frac{d_h}{\varepsilon}\right)^2 - 0.338\left(\frac{d_h}{\varepsilon}\right)^3\right) \tag{A.35}$$

Plate porosity

$$p_h = \frac{A_h}{A_T} \tag{A.36}$$

Pressure drop due to dry air

$$\Delta P_{D,n}[bar] = \frac{1\text{x}10^{-5}}{2K_h^2}\left(\frac{1}{A_h}\frac{V_n}{\rho_V}[m^3/s]\right)^2(\rho_V[kg/m^3])(1 - p_h^2), n \in Sep + Cat \tag{A.37}$$

Pressure drop due to superficial tension

$$\Delta P_{\sigma,n}[bar] = \frac{4\sigma_n}{d_h}, n \in Sep + Cat \tag{A.38}$$

Total pressure drop

$$\Delta P_n = \Delta P_{L,n} + \Delta P_{D,n} + \Delta P_{\sigma,n}, n \in Sep + Cat \tag{A.39}$$

A.6. Index reduction model derivatives

In order to reduce the index of the DAE problem stated in the Section Index reduction technique and simplified differential algebraic model (DAE2r), the differential energy balance was replaced by an algebraic equation that involved the derivatives of certain properties. Based on the work of Lozano et al. [27] and Rahul et al. [57] the following model was proposed.

Derivative of the specific liquid enthalpy of each component with respect to the temperature.

$$\frac{dH_{L,i}(T)}{dT} = \frac{d}{dT}\left(H_{L,i}(T_b) + \Delta H_{vap,i}(T_b) + \int_{T_b}^{T} Cp_{L,i}\, dT\right) = Cp_{L,i} = C_{1l,i} + C_{2l,i}T + C_{3l,i}T^2 + C_{4l,i}T^3 + C_{5l,i}T^4 \tag{A.40}$$

Derivative of the specific mixture liquid enthalpy with respect to time.

$$\begin{aligned}\frac{dH_L}{dt} = \frac{d}{dt}\left(\sum_{i\in C} x_i H_{L,i}\right) = \sum_{i\in C} x_i \frac{dH_{L,i}}{dt} + \sum_{i\in C} H_{L,i}\frac{dx_i}{dt} = \sum_{i\in C} x_i \frac{dH_{L,i}}{dT}\frac{dT}{dt} + \sum_{i\in C} H_{L,i}\frac{dx_i}{dt} \\ = \frac{dT}{dt}\left(\sum_{i\in C} x_i \frac{dH_{L,i}}{dT}\right) + \sum_{i\in C} H_{L,i}\frac{dx_i}{dt}\end{aligned} \tag{A.41}$$

Derivative of the saturation pressure of each component with respect to temperature.

$$\frac{dP_i^{sat}}{dT} = P_i^{sat}\left[\frac{-C_{2sp,i}}{\left(T + C_{3sp,i}\right)^2} + C_{4sp,i} + \frac{C_{5sp,i}}{T} + C_{6sp,i}C_{7sp,i}T^{C_{7sp,i}-1}\right] \tag{A.42}$$

Phase equilibrium constant.

$$K_i = \frac{\gamma_i P_i^{sat}}{\varphi_i P} \tag{A.43}$$

Derivative of the phase equilibrium constant with respect to time (assuming fugacity coefficient constant in time).

$$\frac{dK_i}{dt} = \frac{1}{P}\left[P_i^{sat}\frac{d\gamma_i}{dt} + \gamma_i\frac{dP_i^{sat}}{dt}\right] = \frac{1}{P}\left[P_i^{sat}\frac{d\gamma_i}{dt} + \gamma_i\frac{dP_i^{sat}}{dT}\frac{dT}{dt}\right] \tag{A.44}$$

Derivative of the activity coefficient with respect to time.

$$\frac{d\gamma_i}{dt} = \frac{\partial\gamma_i(x_j,T)}{\partial T}\frac{dT}{dt} + \sum_{j\in C}\frac{\partial\gamma_i(x_j,T)}{\partial x_j}\frac{dx_j}{dt} \tag{A.45}$$

Derivative of the activity coefficient with respect to temperature (numerical perturbation).

$$\frac{\partial\gamma_i}{\partial T} \approx \frac{\gamma_i(T+\Delta T) - \gamma_i(T)}{\Delta T} \tag{A.46}$$

Derivative of the activity coefficient with respect to composition (numerical perturbation).

$$\frac{\partial \gamma_i}{\partial x_j} \approx \frac{\gamma_i(x_j + \Delta x_j) - \gamma_i(x_j)}{\Delta x_j} \tag{A.47}$$

The derivative of temperature with respect to time is calculated from the summation equation.

$$\sum_{j \in C} (y_i - x_i) = 0 \tag{A.48.a}$$

$$\sum_{i \in C} (K_i x_i - x_i) = \sum_{i \in C} (K_i x_i) - 1 = 0 \tag{A.48.b}$$

$$\frac{d}{dt}\left(\sum_{i \in C} (K_i x_i) - 1\right) = 0 \tag{A.48.c}$$

$$\sum_{i \in C} \left(\left(K_i \frac{dx_i}{dt}\right) + \left(x_i \frac{dK_i}{dt}\right)\right) = 0 \tag{A.48.d}$$

$$\sum_{i \in C} \left(K_i \frac{dx_i}{dt}\right) + \sum_{i \in C} \left(x_i \frac{dK_i}{dt}\right) = \sum_{i \in C} \left(K_i \frac{dx_i}{dt}\right) + \sum_{i \in C} \left(x_i \frac{1}{P}\left[P_i^{sat} \frac{d\gamma_i}{dt} + \gamma_i \frac{dP_i^{sat}}{dT}\frac{dT}{dt}\right]\right) = 0 \tag{A.48.e}$$

$$\sum_{i \in C} \left(K_i \frac{dx_i}{dt}\right) + \sum_{i \in C} \left(x_i \frac{1}{P}\left[P_i^{sat} \left(\frac{\partial \gamma_i(x_j, T)}{\partial T}\frac{dT}{dt} + \sum_{j \in C} \frac{\partial \gamma_i(x_j, T)}{\partial x_j}\frac{dx_j}{dt}\right) + \gamma_i \frac{dP_i^{sat}}{dT}\frac{dT}{dt}\right]\right) = 0 \tag{A.48.f}$$

$$\frac{dT}{dt} = \frac{-\frac{1}{P}\sum_{i \in C}\left[x_i P_i^{sat} \sum_{j \in C} \frac{\partial \gamma_i(x_j, T)}{\partial x_j}\frac{dx_j}{dt}\right] - \sum_{i \in C}\left(K_i \frac{dx_i}{dt}\right)}{\frac{1}{P}\left(\sum_{i \in C} x_i P_i^{sat} \frac{\partial \gamma_i(x_j, T)}{\partial T} + \sum_{i \in C} x_i \gamma_i \frac{dP_i^{sat}}{dT}\right)} \tag{A.48.g}$$

Appendix B - OCP representation as NLP problem and solution algorithms

The treatment of a constrained DAE dynamic optimization problem can be made through two different approaches: optimize and then discretize (O-D) or discretize and then optimize (D-O). The first approximation is an indirect method that solves the problem based on the Pontryagin's maximum principle [29], transforming an optimization problem in a boundary condition problem using adjoint variables. Even though this approximation has strong theoretical foundations, it is inefficient for large scale problems or problems with inequality constraints[25]. The second approximation is a direct method that discretizes the differential equations to work the whole OCP as a NLP. The simultaneous solution through direct transcription discretizes all the variables of the problem (state and control variables) and solves the whole problem in a single level, which means that it just solves the DAE problem once, at the optimal point. This last case generates a large scale NLP problem, whose dispersion and structure can be exploited [25].

For large scale problems the best choice is the direct transcription approach. The discretization alternative used in this work is orthogonal collocation in finite elements due to its precision and numerical stability [25]. The fact of using an orthogonal collocation in finite elements transcripts the DAE problem into an NLP. The specific case of orthogonal collocation using Radau roots has the following advantages:

- It is widely used to solve index two problems [91].
- It is a method that presents a L-stability, which means that as the integration step tends to zero, the stability region tends to infinity [92]. This allows the method to handle with high precision stiff DAE equations.
- It is able to stabilize superior (>1) index DAE problems [59]

The truncation errors for stiff differential equations DAE problems is shown in the Table B**.** below.

Table B.1. Truncation error inside each finite element for the method of orthogonal colocation with Radau point [91]

DAE index	Error in algebraic variables*	Error in differential variables*
0	-	$O(h^{2s-1})$
1	$O(h^{2s-1})$	$O(h^{2s-1})$
2	$O(h^{s})$	$O(h^{2s-1})$

* s is the number of stages (collocation points) of the method and h is the size of the finite element.

The truncation error for the Radau orthogonal collocation method is the lowest truncation error for stiff ODE problems, only outmatched by the Legendre orthogonal collocation method.

Using the discretization by orthogonal collocation in finite elements the representation of the differential equations is transformed into a weighted sum of the variables in an integration step according to the following equation.

$$\sum_{k\in 1}^{K} z_{jk}\frac{dl_k(\tau_k)}{d\tau} = h_j f\left(z_{jk}, y_{jk}, u_{jk}, p\right), \forall j \in \{0, \dots, J\} \tag{B.1}$$

where K is the number of collocation points, J is the number of finite elements, $f\left(z_{jk}, y_{jk}, u_{jk}, p\right)$ is the right hand-side of the differential equations, h_j is the size of the finite element, and $\frac{dl_k(\tau_k)}{d\tau}$ is the derivative of the Lagrange polynomial shown below.

$$x_j(t) = \sum_{k\in 1}^{K} l_k(\tau) x_{jk}\,, \forall x \in \{y, z, u\} \tag{B.2}$$

$$l_k(\tau) = \prod_{n=0,\neq k}^{K} \frac{\tau - \tau_n}{\tau_k - \tau_n}, \forall k \in \{1, \dots, K\} \tag{B.3}$$

where τ_k is the respective root of the orthogonal polynomial. It can be noticed that the control and algebraic variables can also be represented by Lagrange polynomials [91]. The derivatives of the Lagrange polynomial are evaluated at each collocation point k.

Like in every other method of integration of differential equations, it is necessary to define the initial conditions for the differential variables. These differential variables have to be differentiable during the whole time interval, which is ensured by the continuity at the finite element boundary.

$$y_{1,0} = y(t_0) = y_0 \tag{B.4}$$

$$y_{j+1,0} = \sum_{k=0}^{K} l_k(1) y_{jk}\ , \forall j \in \{1, \dots, J-1\} \tag{B.5}$$

Using this representation, the differential equations of the original formulation can be replaced by algebraic equations. Note that the manipulated and algebraic variables can be discontinuous between finite elements.

After discretizing the dynamic optimization problem can be reformulated as a general NLP problem.

$$\min J = \mathcal{F}(t_f) + \sum_{j=0}^{J}\sum_{k=0}^{K} \mathcal{f}\left(z_{jk}, y_{jk}, u_{jk}, p_{jk}\right) \tag{B.6.a}$$

$$\text{s.t.} \sum_{k=1}^{K} z_{jk}\frac{dl_k(\tau_k)}{d\tau} - h_j f\left(z_{jk}, y_{jk}, u_{jk}, p\right) = 0, \forall j \in \{0, \dots, J\} \tag{B.6.b}$$

$$y_{1,0} = y(t_0) = y_0 \tag{B.6.c}$$

$$h\left(z_{jk}, y_{jk}, u_{jk}, p_{jk}\right) = 0\ , \forall j \in \{0, \dots, J\}, \forall k \in \{0, \dots, K\} \tag{B.6.d}$$

$$g\left(z_{jk}, y_{jk}, u_{jk}, p_{jk}\right) \leq 0\ , \forall j \in \{0, \dots, J\}, \forall k \in \{0, \dots, K\} \tag{B.6.e}$$

$$x_j(t) = \sum_{k}^{K} l_k(\tau) x_{jk}\,, \forall x \in \{y, z, u\} \tag{B.6.f}$$

$$y_{j+1,0} = \sum_{k=0}^{K} l_k(1) y_{jk} \ , \forall j \in \{1, \dots, J-1\} \quad \text{(B.6.g)}$$

Here the control, algebraic and differential variables have been included into x. In the same manner, all the resulting constraints can be grouped in a set of constraints c. The problem that is intended to be solved is then summarized in the Eq. B.7.

$$\min J(x,p) \quad \text{(B.7.a)}$$

$$\text{s.t. } c(x,p) = 0 \quad \text{(B.7.b)}$$

$$x_{Lo} \leq x \leq x_{Up} \quad \text{(B.7.c)}$$

It should be noted that all variables are bounded in the interval $[x_{Lo}, x_{Up}]$ where x_{Lo} and x_{Up} are the lower and upper bounds of the variable x respectively. The optimization methods that are going to be used in this work are deterministic algorithms based on gradients. These algorithms solve the first order or Karush-Kuhn-Tucker (KKT) optimality conditions for NLP problems. These algorithms solve the algebraic equations defined by the gradient of the Lagrange function (Eq. B.8.a), feasibility (Eq. B.8.b), and complementarity (Eq. B.8.c-B.8.d) [91].

$$\nabla_x J(x,p) + \nabla c(x,p) v - E_{Lo} w_{A_{Lo}} + E_{Up} w_{A_{Up}} = 0 \quad \text{(B.8.a)}$$

$$c(x,p) = 0 \quad \text{(B.8.b)}$$

$$E_{Up}^T x = E_{Up}^T x_{Up} \quad \text{(B.8.c)}$$

$$E_{Lo}^T x = E_{Lo}^T x_{Lo} \quad \text{(B.8.d)}$$

where v is the Lagrange multiplier vector, w_{A_L} and w_{A_U} are the active constraints multipliers in their lower and upper bounds respectively, and E_L and E_U are the matrixes that determine that the variables are at their lower or upper bound respectively. These matrixes are defined as:

$$\{E_{Lo}\}_{ij} = \begin{cases} 1 \ if \ the \ variable \ j \ is \ in \ its \ lower \ bound \\ 0 \ otherwhise \end{cases} \quad \text{(B.9.a)}$$

$$\{E_{Up}\}_{ij} = \begin{cases} 1 \ if \ the \ variable \ j \ is \ in \ its \ upper \ bound \\ 0 \ otherwhise \end{cases} \quad \text{(B.9.b)}$$

These methods require the computation of the first and second order derivatives. The convergence is strongly dependent of the precision of such calculations. There are other algorithms that do not require the use of derivatives and are known as direct search algorithms (as the genetic or the simulated annealing algorithms), many of them are derived from heuristics [93].

Three deterministic algorithmic methods implemented in the software General Algebraic Modelling System (GAMS) [94], used to solve NLP problems will be explained below.

B.1. Interior Point methods (IPOPT algorithm)

This method modifies the original NLP problem by imposing a logarithmic barrier for the inequality constraints and it penalizes the objective function with a parameter μ_l as seen in Eq. B.10.

$$\min J(x,p) - \mu^k \left(\sum \ln(x - x_{Lo}) + \sum \ln(x_{Up} - x) \right) \tag{B.10}$$

The problems is solved for a decreasing sequence of barrier parameter $\mu^k \to 0, k \to \infty$. This guarantees that the final results belong to the set of active constraints as when $k \to \infty$ the solution of th barrier problems tends to the solution of the original problem. The set of active constraints may change in each iteration.

The algorithm IPOPT [95] uses the complete space solution method, exploiting the symmetry and disspersity of the Hessian matrix of the Lagrange function for an efficient calculation of its inverse. It can be noted that a complete space is that space that contains any Cauchy sequence formed by the elements of that same space [96], which means that there are no “missing points” in this space, which is useful for the Hessian calculation. Another advantage is that the iterations are made in order to modify all the variables simultaneously, compared to the reduced space algorithms.

In this method, the Hessian matrix does not change significantly after each iteration taking into account the disspersity and structure of the matrix, which allows its decomposition to be made just at the beginning of the algorithm. The disadvantage of this method is that a sequence of barrier parameters must be adequately selected to achieve a fast convergence. Moreover, this method uses a filter line search procedure after every Newton’s type step [95].

B.2. Sequential quadratic programming methods (SNOPT algorithm)

This method is based on a quadratic approximation of the objective function and a linear approximation of the constraints, which means that the quadratic programming problem represents a simplified version of the original formulation in Eq. B.7. This problem is solved sequentially until converging into the original problem, as seen in the Eq. B.11.

$$\min_{\Delta x^k} \left(\nabla J(x^k, p) \Delta x^k + \frac{1}{2} (\Delta x^k)^T H \Delta x^k \right) \tag{B.11.a}$$

$$\text{s.t.} \nabla c(x^k, p) \Delta x^k + c(x^k, p) = 0 \tag{B.11.b}$$

Note that the linearization is made at each new iteration. The quadratic problems are solved in an effective manner with a Newton based step algorithm. Nevertheless, converging to the original problem requires a large number of iterations.

The algorithm SNOPT [97] is based on this method with certain modifications, such as the active set strategies to handle inequalities, linear search for improving the step at every iteration, and the Broyden, Fletcher, Goldfarb and Shanno (BFGS) approximation of the Hessian matrix. As it does not compute the second derivatives of the problem directly, it may iterate faster but cannot exploit directly that information, resulting in a slower convergence [98].

B.3. Generalized reduced gradient methods (CONOPT algorithm)

This method does a variable classification similar to the SIMPLEX algorithm for linear programming (LP). It defines superbasic variables, which are the ones that are updated by the optimization method, basic variables, which are the ones defined by the equality constraints, and nonbasic variables, which are the variables at their bounds. This differentiation makes the algorithm efficient and its convergence is fast for problems with few degrees of freedom [99], [100] since the search is done over a few variables. As a reduced space method, once a feasible solution is found it will not lose feasibility, which

means that in the worst case the solution will be feasible and better than the initial point, but not optimal [101].

The CONOPT [82] algorithm is based on the Generalized Reduced Gradient method but is specifically designed for large and sparse models.

Independently of the solution algorithm that will be used in this problem, the software GAMS has been selected as programming environment. GAMS has been successfully used for the optimal control in several case studies of distillation [8], [9], [31], [39], [45]. One of the most significant advantages of this software is an advanced solver for the resolution of large-scale problems and a great flexibility when testing several solution algorithms [100]. Its evaluation techniques for the first and second order derivatives implemented on it (*Automatic differentiation*) makes its solver a more robust, exact and computational efficient tool compared to the regular differentiation methods like finite differences for the Jacobian and BFGS for the Hessian matrix [98].

Appendix C – Second Case Study

A second case study has been proposed to apply the methodology developed during this work. This second case study corresponds to the results obtained by Gómez et al. [18], where a MINLP optimization for the design of an ETBE production CD column was proposed. This problem was solved using two different models, an equilibrium model (EQ) which, as the model implemented in this work, assumes thermodynamic equilibrium in all the separation stages; and a non-equilibrium model (NEQ), which uses transport phenomena equations to represent the mass and energy transfer in each stage. The results obtained by this author gave the optimal column design and operation parameters according to the models there implemented.

The characteristics of this column differ from the one studied by Miranda et al. [41] and which is the main case study of this work.

Table C.1. Distillation column characteristics from [18]

Characteristic	Unit	NEQ	EQ
Number of stages $\boldsymbol{NT}$	[-]	45	46
Number of reactive stages	[-]	13	11
Position of the catalyst	Stage	13,14,15,18,20 22,23,24,28,29 31,34,36	17,19,21,22,23 25,27,32,35 37
Ethanol Feed Stage	Stage	13	15
Butenes Feed Stage	Stage	36	38
$\boldsymbol{x_{NT,ETBE}^{min}}$	[mol/mol]	0.95	0.95
Ethanol feed flow $\boldsymbol{F_{EtOH}}$	[kmol/min]	1.7118	1.7118
Ethanol feed temperature	[K]	320	320
Butenes feed flow $\boldsymbol{F_{but}}$	[kmol/min]	5.4678	5.4678
Butenes feed temperature	[K]	400	400
Condenser pressure	[bar]	9.5	9.5
Stage height $\boldsymbol{h_s}$	[m]	0.15	0.15
Pitch	[m]	8E-03	8E-03
Tray thickness $\boldsymbol{\varepsilon}$	[m]	2E-03	2E-03
Hole diameter $\boldsymbol{d_h}$	[m]	2E-03	2E-03

Regarding the first case study, there are some differences which changed the optimization problem formulation. The butenes feed flow was fixed from the beginning, such as other geometrical constants.

The most important is the stage height, which was fixed in this case, contrary to the other case where the total column height was specified.

The profiles shown below correspond to the optimal design results using the NEQ configuration.

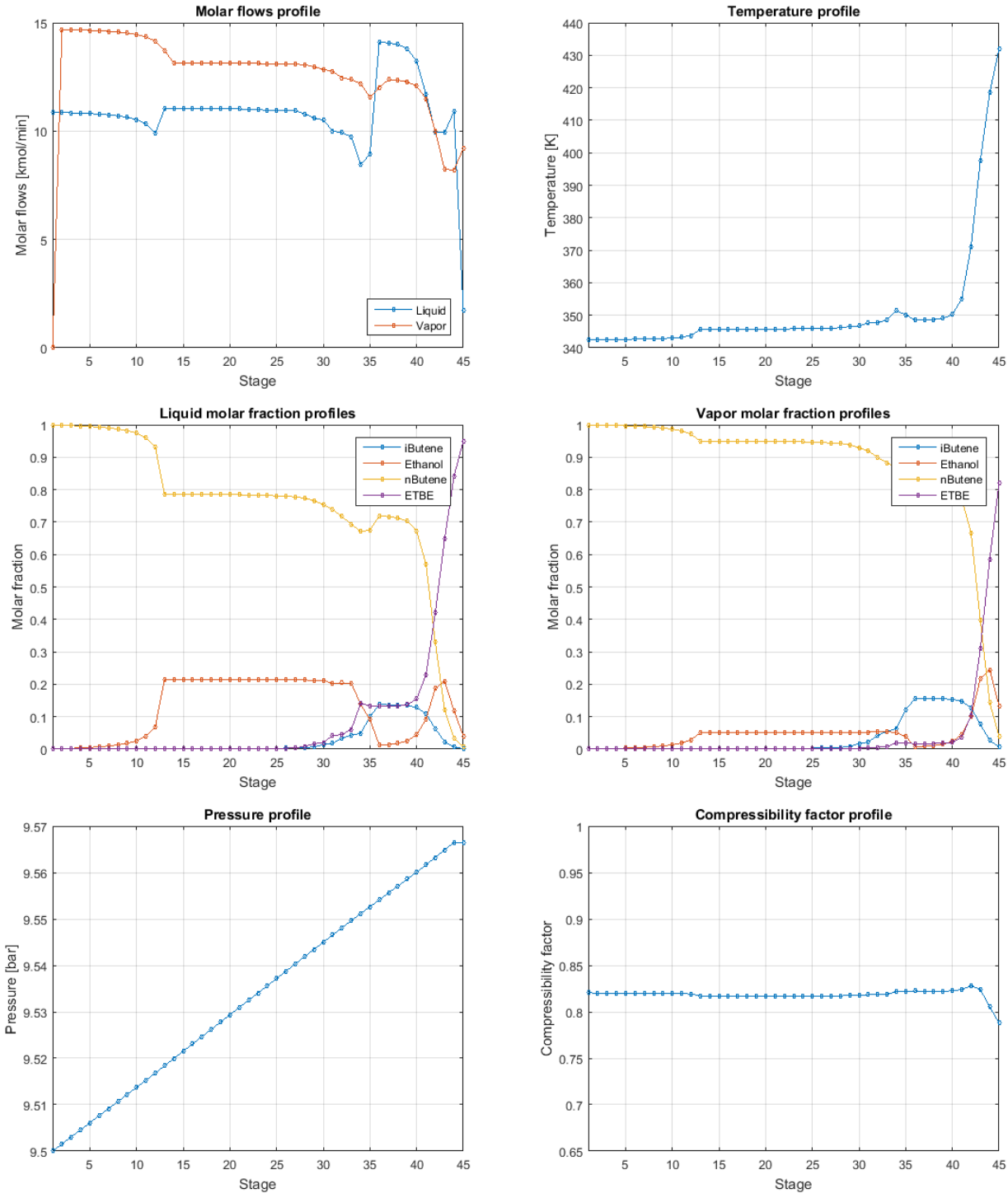

Figure C.1. Profiles of the optimal design solution for the NEQ

The obtained profiles show an expected behavior. The ETBE appears in the trays with catalyst as the reaction is the only source of this component. There is a pressure drop of 0.08 bar for the whole column. The compressibility factor is around 0.82 for the whole column and it lowers its value for the last stages, since the temperature increases considerably to achieve the higher minimum composition. The operation data such as reflux ratio and reboiler duty is presented in the Table C.2.

A comparison between the results obtained by implementing the model proposed in this work with the author's parameters and the ones obtained by the optimal design in this work and were depicted in the Table C.2.

Table C.2. Optimal design results

		NEQ		EQ	
Solution source	**Units**	**Gómez et al.**	**This work**	**Gómez et al.**	**This work**
Column Diameter D_C	[m]	0.093	0.0835	0.084	0.0464
Reboiler Duty Q_R	[kJ/min]	408.96	450.281	388.38	234.138
Molar reflux ratio RR	[-]	5.07	5.946	4.5	2.61
Weir height h_W	[m]	3.2E-02	1.9E-02	*5.0E-02*	1.9E-02
Weir length L_W	[m]	7.4E-02	6.7E-02	*6.7E-02*	3.7E-02
Active area A_a	[m^2]	4.9E-03	3.9E-03	*3.9E-03*	1.2E-03
ETBE bottoms composition $x_{NT,ETBE}$	[mol/mol]	**0.88061**	0.95000	**0.77918**	0.95000
Isobutene conversion	[mol/mol]	0.91771	0.99899	0.81239	0.99731
Entrainment flooding?		No	No	No	No
Downcomer flooding?		No	No	No	No
Weeping?		**Yes**	No	**Yes**	No
Profit ETBE	[$/year]	20768	20936	20787	20912
Investment cost	[$/year]	10260	10767	10239	10534
Operating cost	[$/year]	35145	34689	35085	34646
Total Cost	[$/year]	24639	24519	24537	24268

* The results on italics do not correspond to data given by Gómez et al. [18], but obtained by the model used in this work. The values in bold are highlighted since reflect a violation of the design constraints.

It can be noted how the different models used converged to different solutions. The fact of implementing the pressure drop across the column affected considerably the equilibrium in the lower stages, which finally resulted in different bottoms composition of ETBE. It is also worthy to note that the considerable large column diameters decreased the minimum weeping vapor hole velocity to the point that in both cases this phenomenon happens.

Nomenclature

Subscripts

0: Referring to the formation conditions.
A: Referring to the Adsorption.
A_L: Belonging to the set of variables on its lower bound.
A_U: Belonging to the set of variables on its upper bound.
a: Referring to the active area.
b: Referring to boiling conditions.
but: Referring to the butenes feed.
C: Referring to the column.
C: Referring to critical conditions.
$Cond$: Referring to the condenser.
cat: Catalyst.
cl: Referring to the clear liquid.
D: Diameter.
DC: Referring to the downcomers.
$Econ$: Referring to the Economic part of the objective function.
Eq: Referring to the Equilibrium.
$EtOH$: Referring to the Ethanol.
$EO-NMPC$: Referring to the Economic Oriented Non Linear Model Predictive Control objective.
$ETBE$: Referring to the Ethyl *tert*-butyl ether.
F: Referring to the feed stream.
f: Referring to the final time.
H: Referring to the hot service (steam).
h: Referring to the holes.
I: Referring to the Isobutene.
Inv: Referring to the investment.
i: Component of the set C.
ij: Row i, column j in a matrix.
i, j, k: Component of the set C.
j: Finite element.
k: Orthogonal collocation point.
L: Referring to the liquid phase.
Lo: Lower bound.
m: Referring to the mixture.
$NMPC$: Referring to the Non Linear Model Predictive Control objective.
NT: Referring to the last stage (reboiler).
n: Stage of the set N.
nB: Referring to the nButene.
Op: Referring to the operation.
ow: Referring to the over weir.
p: Objective of the set Φ.
Q_{Reb}: Referring to the reboiler duty.

q: Referring to the cross area.
Reb: Referring to the reboiler.
RR: Referring to the molar reflux ratio.
$rate$: Referring to the Reaction rate.
ref: Referring to the reference value (298K in temperature)
S: Referring to the stage.
T: Referring to the total height or area.
$Track$: Referring to the Tracking part of the objective function.
Up: Upper bound.
V: Referring to the vapor phase.
vap: Referring to vaporization.
W: Referring to the cold service (water).
W: Referring to the weir.
σ: Referring to superficial tension.

Superscript
ig: Referring to ideal gas.
k: Iteration.
Lo: Lower bound.
min: Minimum.
max: Maximum.
Ref: Reference.
T: Transpose.
Up: Upper bound.

Latin symbols
A: Area [m2].
A: Parameter for the SRK EOS.
AF: Annualizing factor [1/year].
a: Parameter for the SRK EOS.
a: Parameter for NRTL.
B: Parameter for the SRK EOS.
b: Parameter for the SRK EOS.
b: Parameter for NRTL.
C: Cost.
C: Coefficient of a physical property model.
C: Parameter for NRTL.
Cat: Catalyst filled trays.
Cp: Heat capacity [kJ/kmol.K].
C_{sbf}: Capacity parameter
c: Set of constraints.
d: Diameter [m].
E: Variables in bounds determination matrices.
F: Feed [kmol/hr].

F: Cost factor.
$\mathcal{F}$: Terminal objective function.
Fp: Flow parameter.
f: Differential equations.
ℓ: Moving or trajectory objective function.
fa: Airation factor.
G: Parameter for NRTL.
g: Algebraic equations.
g: Inequality constraints.
g: Gravity acceleration 9.8 m/s2.
H: Enthalpy [kJ/kmol].
H: Total height [m].
h: Discretization in orthogonal collocation.
h: Height [m].
h: Equality constraints.
J: Objective function.
J: Total amount of collocation points.
K: Total amount of finite elements.
K: Equilibrium constant.
K: (Hole) Coefficient.
L: Length [m].
L: Liquid flow [kmol/hr].
$\mathcal{L}_1$: One dimensional norm.
l: Coefficient of Lagrange polynomial.
M: Molar holdup [kmol].
$M\&S$: Marshall and Swift parameter.
m: Mass [kg].
m: Parameter for the SRK EOS.
P: Pressure [bar].
P: Perturbation.
p: Parameter vector.
p: Porosity.
$pitch$: Pitch between holes in the tray.
Q: Heat Duty [kJ/hr]
R: Ideal gas constant 8.314 J/mol.K
$\mathcal{R}$: Reaction rate [kmol/kg_{cat}]
RR: Reflux ratio.
s: Number of orthogonal collocation points.
S: Cross section area [m^2].
S: Parameter for NRTL.
Sep: Separation trays.
T: Absolute temperature [K].
t: Time [hr]

U: Internal energy [kJ].
u: Control variables.
u: Velocity [m/s].
V: Vapor flow [kmol/hr]
v: Lagrange multiplier vector.
w: Bound activation multiplier.
x: Optimization variables.
x: Molar composition in the liquid.
y: Differential variables.
y: Molar composition in the vapor.
Z: Compressibility factor.
z: Algebraic variables.
z: Molar composition in the feed.

Greek symbols

α: Weighting parameter.
α: Parameter for the SRK EOS.
α: Parameter for NRTL.
β: Angle for downcomer determination.
ΔH: Vaporization enthalpy [kJ/kmol].
ΔP: Pressure drop [bar].
ε: Parameter for NRTL.
ε: Tray thickness [m].
γ: Activity coefficient.
κ: Reaction rate constant.
μ: IPOPT barrier parameter.
ν: Stoichiometric coefficient.
ρ: Mass density [kg/m^3].
$\bar{\rho}$: Molar density [kmol/m^3].
σ: Surface tension [N/m]
σ: Standard deviation.
τ: Radau root of the orthogonal polynomial.
τ: Parameter for NRTL.
φ: Fugacity coefficient.
Φ: Set of objectives.
ϕ: Objective.
ω: Acentricity factor.

Miscellaneous-Abbreviations

A15: Amberlyst 15 catalyst.
ACC: Annualized Capital Cost.
AMPL: A Mathematical Programming Language.
AOP: Annual Operation Plan.
BFGS: Broyden, Fletcher, Goldfarb and Shanno.

CD: Catalytic Distillation.
DAE: Differential Algebraic Equation.
DAE1: Detailed differential algebraic model.
DAE2: Simplified differential algebraic model.
DAE2h: Index Hybrid differential algebraic model.
DAE2r: Index reduced simplified differential algebraic model.
DIPE: Diisopropyl ether.
DME: Dimethyl ether.
D-O: Discretize then Optimize.
EQ: Equilibrium model.
EOS: Equation Of State.
EO-NMPC: Economic Oriented Non Linear Model Predictive Control.
ETBE: Ethyl *tert*-butyl-ether.
FORTRAN: FORmula TRANslation.
GAMS: General Algebraic Modelling System.
gPROMS: general PROcess Modeling System.
IPOPT: Interior POint OPTimizer.
KKT: Karush-Kuhn-Tucker.
LP: Linear Programming.
LQ: Linear Quadratic.
MATLAB: MATrix LABoratory.
MESH: Mass, Equilibrium, Sum, entHalpy equations.
MIDO: Mixed Integer Dynamic Optimization.
MIMO: Multiple Input Multiple Output.
MINLP: Mixed Integer NonLinear Programming.
MPEC: Mathematical Programming with Equilibrium Constraints.
MPC: Model Predictive Control
MPCC: Mathematical Programming with Complementarity Constraints.
MTBE: Methyl *tert*-butyl-ether.
NEQ: Non Equilibrium model.
NLP: NonLinear Programming.
NMPC: Non Linear Model Predictive Control.
NRTL: Non Random Two Liquid.
OCP: Optimal Control Problem.
ODCP: Optimal Design and Control Problem
ODE: Ordinary Differential Equation.
O-D: Optimize then Discretize.
PI: Proportional, and Integral controller.
PID: Proportional, Integral, and Differential controller.
RD: Reactive Distillation.
RTO: Real-Time Optimization.
SNOPT: Sparse NOnlinear OPTimizer.
SQP: Sequential Quadratic Programming.
SRK. Soave-Redlich-Kwong.

TAME: *tert* amyl methyl ether.
TEEE: *tert* amyl ethyl ether.
TML: TetraMethylLead.
TEL: TetraEthylLead.
UNIFAC: UNIQUAC Functional-group Activity Coefficients.
VOC: Volatile Organic Compounds.

References

[1] W. L. Luyben and C.-C. Yu, *Reactive Distillation Design and Control*. 2005.

[2] D. C. White, “Optimize Energy Use in Distilation,” *Am. Inst. Chem. Prog.*, no. March, p. 7, 2014.

[3] P. Fact, “Distillation Column Modelling Tools,” *Chem. Proj. Fact Sheet*, 2001.

[4] T. Keller, B. Dreisewerd, and A. Görak, “Reactive distillation for multiple-reaction systems: Optimisation study using an evolutionary algorithm,” *Chem. Process Eng. - Inz. Chem. i Proces.*, vol. 34, no. 1, pp. 17–38, 2013.

[5] K. Sundmacher and A. Kienle, *Reactive distillation: status and future directions*, vol. 3. 2006.

[6] R. Ross, J. D. Perkins, E. N. Pistikopoulos, G. L. M. Koot, and J. M. G. Van Schijndel, “Optimal design and control of a high-purity industrial distillation system,” in *Computers and Chemical Engineering*, 2001, vol. 25, no. 1, pp. 141–150.

[7] J. G. Ziegler and N. B. Nichols, “Optimum settings for automatic controllers,” *InTech*, vol. 42, no. 6, pp. 94–100, 1995.

[8] V. Bansal, J. D. Perkins, E. N. Pistikopoulos, R. Ross, and J. M. G. Van Schijndel, “Simultaneous design and control optimisation under uncertainty,” *Comput. Chem. Eng.*, vol. 24, no. 2–7, pp. 261–266, 2000.

[9] R. L.-N. de la Fuente and A. Flores-Tlacuahuac, “Integrated Design and Control Using a Simultaneous Mixed-Integer Dynamic Optimization Approach,” *Ind. Eng. Chem. Res.*, vol. 48, no. 4, pp. 1933–1943, 2009.

[10] M. G. Sneesby, M. O. Tadé, and T. N. Smith, “Multiplicity and Pseudo-Multiplicity in MTBE and ETBE Reactive Distillation,” *Chem. Eng. Res. Des.*, vol. 76, no. 4, pp. 525–531, 1998.

[11] H. E. P. and its Offices, “Bio-ETBE: The Right Road to High Quality 21st Century Motor Fuels,” Washington, 2012.

[12] V. M. Zavala and A. Flores-Tlacuahuac, “Stability of multiobjective predictive control: A utopia-tracking approach,” *Automatica*, vol. 48, no. 10, pp. 2627–2632, 2012.

[13] M. M. Sharma and S. M. Mahajani, “Industrial Applications of Reactive Distillation,” in *Reactive Distillation*, vol. 3, 2002, pp. 1–29.

[14] D. V Quang, P. Amigues, J. F. Gaillard, J. Leonard, and J. L. Nocca, “Process for manufacturing a tertiary alkyl ether by reactive distillation.” Google Patents, 11-Jul-1989.

[15] R. Jacobs and R. Krishna, “Multiple solutions in reactive distillation for methyl tert-butyl ether synthesis,” *Ind. Eng. Chem. Res.*, vol. 32, no. 8, pp. 1706–1709, Aug. 1993.

[16] T. L. Marker, “Hydrocarbon conversion by catalytic distillation.” Google Patents, 07-Mar-1995.

[17] J. L. Bravo, A. Pyhalahti, and H. Jarvelin, “Investigations in a catalytic distillation pilot plant. Vapor/liquid equilibrium kinetics, and mass-transfer issues,” *Ind. Eng. Chem. Res.*, vol. 32, no. 10, pp. 2220–2225, Oct. 1993.

[18] J. M. Gómez, J.-M. Reneaume, M. Roques, M. Meyer, and X. Meyer, “A Mixed Integer Nonlinear Programming Formulation for Optimal Design of a Catalytic Distillation Column Based on a Generic Nonequilibrium Model,” *Ind. Eng. Chem. Res.*, vol. 45, no. 4, pp. 1373–1388, Feb. 2006.

[19] A. Quitain, H. Itoh, and S. Goto, “Reactive Distillation for Synthesizing Ethyl tert-Butyl Etherfrom Bioethanol.,” *J. Chem. Eng. JAPAN*, vol. 32, no. 3, pp. 280–287, 1999.

[20] T. L. Marker, G. A. Funk, P. T. Barger, and H. U. Hammershaimb, “Two-stage process for producing diisopropyl ether using catalytic distillation.” Google Patents, 28-Apr-1998.

[21] C. A. Gonz??lez-Rugerio, R. Fuhrmeister, D. Sudhoff, J. Pilarczyk, and A. G??rak, “Optimal design of catalytic distillation columns: A case study on synthesis of TAEE,” *Chem. Eng. Res. Des.*, vol. 92, no. 3, pp. 391–404, 2014.

[22] R. A. Scala, “Motor gasoline toxicity,” *Toxicol. Sci.*, vol. 10, no. 4, pp. 553–562, 1988.

[23] T. Lidderdale, “Motor gasoline outlook and state MTBE bans,” *US Energy Inf. Adm. DOE, …*, 2003.

[24] A. M. Brownstein and A. M. Brownstein, “Chapter 10 – The Uncertain Future,” in *Renewable Motor Fuels*, 2015, pp. 101–111.

[25] L. T. Biegler, “8. Introduction to Dynamic Process Optimization,” in *Nonlinear Programming*, Society for Industrial and Applied Mathematics, 2010, pp. 213–249.

[26] “2. Theory of DAE’s,” in *Numerical Solution of Initial-Value Problems in Differential-Algebraic Equations*, Society for Industrial and Applied Mathematics, 1995, pp. 15–39.

[27] F. Lozano Santamaría and J. M. Gómez, “Index Hybrid Differential–Algebraic Equations Model Based on Fundamental Principles for Nonlinear Model Predictive Control of a Flash Separation Drum,” *Ind. Eng. Chem. Res.*, vol. 54, no. 7, pp. 2145–2155, Feb. 2015.

[28] F. L. Santamaría and J. M. Gómez, “Economic Oriented NMPC for an Extractive Distillation Column Using an Index Hybrid DAE Model Based on Fundamental Principles,” *Ind. Eng. Chem. Res.*, vol. 54, no. 24, pp. 6344–6354, Jun. 2015.

[29] L. Bittner, “L. S. Pontryagin, V. G. Boltyanskii, R. V. Gamkrelidze, E. F. Mishechenko, The Mathematical Theory of Optimal Processes. VIII + 360 S. New York/London 1962. John Wiley & Sons. Preis 90/–,” *ZAMM - Zeitschrift für Angew. Math. und Mech.*, vol. 43, no. 10–11, pp. 514–515, 1963.

[30] D. H. Pike and M. E. Thomas, “Optimal Control of a Continuous Distillation Column,” *Ind. Eng. Chem. Process Des. Dev.*, vol. 13, no. 2, pp. 97–102, Apr. 1974.

[31] M. J. Mohideen, J. D. Perkins, and E. N. Pistikopoulos, “Optimal Design of Dynamic Systems under Uncertainty,” *AIChE J.*, vol. 42, no. 8, pp. 2251–2265, 1996.

[32] Y. H. Kim, “Optimal design and operation of a multi-product batch distillation column using dynamic model,” vol. 38, pp. 61–72, 1999.

[33] V. Bansal, R. Ross, J. D. Perkins, and E. N. Pistikopoulos, “The interactions of design and control: double-effect distillation,” *J. Process Control*, vol. 10, no. 2, pp. 219–227, 2000.

[34] L. T. Biegler, A. M. Cervantes, and A. Wächter, “Advances in simultaneous strategies for

dynamic process optimization," *Chem. Eng. Sci.*, vol. 57, no. 4, pp. 575–593, 2002.

[35] V. Bansal, J. D. Perkins, and E. N. Pistikopoulos, "A Case Study in Simultaneous Design and Control Using Rigorous, Mixed-Integer Dynamic Optimization Models," *Ind. Eng. Chem. Res.*, vol. 41, no. i, pp. 760–778, 2002.

[36] M. C. Georgiadis, M. Schenk, E. N. Pistikopoulos, and R. Gani, "The interactions of design, control and operability in reactive distillation systems," *Comput. Chem. Eng.*, vol. 26, no. 4–5, pp. 735–746, 2002.

[37] K. H. Low and E. Sorensen, "Simultaneous optimal design and operation of multipurpose batch distillation columns," *Chem. Eng. Process. Process Intensif.*, vol. 43, no. 3, pp. 273–289, 2004.

[38] A. U. Raghunathan, M. Soledad Diaz, and L. T. Biegler, "An MPEC formulation for dynamic optimization of distillation operations," *Comput. Chem. Eng.*, vol. 28, no. 10, pp. 2037–2052, 2004.

[39] P. Panjwani, M. Schenk, M. C. Georgiadis, and E. N. Pistikopoulos, "Optimal design and control of a reactive distillation system," *Eng. Optim.*, vol. 37, no. 7, pp. 733–753, Oct. 2005.

[40] A. Woinaroschy, "Time-optimal control of startup distillation columns by iterative dynamic programming," *Ind. Eng. Chem. Res.*, vol. 47, no. 12, pp. 4158–4169, 2008.

[41] M. Miranda, J. M. Reneaume, X. Meyer, M. Meyer, and F. Szigeti, "Integrating process design and control: An application of optimal control to chemical processes," *Chem. Eng. Process. Process Intensif.*, vol. 47, no. 11, pp. 2004–2018, 2008.

[42] T. Damartzis and P. Seferlis, "Optimal design of staged three-phase reactive distillation columns using nonequilibrium and orthogonal collocation models," *Ind. Eng. Chem. Res.*, vol. 49, no. 7, pp. 3275–3285, 2010.

[43] L. L. Simon, H. Kencse, and K. Hungerbuhler, "Optimal rectification column, reboiler vessel, connection pipe selection and optimal control of batch distillation considering hydraulic limitations," *Chem. Eng. Process. Process Intensif.*, vol. 48, no. 4, pp. 938–949, 2009.

[44] A. Alizadeh Moghadam, I. Aksikas, S. Dubljevic, and J. F. Forbes, "Infinite-dimensional LQ optimal control of a dimethyl ether (DME) catalytic distillation column," *J. Process Control*, vol. 22, no. 9, pp. 1655–1669, 2012.

[45] M. A. Ramos, P. García-Herreros, J. M. Gómez, and J. M. Reneaume, "Optimal control of the extractive distillation for the production of fuel-grade ethanol," *Ind. Eng. Chem. Res.*, vol. 52, no. 25, pp. 8471–8487, 2013.

[46] M. Bauer and I. K. Craig, "Economic assessment of advanced process control - A survey and framework," *Journal of Process Control*, vol. 18, no. 1. pp. 2–18, 2008.

[47] J. B. Rawlings and R. Amrit, "Optimizing Process Economic Performance Using Model Predictive Control," *Nonlinear Model Predict. Control*, vol. 384, pp. 119–138, 2009.

[48] R. Huang, "Nonlinear Model Predictive Control and Dynamic Real Time Optimization for Large-scale Processes Nonlinear Model Predictive Control and Dynamic Real Time Optimization for Large-scale Processes," *PhD Thesis*, 2010.

[49] E. F. Camacho and C. Bordons, *Model Predictive Control*, vol. 57, no. 1. 2010.

[50] E. A. N. Idris and S. Engell, “Economics-based NMPC strategies for the operation and control of a continuous catalytic distillation process,” *J. Process Control*, vol. 22, no. 10, pp. 1832–1843, 2012.

[51] X. Yang and L. T. Biegler, “Advanced-multi-step nonlinear model predictive control,” *J. Process Control*, vol. 23, no. 8, pp. 1116–1128, 2013.

[52] K. Ramesh, S. R. Abd Shukor, and N. Aziz, *Nonlinear Model Predictive Control of a Destillation Column Using NARX Model*, vol. 27. Elsevier Inc., 2009.

[53] C. Venkateswarlu and a D. Reddy, “Nonlinear Model Predictive Control of Reactive Distillation Based on Stochastic Optimization,” *Ind. Eng. Chem. Res.*, vol. 47, no. 18, pp. 6949–6960, 2008.

[54] J. L. Purohit, S. C. Patwardhan, and S. M. Mahajani, “DAE-EKF-based nonlinear predictive control of reactive distillation systems exhibiting input and output multiplicities,” *Ind. Eng. Chem. Res.*, vol. 52, no. 38, pp. 13699–13716, 2013.

[55] S. Schulz, “Four Lectures on Differential-Algebraic Equations,” p. 41, 2003.

[56] A. Kumar and P. Daoutidis, “Control of Nonlinear Differential Algebraic Equation Systems : An Overview,” in *Nonlinear Model Based Process Control*, Dordrecht: Springer Netherlands, 1998, pp. 311–344.

[57] M. Rahul, M. V. P. Kumar, D. Dwivedi, and N. Kaistha, “An efficient algorithm for rigorous dynamic simulation of reactive distillation columns,” *Comput. Chem. Eng.*, vol. 33, no. 8, pp. 1336–1343, 2009.

[58] P. I. Barton, “Introduction Industrial Experience With Dynamic Simulation,” p. 291, 1997.

[59] J. S. Logsdon and L. T. Biegler, “Accurate solution of differential-algebraic optimization problems,” *Ind. Eng. Chem. Res.*, vol. 28, no. 11, pp. 1628–1639, Nov. 1989.

[60] M. Al-Arfaj, “Quantitative heuristic design of reactive distillation,” Lehigh University, 1999.

[61] B. N. M. van Leeuwen, A. M. van der Wulp, I. Duijnstee, A. J. A. van Maris, and A. J. J. Straathof, “Fermentative production of isobutene.,” *Appl. Microbiol. Biotechnol.*, vol. 93, no. 4, pp. 1377–87, Feb. 2012.

[62] M. G. Sneesby, M. O. Tade, R. Datta, and T. N. Smith, “ETBE Synthesis via Reactive Distillation. 1. Steady-State Simulation and Design Aspects,” *Ind. Eng. Chem. Res.*, vol. 36, pp. 1855–1869, 1997.

[63] L. Domingues, C. I. C. Pinheiro, N. M. C. Oliveira, J. Fernandes, and A. Vilelas, “Model Development and Validation of Ethyl tert-Butyl Ether Production Reactors Using Industrial Plant Data,” *Ind. Eng. Chem. Res.*, vol. 51, pp. 15018–15031, 2012.

[64] M. A. Al-Arfaj and W. L. Luyben, “Control Study of Ethyl tert -Butyl Ether Reactive Distillation,” *Ind. Eng. Chem. Res.*, vol. 41, no. 16, pp. 3784–3796, 2002.

[65] L. Domingues, C. I. C. Pinheiro, and N. M. C. Oliveira, “Optimal design of reactive distillation systems: Application to the production of ethyl tert-butyl ether (ETBE),” *Comput. Chem. Eng.*, vol. 64, pp. 81–94, 2014.

[66] K. L. Jensen and R. Datta, “Ethers from Ethanol. 1. Equilibrium Thermodynamic Analysis of the

Liquid-Phase Ethyl tert-Butyl Ether Reaction," *Ind. Eng. Chem. Res.*, vol. 34, no. 1992, pp. 392–399, 1995.

[67] Rohm and Haas Company, "AMBERLYST™ 15WET Industrial Grade Strongly Acidic Catalyst For Catalysis and Separation technologies," Philadelphia, 2003.

[68] H. Kister, "Distillation design." p. 710, 1992.

[69] J. M. Douglas, "Conceptual design of chemical processes." p. 601, 1988.

[70] J. D. Seader, W. D. Seider, D. R. Lewin, L. Boulle, and A. Rycrof, *Separation Process Principles, 3rd Edition*. 2006.

[71] J. C. CICILE, "Distillation. Absorption - Colonnes à plateaux : dimensionnement," *Tech. L'INGÉNIEUR*, 1994.

[72] M. F. Cardoso, R. L. Salcedo, S. F. De Azevedo, and D. Barbosa, "Optimization of reactive distillation processes with simulated annealing," *Chem. Eng. Sci.*, vol. 55, no. 21, pp. 5059–5078, 2000.

[73] A. R. Ciric and D. Gu, "Synthesis of Nonequilibrium Reactive Distillation Processes by MINLP 0ptimization," *AIChe J.*, vol. 40, no. 9, pp. 1479–1487, 1994.

[74] L. T. Biegler, "A Survey on Sensitivity-based Nonlinear Model Predictive Control," *10th IFAC Int. Symp. Dyn. Control Process Syst.*, no. 2004, pp. 499–510, 2013.

[75] L. Grüne, W. Semmler, and M. Stieler, "Using nonlinear model predictive control for dynamic decision problems in economics," *J. Econ. Dyn. Control*, vol. 60, pp. 112–133, 2015.

[76] R. Huang, L. T. Biegler, and E. Harinath, "Robust stability of economically oriented infinite horizon NMPC that include cyclic processes," *J. Process Control*, vol. 22, no. 1, pp. 51–59, 2012.

[77] R. Huang, E. Harinath, and L. T. Biegler, "Lyapunov stability of economically oriented NMPC for cyclic processes," *J. Process Control*, vol. 21, no. 4, pp. 501–509, 2011.

[78] R. Amrit, J. B. Rawlings, and L. T. Biegler, "Optimizing process economics online using model predictive control," *Comput. Chem. Eng.*, vol. 58, pp. 334–343, 2013.

[79] V. M. Zavala, "Real-Time Optimization Strategies for Building Systems†," *Ind. Eng. Chem. Res.*, vol. 52, no. 9, pp. 3137–3150, 2013.

[80] a Flores-Tlacuahuac, P. Morales, and M. Rivera-Toledo, "Multiobjective Nonlinear Model Predictive Control of a Class of Chemical Reactors," *Ind. Eng. Chem. Res.*, vol. 51, no. 17, pp. 5891–5899, 2012.

[81] A. Gopalakrishnan and L. T. Biegler, "Economic Nonlinear Model Predictive Control for periodic optimal operation of gas pipeline networks," *Comput. Chem. Eng.*, vol. 52, pp. 90–99, 2013.

[82] A. Drud, "CONOPT: A GRG code for large sparse dynamic nonlinear optimization problems," *Math. Program.*, vol. 31, no. 2, pp. 153–191, 1985.

[83] M. R. Bussieck and A. Meeraus, "General Algebraic Modeling System (GAMS)," in *Modeling Languages in Mathematical Optimization, J. Kallrath (Ed.)*, vol. 88, Springer US, 2004, pp. 137–157.

[84] M. G. Sneesby, M. O. Tadé, R. Datta, and T. N. Smith, “ETBE Synthesis via Reactive Distillation. 2. Dynamic Simulation and Control Aspects,” *Ind. Eng. Chem. Res.*, vol. 36, no. 5, pp. 1870–1881, 1997.

[85] C. Bendtsen and P. G. Thomson, “Numerical solution of differential algebraic equations,” *Tech. Rep. IMM-REP-1999-8*, 1999.

[86] R. H. Aungier, “A Fast, Accurate Real Gas Equation of State for Fluid Dynamic Analysis Applications,” *J. Fluids Eng.*, vol. 117, no. June 1995, pp. 277–281, 1995.

[87] P. C.-N. Mak, “Thermodynamic properties from cubic equations of state,” 1988.

[88] I. Aspen Technology, “Aspen Plus ® User Guide,” *Aspen Technol. Inc.*, p. 936, 2000.

[89] B. E. Poling, J. M. Prausnitz, J. P. O ’connell, N. York, C. San, F. Lisbon, L. Madrid, M. City, M. New, D. San, J. S. Singapore, and S. Toronto, “THE PROPERTIES OF GASES AND LIQUIDS McGRAW-HILL.”

[90] F. J. Zuiderweg, “Sieve trays. A view on the state of the art,” *Chem. Eng. Sci.*, vol. 37, no. 10, pp. 1441–1464, 1982.

[91] L. T. Biegler, “10. Simultaneous Methods for Dynamic Optimization,” in *Nonlinear Programming*, Society for Industrial and Applied Mathematics, 2010, pp. 287–324.

[92] E. Hairer and G. Wanner, “Stability Function of Implicit RK-Methods,” 1996, pp. 40–50.

[93] L. T. Biegler, “1. Introduction to Process Optimization,” in *Nonlinear Programming*, Society for Industrial and Applied Mathematics, 2010, pp. 1–16.

[94] G. D. Corporation, “General Algebraic Modeling System (GAMS) Release 24.2.1.” 2013.

[95] A. Wächter and L. T. Biegler, “On the implementation of an interior-point filter line-search algorithm for large-scale nonlinear programming,” *Math. Program.*, vol. 106, no. 1, pp. 25–57, Apr. 2005.

[96] W. A. Sutherland, *Introduction to metric and topological spaces.* Oxford: Oxford University Press., 2009.

[97] P. E. Gill, W. Murray, and M. A. Saunders, “SNOPT: An SQP Algorithm for Large-Scale Constrained Optimization,” *SIAM J. Optim.*, vol. 12, no. 4, pp. 979–1006, 2002.

[98] L. T. Biegler, “7. Steady State Process Optimization,” in *Nonlinear Programming*, Society for Industrial and Applied Mathematics, 2010, pp. 181–212.

[99] J. T. Betts and P. D. Frank, “A sparse nonlinear optimization algorithm,” *J. Optim. Theory Appl.*, vol. 82, no. 3, pp. 519–541, 1994.

[100] Bruce A. McCarl et. al., “McCarl Expanded GAMS User Guide, GAMS Release 24.2.1.” Washington, DC, USA, 2013.

[101] S. S. Keerthi and E. G. Gilbert, “Optimal infinite-horizon feedback laws for a general class of constrained discrete-time systems: Stability and moving-horizon approximations,” *J. Optim. Theory Appl.*, vol. 57, no. 2, pp. 265–293, 1988.